

Integrated System for Improved Grade Control
in Open Pit Mines

by

Yaroslav Valentynovych Vasylchuk

A thesis submitted in partial fulfillment of the requirements for the degree of

Master of Science

in

Mining Engineering

Department of Civil and Environmental Engineering
University of Alberta

© Yaroslav Valentynovych Vasylchuk, 2016

Abstract

Grade control establishes the final destinations for mined material (plant, stockpile, waste dump, etc.) at the time of mining. Correct decisions bring profit to a mining company while incorrect decisions bring losses. There are several potential sources of misclassification of mined material: i) unreasonable prediction of grade, ii) failing to account for the consequences of incorrect decisions, iii) ignoring blast movement of rocks, and iv) imprecise selection of mined material using large polygons.

This thesis provides tools for addressing some sources of misclassification. A reasonable range of grid sizes for grade control models is determined. The use of simulation and utility theory for grade control classification are illustrated with a series of examples. A program for predicting approximate blast movement of rocks is developed. Grade control dig limits are replaced with truck-by-truck determination of the optimal destination. The new selection paradigm combines all of these considerations in a unified approach.

Acknowledgements

I want to express my sincere gratitude to Dr. Clayton Deutsch, my thesis supervisor and mentor. His tremendous intellect, bright ideas, and patience helped me to produce this piece of research. I admire his unique ability to inspire and make everything happen in an easiest way.

I would like to thank the Centre for Computational Geostatistics for the financial support during the period of my study and an excellent research environment. My CCG colleagues, Dr. Yevgeniy Zagayevskiy, Mostafa Hadavand, and Amir Razavi, were constantly helping me with wise advice and were encouraging my enthusiasm.

The selfless love of my wife and my parents made it possible for me to go through this thorny path. Our everyday conversations charged me with energy and positive emotions, and gave me a desire to keep going and achieve.

Contents

1	Introduction	1
1.1	Background	1
1.1.1	Problem Definition	2
1.1.2	Problem Solution	4
1.2	Thesis Statement and Outline	5
2	Literature Overview	7
2.1	Geological Characterization	7
2.2	Valuation and Decision Making	10
2.3	Blast Movement of Rock	13
2.4	Ore and Waste Zone Delimitation	16
3	Optimal Grid Size for Estimation	18
3.1	Motivation	18
3.2	Methodology	19
3.3	Experimental Results	21
3.4	Limitations	23
4	Simulation versus Estimation	24
4.1	The Concept of Utility in Grade Control	24
4.2	Decision Making Using Uncertainty	26
4.3	Profitability of Estimation Versus Simulation	31
4.4	Limitations and Recommendations	34

5	Background of the Blast Movement Problem	37
5.1	Accounting for Blast Movement in Grade Control	39
5.2	Common Problems for Blast Movement Measurement	42
5.3	Calculating Approximate Blast Movement	43
5.4	Examples of Blast Movement Modeling	49
5.5	Conclusions	60
6	Truck-By-Truck Selection	62
6.1	Motivation	62
6.2	The Importance of a Flexible Grade Control	64
6.3	Choice of truck-based units	68
6.4	Conclusions and Limitations	74
7	Red Dog Case Study	76
7.1	Purpose	76
7.2	Background	78
7.3	Construction of Reference Distribution	80
7.4	Optimal Grid Size	94
7.5	Estimation Versus Simulation	97
7.6	Blast Movement	99
7.7	Truck-by-Truck Selection	104
7.8	Conclusions and Limitations	117
8	Conclusions	120
8.1	Summary of Contributions	120
8.2	Limitations	123
8.3	Future Work	125
	References	127
	Appendix A Input for Blast Movement Program	136

List of Tables

4.1	Effectiveness of ore/waste selection for the case with many grade control decisions and normal distribution of data	32
4.2	Effectiveness of ore/waste selection for the case with many grade control decisions and and log-normal distribution of data	32
4.3	Effectiveness of ore/waste selection for the case with two grade control decisions and normal distribution of data	33
4.4	Effectiveness of ore/waste selection for the case with two grade control decisions and log-normal distribution of data	33
6.1	Comparison of two estimation methods	66
7.1	Effectiveness of ore/waste classification at different grid sizes for Red Dog mine)	96
7.2	Technological parameters of equipment related to the TBT selection	106
7.3	Percentage of misclassified blocks produced by the TBT method with different degrees of navigation accuracy	114
7.4	Percentage of misclassified blocks produced by the DL method with different degrees of navigation accuracy	115
7.5	Percentage of misclassified blocks produced by the TBT method with different degrees of navigation accuracy (accounting for sampling errors)	115

7.6	Percentage of misclassified blocks produced by the DL method with different degrees of navigation accuracy (accounting for sampling errors)	116
A.1	Parameter file for BMOV program	136
A.2	An example of vertices file	137
A.3	An example of surface file	137

List of Figures

2.1	Schematic illustration of the problem of optimal estimation grid size	10
2.2	An example loss function	11
2.3	Typical dig limits	16
3.1	Misclassification errors	20
3.2	PME versus OK grid size for 2 set of parameters	21
3.3	Experimental results for error with different grid size	22
4.1	A simple utility function	26
4.2	Asymmetric loss functions	27
4.3	Range of possible decisions	28
4.4	Two gade control decisions case loss function	30
4.5	Penalties for estimation and simulation	34
5.1	A schematic illustration of rectangular (left) and staggered (right) drilling patterns	37
5.2	A schematic illustration of the detonation wave passing through the column of charge	39
5.3	A schematic movement of rocks for the V-cut firing sequence . .	41
5.4	A shematic illustration of the mapping principle of <i>bmov</i>	46
5.5	3-D models of mine area before and after blasting (first simple example)	51

5.6	3-D models colored according to position index values (first simple example)	52
5.7	3-D models with assigned grades (first simple example)	53
5.8	3-D models with assigned grades (second simple example)	54
5.9	3-D models with assigned grades (third simple example)	55
5.10	3-D models representing the mine area before and after blasting (more complex example)	56
5.11	3-D models with assigned grades (more complex example, top view)	58
5.12	3-D models with assigned grades (more complex example, bottom view)	59
6.1	Bench 4270 estimated by ID cubed and BEI method	65
6.2	The ID cubed estimate (dashed lines) superimposed onto the BEI estimate	65
6.3	Bench 4270 with green areas representing the parts where two estimates coincide and brown areas where they do not	66
6.4	Bench 4270 discretized by units representing one truck load	67
6.5	Reference model for simple grade control case	69
6.6	Reference model for complex grade control case	70
6.7	Ore/waste maps for two grade control cases	71
6.8	Ore/waste for two grade control methods	72
6.9	Percentage of maximum profit across the range of TBT sizes for simple grade control case	73
6.10	Percentage of maximum profit across the range of TBT sizes for complex grade control case	73
6.11	Difference with respect to profit between two grade control methods for both grade control cases	74
7.1	A schematic illustration of stockpile constraints at Red Dog	79

7.2	Mine Bench 20177 with BH colored according to contents of each variable	82
7.3	Comparison of bi-variate plots of original and PPMT transformed variables	84
7.4	Variogram models for all four variables in Normal Scores	86
7.5	Simulated reference models for all four variables	87
7.6	Q-Q plots between original and simulated data for all four variables	88
7.7	Comparison of histograms of original and simulated data for all four variables	89
7.8	Variogram reproduction for all four variables	90
7.9	Bi-plots of data in original units versus bi-plots of simulated data	92
7.10	Reference ore/waste map for the Red Dog case study	94
7.11	Ordinary kriging ore/waste indicator maps	95
7.12	Percentage of misclassified blocks for different grid sizes (Red Dog case study)	96
7.13	Ore/waste maps at 3'×3'×25' resolution	98
7.14	Topographic surfaces for Bench 20177	100
7.15	3-D models for the dig limits case	102
7.16	The output of BMOV	103
7.17	Ore/waste indicator map with digitized dig limits for the selection of ore	107
7.18	Reference ore/waste indicator maps discretized by the units equal to one truck load	107
7.19	Possible directions of displacement from modeled positions for each type of excavating equipment	108
7.20	A mine block boundary constraint	109
7.21	An overlap constraint	109
7.22	Ore/waste indicator map with digitized dig limits for the selection of ore (case with sample errors)	111

7.23	Change in expected profit for each scoop of excavating equipment due to 3' offset	112
7.24	Change of ore/waste indicator maps for 'front end loader-truck' units due to 3' offset (TBT method)	112
7.25	Change of ore/waste indicator maps for 'front end loader-truck' units due 3' offset (DL method)	113
7.26	Change of ore/waste indicator maps for 'hydraulic excavator-truck' units due 3' offset (TBT method)	113
7.27	Change of ore/waste indicator maps for 'hydraulic excavator-truck' units due 3' offset (DL method)	113
7.28	Change of ore/waste indicator maps for 'electric rope shovel-truck' units due 3' offset (TBT method)	114
7.29	Change of ore/waste indicator maps for 'electric rope shovel-truck' units due to dispatching errors (DL method)	114

List of Abbreviations

AMC	Approximate model of coregionalization
Ba	Barium
BEI	Break even indicator estimation method
BH	Blasthole
BLUE	Best linear unbiased estimator
BMM	Blast movement monitor
CAD	Computer-aid design
DH	Drillhole
DL	Dig limits-based selection method
Fe	Iron
ft	foot
GPS	Global positioning system
GSLIB	Geostatistical Software Library
GSS	Grid size/sample spacing ratio
ID	Inverse distance estimation method
kg	kilogram
LMC	Linear model of coregionalization
MAF	Minimum/maximum auto-correlation factors
MDE	Multivariate density estimation
m	meter
NN	Nearest neighbor estimation method
NS	Normal score
OK	Ordinary kriging estimation method
Pb	Lead
PCA	Principal component analysis
PME	Percentage of misclassification errors
PPMT	Projection pursuit multivariate transform
RC	Reverse circulation drilling

SIM	Simulation approach for grade control
SGS	Sequential Gaussian simulation
SK	Simple kriging estimation method
SCT	Stepwise conditional transformation
SMU	Selective mining unit
TBT	Truck-by-truck selection method
Zn	Zinc

Chapter 1

Introduction

1.1 Background

The success of a mine is dependent on correct grade control. Grade control is the process of determining the final destination of mined material; it directly influences the profitability of the operation. Any errors will be a direct cost or loss of profit. Thus, it is of great concern to mine operators. Appropriate grade control starts from quality assurance and quality control programs for collecting, storing and assaying geological data. The next step is obtaining the best possible predictions of all required grade variables. Then, these predictions are used to determine the optimal destination, that is, the destination with the least loss and greatest profit. The final step is for mine operators to correctly move the material to the planned destination.

The predictions are obtained using samples from drillholes (DH) and blastholes (BH). DH samples are a reliable but expensive source of information obtained using diamond and/or reverse circulation drilling. Due to the high cost of drilling, DH samples are widely spaced. The most closely spaced source of information for daily grade control tasks is BH samples. Blastholes are closely spaced due to blasting technology requirements (Rossi & Deutsch, 2014).

After obtaining samples, a grid is chosen, the grades are estimated for grid

blocks, and the destination of mined material is determined. Blasting causes the movement of rocks. Thus, the pre-blast positions of grades should be adjusted according to the post-blast muckpile geometry. The selectivity of excavation depends on the available data and the working parameters of the excavating equipment. The destination for mined material should be established on a truck load basis. The scale of selectivity cannot be smaller and could be larger if the blastholes are not well sampled or if the blast movement is not understood.

Grade control should be a flexible procedure accounting for the uncertainty of the prediction and site specific characteristics of mining operation.

1.1.1 Problem Definition

In common grade control practice, there are several potential reasons of the misclassification errors:

i) Geostatistical estimation is done on a grid of blocks. Each node corresponds to a center of a block unit. Each block is estimated based on the chosen algorithm. The blocks are commonly chosen to correspond to a specified selective mining unit (SMU), which could be the bench height by 10×10 meters (Dimitrakopoulos & Godoy, 2014) or larger. The SMU size is often larger than the blasthole sample spacing (4-7 meters). Considering also the bench height is 10 meters or more, the volume of an SMU block could be much larger than the volume of one truck load; at the time of grade control the selectivity may be smaller than the chosen SMU size.

ii) Grade control typically relies on estimation methods (Dimitrakopoulos & Godoy, 2014; Verly, 2005) such as Inverse distance (ID), Nearest Neighbor (NN), Simple or Ordinary Kriging (Dimitrakopoulos & Godoy, 2014; Detour Gold, 2012). These methods provide deterministic estimates and do not account for non-linear recovery and uncertainty in profit. Therefore, they may not be suitable for multiple variables and complex profit calculations. They may not provide optimal decisions when the penalties for different types of

misclassification errors are complex.

iii) Grade estimates are typically used to develop boundaries (dig limits) for delimiting ore and waste or different destinations including leach pads and stockpiles (Dimitrakopoulos & Godoy, 2014; Verly, 2005). It is difficult to delimit ore and waste zones precisely accounting for the mining practice; this can lead to increased dilution and ore loss. The use of dig limits is improved using expected profit maps, optimization, and accounting for mine specific selectivity constraints (Norrena, 2007; Isaaks, Treloar, & Elenbaas, n.d.).

iv) In some cases, conventional grade control does not account for blast movement. Most mines use drilling and blasting to break rocks prior to excavation and hauling. Due to the energy of explosion, the rock moves with blasting. Depending on the type of rocks, the displacement of grades can be up to 10-15 meters (Thornton, Sprott, & Brunton, 2005; Thornton, 2009b). This means the pre-blast estimates are not final. The post-blast mapping of grades is of great importance for grade control.

v) Misclassification errors may be introduced by the excavating process itself. Navigation and human errors are inevitable. They impact the quality of grade control for different types of equipment. Generally, several scoops of the excavating equipment comprise a truck load. The profit from these scoops determines the profit of the entire truck load. Therefore, the geometric parameters of shovels and working constraints significantly impact the final grade control decisions. This impact should be understood beforehand and taken into account.

vi) Sampling errors are inevitable. They reduce the quality of the estimates for grade control. The influence of sampling errors on simulation and truck-based selection of rocks should be understood. The possibility of incurring sampling error should be taken into account.

1.1.2 Problem Solution

This thesis addresses the problems outlined above. It serves as a guide for the implementation of simulation and other aspects for improved grade control.

The optimal estimation grid size is studied. A range of different grid sizes is considered relative to a reference model. A number of influencing factors are taken into consideration. Recommendations on the optimal estimation grid size are provided.

Stochastic methods are an alternative to the deterministic approach. The use of multiple realizations appears challenging due to the ambiguity introduced by multiple realizations, but the grade control decisions could be optimized over all realizations simultaneously. Many researchers attempt to adapt stochastic methods for better classification of mined material (Isaaks, 1991; Glacken, 1996; Godoy, Dimitrakopoulos, & Costa, 2001; Deutsch, Magri, & Norrena, 2000; Dimitrakopoulos & Godoy, 2014; Verly, 2005; Neufeld, Norrena, & Deutsch, 2007). A minimum loss/maximum profit grade control approach is adjusted to current practice. Simulation is used to obtain multiple realizations and assess the uncertainty in profit. The selection decisions can be based either on maximum expected profit or minimum expected loss. This approach is adjustable and capable of handling many variables and complex processes.

A solution is provided for blast movement assessment. A program for mapping the pre-blast grades onto post-blast muckpile geometry is introduced. The program works in 3-D with the pre- and post-blast topographies of any complexity. It is possible to calibrate the program for any particular mine site. A series of examples on how to use the program are provided.

A truck-by-truck (TBT) selection paradigm is presented. The use of dig limits is replaced by the truck-based classification of grades. The method uses the expected profit of each truck load for making the grade control decisions. TBT eliminates the errors introduced by arbitrary dig limits and more closely models the actual selection process at the mine site.

The selection of mined material by different types of excavating equipment is modeled. The mined volumes and the sequence of each consecutive scoop in the course of digging is simulated. Dispatching GPS errors are investigated by assigning random offsets to the position of each scoop. The results of the simulation are summarized by the amount of misclassification errors. Recommendations on improving grade control at this stage of mining process are provided.

The influence of sampling errors on grade control is taken into account using the method from Neufeld, Lyall, and Deutsch (2006). A random error is added to the sample values. The impact of the sample errors on the amount of the misclassified mined material is estimated. In practice, of course, we would not add errors and would work with the mine and laboratory staff to ensure that errors are minimized.

A new integrated grade control system is introduced. A comprehensive case study using all the elements of the system is presented. Different aspects of the system could be used, depending on the needs of a particular mine.

1.2 Thesis Statement and Outline

The new integrated system for grade control is based on the maximum profit/minimum loss classification of mined material by means of simulation. It accounts for the displacement of grades after blasting and the working parameters of excavating equipment. Sampling and navigating errors are addressed. Limitations of the research are summarized.

Chapter 2 contains an overview of the existing estimation and simulation techniques in the context of grade control. Literature references addressing the blast movement issue and the maximum profit/minimum loss grade control paradigm are provided.

Chapter 3 is devoted to determining the optimal estimation grid size. A

numerical experiment is followed by practical recommendations.

Chapter 4 presents a numerical study on the effectiveness of different estimation techniques versus simulation. The performance of the estimation methods and simulation is measured by their ability to correctly classify ore and waste blocks. The results are repeated for different loss functions. Recommendations on estimation methods and conditional simulation are provided.

Chapter 5 introduces a new program for mapping grades onto the post-blast muckpile geometry. The principle is explained in detail and demonstrated with a series of examples.

Chapter 6 discusses the truck-by-truck (TBT) selection paradigm compared to the conventional dig limits approach.

Chapter 7 presents a case study using data from Red Dog Mine, Alaska. A mine block is classified either ore or waste at the optimal grid size. Then, the influence of the blast movement of grades on the ore/waste selection is estimated. Three types of excavating equipment is simulated for both the TBT and dig limit approaches. The profitability of each method and the optimal type of equipment are determined. Dispatching and sampling errors are considered.

Chapter 8 discusses limitations of this research. It also provides conclusions and recommendations on improving grade control in open pit mines.

Chapter 2

Literature Overview

2.1 Geological Characterization

There are number of methods to construct geological models of deposits. They vary from simple deterministic estimation methods to complex multivariate simulation techniques.

Inverse distance (ID) is a simple interpolation method. It estimates unsampled locations using nearby data weighted by distance. Usually, the estimation is limited by a search neighborhood. Further information can be found in Shepard (1968). Nearest Neighborhood interpolation is another simple deterministic method. The unknown locations are estimated by assigning the value of the closest sample data available.

Kriging techniques are widely used in geostatistics. Kriging is similar to ID in terms of calculating the estimate by weighting data. Kriging uses spatial correlations between the data and is often referred to as BLUE (Best Linear Unbiased Estimator). Kriging estimates are smooth and, therefore, should not be used for applications where extreme values are important. As mentioned earlier, kriging estimates are not able to address the non-linearity of some technological processes (e.g. metal recovery). Ordinary kriging (OK) is a robust estimator and can be used in grade control when the economic con-

sequences of the underestimation and overestimation decisions are nearly the same (Vasylchuk & Deutsch, 2015a). The theory of kriging is formulated in numerous publications (Matheron, 1963; Journel & Huijbregts, 1978; Isaaks & Srivastava, 1989; Cressie, 1990; Deutsch & Journel, 1998).

Simulation is a way to model the uncertainty in grades. It generates multiple equiprobable realizations and captures the extreme values. A popular simulation technique is Sequential Gaussian Simulation (SGS) (Isaaks, 1991). The data are transformed to Gaussian space (normal score transformation). Then, a distribution conditional to nearby data and previously simulated values is constructed using the normal equations (simple kriging). A value is drawn from the conditional distribution. The path through all node locations is chosen randomly. SGS reproduces uncertainty, histograms, variograms and multivariate relationships. Most of these techniques are in the GSLIB software (Deutsch & Journel, 1998). The ways to use simulation in grade control are explained in the next subsection and Chapter 4.

Geostatistical resource estimation often requires modeling multiple variables. For example, the recovery of a metal of interest may be dependent on the concentration of other metals or non-metal chemical compounds in mined material.

Estimation of multiple variables directly is possible by means of cokriging. Cokriging is usually used when a variable of interest is sparse but a secondary data is abundant (Rossi & Deutsch, 2014). It needs a linear coregionalization model (LMC) to model the mutual behavior of the variables. The method differs from kriging only in the number of variables. More information on cokriging is available in Journel (1989) and Isaaks and Srivastava (1989). Collocated cokriging is a form of cokriging with substantial simplifications. The LMC model is replaced by the Markov model (Zhu, 1991) or the approximate model of coregionalization (AMC)(Wang & Deutsch, 2009).

Cosimulation could be performed in the GSLIB program *sgsim*. It allows

co-simulating up to two variables. The cosimulation of more variables may require specialized techniques. Multivariate transformation/decorrelation of variables have been developed. A short outline of the existing multivariate transformation techniques is provided below (J.L. Deutsch, personal communication, March 24, 2015). The most popular multivariate transformation methods include: i) principal component analysis (PCA), ii) minimum/maximum auto-correlation factors (MAF), iii) multivariate density estimation (MDE), iv) stepwise conditional transformation (SCT), v) projection pursuit multivariate transform (PPMT).

SCT and PPMT are, perhaps, the most advanced transformation techniques in geostatistics at the moment. They allow modeling complex multivariate relationships between variables, relationships with constraints, non-linear relationships and other features. SCT employs a stepwise normal score (NS) transformation of variables with respect to a reference variable. Then, the NS variables are simulated and back-transformed to the original values in the reverse stepwise manner. Advantages and disadvantages of using this transformation technique are outlined in (Leuangthong, 2003; Rossi & Deutsch, 2014). PPMT is a fast and easy way to transform multiple variables. The method uses aspects from Projection Pursuit Density Estimation algorithm (PPDE) (Friedman, 1987). It normal score transforms and decorrelates any number of variables at once. The reader will find more information in Barnett, Manchuk, and Deutsch (2014).

The resolution of geological models is another issue. Usually, it is chosen to correspond to the working parameters of the excavating equipment used at a mine; which is expressed by a selective mining unit (SMU)(Leuangthong, Neufeld, & Deutsch, 2003). Short-term models, however, are a different case. Grade control requires the boundaries to be defined; mining does not extract large blocks, but mines with specific loading equipment.

There is a rule of thumb related to geostatistical modeling of predictions:

estimation grid size should be about $1/3$ or $1/4$ (David, 1977, p. 283) of the sample spacing. It will be useful to check this rule and define the optimal estimation grid size/sample spacing relation (see Figure 2.1) (Vasylchuk & Deutsch, 2015c).

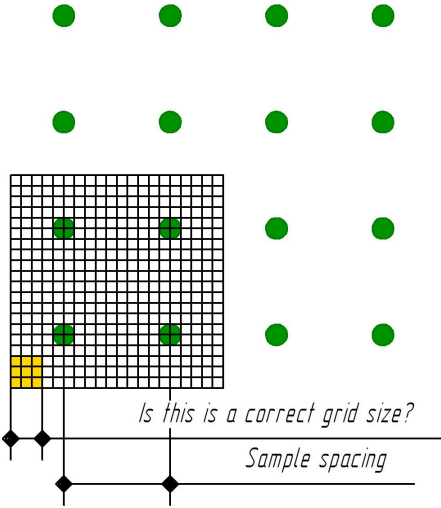


Figure 2.1: Schematic illustration of the problem of optimal estimation grid size

2.2 Valuation and Decision Making

Decision making is an important part of grade control. The basis of economic decisions in presence of uncertainty is important. D. Bernoulli proposed his hypothesis of expected utility in 1738 (Bernoulli, 1954). Before, mathematicians hypothesized that humans made their economic decisions based on the expected value. The expected value in this case is the monetary value of an event multiplied by the probability of this event to occur. There are cases, such as the St. Petersburg Paradox (Bernoulli, 1954), when the expected value principle does not explain human decision making. Bernoulli conjectured that people made their decisions based on the utility they can take from them.

The expected utility principle can be used in grade control. The classification decision at mines is linked to economic consequences. For example, it can

be more expensive to process waste as ore than put ore on a waste dump. On a small scale, some of our decisions inevitably will be erroneous. The idea is to incur the minimum economic loss possible (Vasylchuk & Deutsch, 2015a).

The economic consequences of the decisions can be characterized by loss or profit functions, which determine how much the decision is penalized or how much profit it brings. An example of a loss function is presented in Figure 2.2. It is possible to minimize the expected loss. For example, the minimization of the quadratic and absolute loss functions are well established and exact (Giles (n.d.) and University of Colorado (n.d.) respectively). The loss functions may be various in shape and complexity reflecting technological processes and the level of the company’s risk tolerance. The use of loss functions for geostatistical applications is established in Journel (1984) and Srivastava (1987).

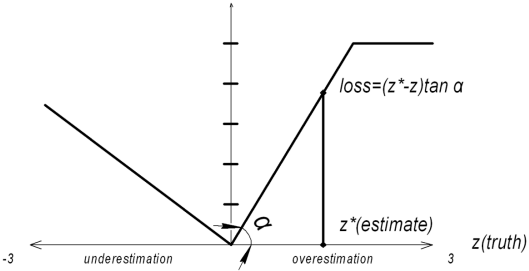


Figure 2.2: An example loss function (Vasylchuk & Deutsch, 2015a)

Numerous research consider optimization of grade control with simulation (Isaaks, 1991; Srivastava, 1987; Glacken, 1996; Deutsch et al., 2000; Godoy et al., 2001; Verly, 2005; Neufeld et al., 2007; Dimitrakopoulos & Godoy, 2014). Conditional simulation is used as the tool for obtaining the expected profit or expected loss. Two basic approaches use minimum expected loss (Isaaks, 1991) and maximum expected profit (Glacken, 1996) as the basis for the grade control decisions. These two approaches are the same in principle. They both are able to incorporate recovery, cutoff grades, the price for commodities, and the costs for mining into decision making. The difference is in a way the uncertainty is processed for decision making. A common way is to use utility and penalty

functions.

Glacken (1996) does not use the cost of mining in the utility function calculations and incorporates additional coefficients for wrong decisions. The coefficients reflect the company's attitude to the treatment of waste material as ore (risk aversion) and to the lost opportunity cost due misclassifying ore as waste. For example, setting the coefficient for underestimation to 0 means the company cares less about the potential ore loss than treating the waste material as ore.

Deutsch et al. (2000) suggest setting both the risk aversion and lost opportunity cost coefficients to 1. In this case, the lost opportunity cost is also taken into account when making the grade control decisions. Other values for both coefficients could be used.

A 'cost of processing waste' coefficient is used in Neufeld et al. (2007). The coefficient scales up or down the loss for underestimation depending on the price of treating waste as ore. Neufeld et al. (2007) also offer the maximum profit approach using operational costs of mining ore and waste.

A more recent study on using the minimum loss principle in grade control is in Vasylchuk and Deutsch (2015a). The method is similar to Isaaks (1991) but it does not take into account the mining and operational costs, recovery and the commodity price. A simpler logic is used: if the decision is correct, it is not penalized; if the decision is wrong, the penalty is dependent on the magnitude of the error with respect to the cutoff grade. The simplification is made in order to determine the best and the most reliable method for grade control. The risk aversion and the lost opportunity cost coefficients are used in the calculations. The coefficients determine the way the underestimation and overestimation decisions are penalized.

The above methods are straightforward to implement when a decision is based on a cutoff grade. The decision making principle remains the same in presence of complex rules: the decision should bring the minimum loss or

maximum profit (Vasylchuk & Deutsch, 2015a). For multiple variables, each decision criteria should be incorporated as a utility or penalty function. Any number of variables can be used for obtaining the final decision. An example of handling multiple variables in grade control using simulation is presented in Chapter 7.

2.3 Blast Movement of Rock

Blast-induced movement of grades influences the effectiveness of grade control. All geostatistical models are pre-blast by default. Their effectiveness is reduced if they are translated onto the post-blast muck pile incorrectly. In some cases, blasting of rocks is not needed at all. Blasting may also be performed so that the rocks movement is relatively insignificant or the displacement vectors of blasted rock mass are very simple. In many cases, however, modeling or measuring the blast movement is required.

There are different ways to account for blast movement (La Rosa & Thornton, 2011): i) visual, ii) theoretical, iii) remote measurements, and iv) cautious blasting (for reduced movement of rocks). The visual methods are the least reliable. Usually, some markers (bags, sticks, balls, dyes, etc.) are placed within the bench volume before blasting and recovered afterwards. The main challenges with this method include: i) the difficulty of recovering markers (a large part of them are never recovered), ii) the difficulty of accounting for the movement in 3-D, and iii) labor intensiveness.

Purely theoretical models have always been attractive to scientists. In blasting, there are theoretical problems that are well understood; and some useful developments are provided to solve them (e.g. the problem of the concentrated blast in the ground (Lavrentev & Shabat, 1973, pp. 387-390)). Many other contributions to mathematical modeling of blasts were made during 1950'-1980'. A great deal of attention is paid to the statistics of post-blast fragments (Kutuzov

& Rubtsov, 1970; Kuznetsov, 1977), the theory of detonation (Persson, Holmberg, & Lee, 1993) and the behavior of stress waves in rocks (Field & Ladegaard-Pedersen, 1971; Shapurin & Eschenko, 1970). Some of these theoretical developments find their implementation in modern software (Maerz, Palangio, & Franklin, 1996; Franklin & Katsabanis, 1996) and statistical blast fragmentation models (Cunningham, 2005; Ouchterlony, 2005).

Unfortunately, neither mathematicians nor mining engineers are able to completely understand the physics of the blast fragmentation and movement of rocks. A full-scale blast involves many variables and aspects that are difficult to define and control due to the short time frame and randomness of blasting.

Attempts are made to model blasts using computer methods. Some simple 2-D models of blast movement are presented in Preece, Tidman, and Chung (1997) and Yang, Kavetsky, and McKenzie (1989). The common approach for modeling blast movement is discretizing the pre-blast mine bench into small elements (Tordoir, Weatherley, Onederra, & Bye, 2009; Preece, Tawadrous, Silling, & Wheeler, 2015) and then modeling the trajectory of each pre-blast particle during blasting. The 3-D modeling approach looks realistic but needs calibration with real data. A study shows that a method from Tordoir et al. (2009) may produce significant errors in the prediction of horizontal displacement of rocks (La Rosa & Thornton, 2011).

Cautious blasting, undoubtedly, is the best way to prevent rocks from significant displacement. The reader can find the information on the principles of cautious (or controlled) blasting in Konya and Walter (1991, pp. 176-193). Using this method may require precise blast initiation systems coupled with programmed electronic detonators (Lusk, Silva, & Eltschlager, 2013). The energy of a cautious blast is reduced and, therefore, fragmentation is decreased. This makes cautious blasting cost more than regular blasting.

Full control of blast movement is not possible. Some displacement of blasted material will occur. Cautious blasting should be combined with blast movement

measurement. A system for measuring blast movement consists of transmitters placed inside the pre-blast bench and a detecting equipment able to determine the coordinates of transmitters before and after blasting (La Rosa & Thornton, 2011; Thornton, 2009b). Software uses the coordinates of the transmitters for constructing blast movement models.

A 2-D method of translating the pre-blast dig limits onto post-blast muck-pile is presented in Firth and Taylor (2003). Magnetic targets are used to obtain the pre- and post-blast coordinates of the displacement vectors of rocks. A more advanced way to measure blast movement in 3-D has been developed by the Julius Kruttschnitt Mineral Research Centre (JKMRC). It is called Blast Movement Monitor system (BMM). Initially, it was developed for improving grade control but brought a significant amount of new knowledge about blasting in rocks in general (Thornton, 2009b). The system consists of transmitters, detecting equipment and software. A comprehensive research and new findings about the nature of blasting are provided in Thornton (2009b) and Thornton (2009a). More information on BMM is in Engmann, Ako, Bisiaux, Rogers, and Kanchibotla (2013) and Thornton et al. (2005).

BMM opens new prospects for grade control if the system is cheap enough for use on a regular basis. The software documented in Isaaks, Barr, and Handayani (n.d.) is able to work with pre- and post-blast topographies in 3-D. It discretizes pre- and post-blast topographic surfaces and assigns a unique trajectory for each pre-blast unit. The pre-blast units are then associated to corresponding post-blast units. It also accounts for the collisions between the pre-blast units during blasting.

The main problems with the blast measurement paradigm are the following:

- i) Limited amount of transmitters. If rocks change their position during blasting significantly, a large amount of data is needed to build post-blast models of grades. It is problematic to use sparse movement vectors for characterizing the entire geology of the mine bench. Increasing the amount of

transmitters leads to increasing the cost of measurement.

ii) The cost of measuring blast movement (transmitters, dedicated drill holes, additional manpower).

iii) Dig limits themselves bring a lot of errors to estimation (Chapters 6 and 7). Sparse blast movement vectors plus inherent errors of dig limits can lower the benefits from using blast movement measurements.

2.4 Ore and Waste Zone Delimitation

Grade control requires delimitation of ore/waste zones using dig limits. An example of dig limits is in Figure 2.3. It is very difficult to handle 3-D models with such simplistic polygons.

In grade control optimization, many researchers aim to optimize the algorithm of drawing the dig limits. The blast movement vectors (Isaaks, Barr, & Handayani, n.d.; Thornton et al., 2005; Engmann et al., 2013; La Rosa & Thornton, 2011) or mining equipment limitations with respect to maximum expected profit (Norrena & Deutsch, 2001; Norrena, 2007; Isaaks, Treloar, & Elenbaas, n.d.) serve as a basis for this optimization.

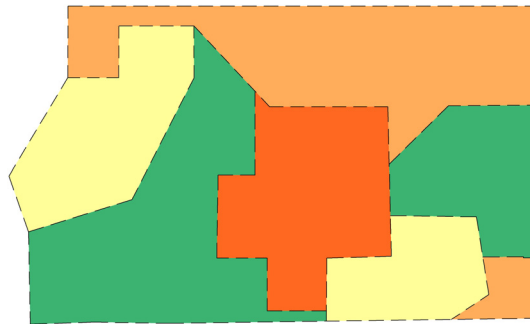


Figure 2.3: Typical dig limits (Rossi & Deutsch, 2014). This figure is not to scale, but is approximately 100 m in the Y direction.

Norrena (2007) offers a method to optimize dig limits accounting for the 'digability' of excavating equipment. Digability is the ability of the equipment to follow the dig limits. Norrena and Deutsch (2001, p. 45) demonstrate

a program to optimize the dig limits with respect to a digability factor and maximum expected profit. The simulated annealing algorithm (Kirkpatrick, Gelatt, & Vecchi, 1983) is used to maximize the total profit using an objective function.

In Wilde and Deutsch (2007a) and Wilde and Deutsch (2007b), the authors propose another optimization algorithm. The method is developed for grade control at the feasibility stage. It replaces the dig limits with a truck-by-truck (TBT) approach. A mine block is discretized by the units representing scoops of excavating equipment. Several scoops comprise a single truck load represented as a mining unit. The authors provide software for optimizing the sequence of the scoops. The authors also use the simulated annealing algorithm for optimizing the total profit.

One more research on optimizing the dig limit outlines minimizing expected loss and accounting for excavation constraints is presented in Isaaks, Treloar, and Elenbaas (n.d.). A program for the dig limits optimization is presented. It optimizes the excavation process using the simulated annealing procedure. The program is similar to the one in Norrena (2007) in terms of the iterative optimization of dig limits. The optimization in Isaaks, Treloar, and Elenbaas (n.d.) is constrained by minimum mining width.

A short discussion on the expediency of using the dig limits approach versus a truck-by-truck method is started in Vasylichuk and Deutsch (2015d). Then, this topic is further developed in Chapters 6 and 7 of this thesis.

Chapter 3

Optimal Grid Size for Estimation

3.1 Motivation

Local estimation of mineral resources could be performed at different grid sizes. The center of each block is called a node. The denser the grid of nodes the higher the resolution. Theoretically, the higher resolution the more information is available about the spatial distribution.

There is a limit after which increasing the resolution would not help resolve any spatial features. The model will not be worse, but using high resolution requires more computational time.

As mentioned in Chapter 2, there are no specific rules for choosing the optimal resolution. The sizes of blocks can correspond to selective mining unit (SMU) size or a fraction of the drillhole (DH) spacing.

The optimal estimation grid size is determined with respect to the sample spacing. Optimal is defined based on the most precise numerical model without excessive use of computer resources; it is not the result of an explicit optimization process. It could be replaced with the term 'reasonable grid size'. The estimation grid size/sample spacing ratio (GSS) is a reasonable parameter

for optimizing the estimation. GSS helps to obtain as much information as possible from geologic samples within a reasonable time.

3.2 Methodology

A numerical experiment is established to build the relationship between the estimation grid size and sample spacing (Vasylchuk & Deutsch, 2015c). Ordinary kriging is chosen as the estimation method. The setup of the experiment consists of the following main steps:

i) The construction of a reference distribution or the "truth". It is a single unconditional *sgsim* (Deutsch & Journel, 1998) realization on a unit 1×1 node grid.

ii) The reference distribution is sampled at 10×10 nodes grid. No information on sampling at less than 1/10th the data spacing is possible.

iii) Ordinary kriging (OK) is performed at different grid sizes in the range from 0.1 to 2 times the sample spacing.

iv) The estimates are regridded to 1×1 node resolution.

v) The effectiveness of estimation is measured through the amount of misclassification errors: either true ore classified as waste or true waste classified as ore. A cutoff grade is used to distinguish between ore and waste at each unsampled location (see Figure 3.1).

iv) The impact of different influencing factors on the quality of estimation is checked.

v) All results are averaged over 100 realizations with different geologic conditions to ensure their reliability.

vi) Final conclusions and recommendations are summarized.

Misclassification errors are also called Type 1 and Type 2 errors in statistical hypothesis testing. The reader can find information on hypothesis testing in Sheskin (2003). The null hypothesis: the unsampled location is ore. If an

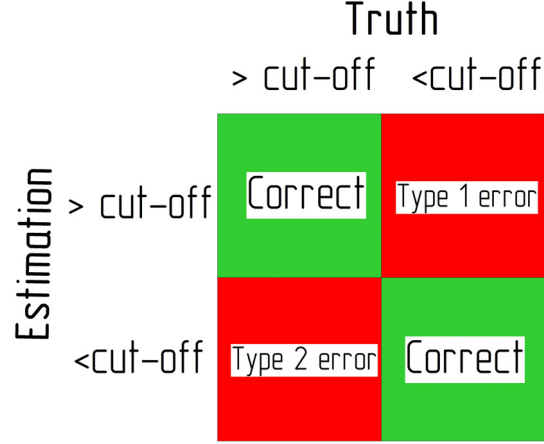


Figure 3.1: Misclassification errors

unsampled location is waste but estimated as ore, it is the Type 1 error (false positive). If the unsampled location is ore but estimated as waste, it is the Type 2 error (false negative). Another way of thinking is to consider two null hypothesis: i) the unsampled location is ore, ii) the unsampled location is waste. Hypotheses are the OK estimates. In this case, we have only the type 1 errors for both hypotheses. The hypotheses can only be falsely accepted. In either approach, the amount of falsely estimated locations is counted. The total amount of the misclassification errors is the summation of these two types of errors. The percentage of the misclassification errors (PME) is expressed as follows:

$$PME = \frac{Errors_{type1} + Errors_{type2}}{Number\ of\ nodes} \times 100\ \% \quad (3.1)$$

The influence of different parameters on PME is checked. These parameters include: i) the variogram range (from 10 to 100 nodes with step 10), ii) the nugget effect contribution (from 0 to 0.5 with step 0.1), iii) the type of the data distribution (normal or log-normal), iv) kriging block discretization (3×3, 4×4, 5×5). Only one influencing parameter changes at a time; others remain at their default values: i) the variogram is omni-directional with a range of 50 nodes, ii) the variogram model is spherical with one nested structure, iii)

the nugget effect contribution is 0.1, iv) the reference distribution of data is normal. The reference distribution is constructed in 2-D. Several Fortran codes are developed to perform the calculations and obtain the final results.

3.3 Experimental Results

PMEs are obtained for each influencing factor. As expected, PME increases with increasing the GSS ratio. PME-OK grid size relation shows a similar trend for all the influencing factors (Figure 3.2).

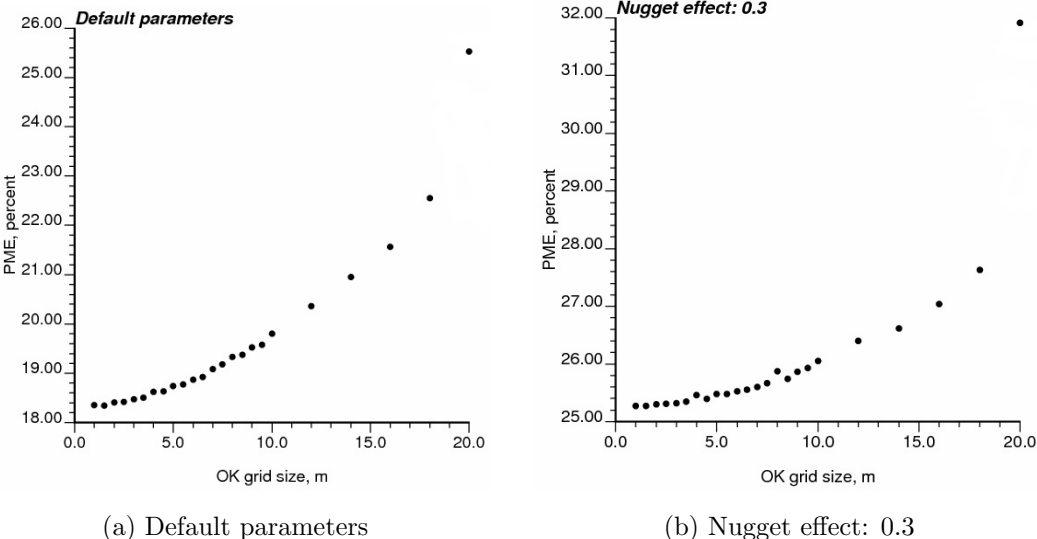


Figure 3.2: PME versus OK grid size for 2 set of parameters

In all cases, the amount of the misclassification errors starts from some initial PME value and then increases. In Figure 3.2, two graphs are increasing but with different minimum PMEs. In order to summarize all results, a general graph is developed to illustrate the relationship between the misclassification errors and the GSS ratio. The misclassification errors are expressed as increments from the initial PME (Vasylchuk & Deutsch, 2015c). The graph in Figure 3.3 is the summary of all the results obtained during the experiment.

The optimal kriging grid size is the one that ensures the best possible estimation with the least amount of misclassification errors (PME). The optimal kriging grid size expressed with respect to sample spacing (GSS ratio) ensures that the incremental error (Figure 3.3) is close to 0 percent (minimum PME).

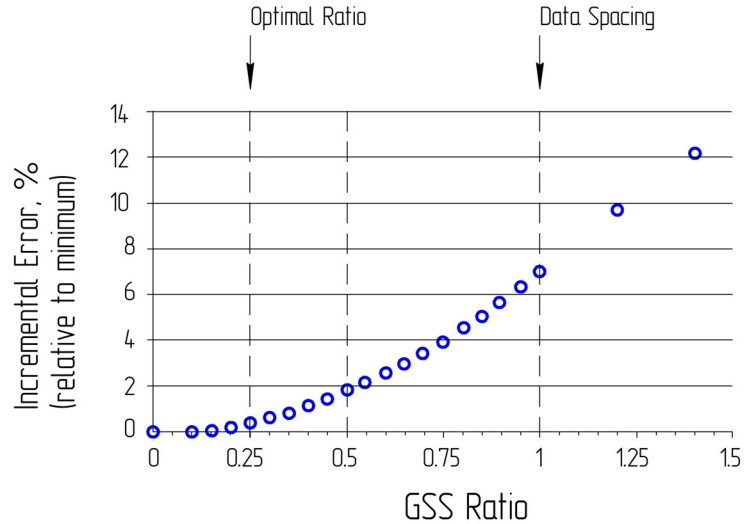


Figure 3.3: Experimental results for error with different grid size (Vasylchuk & Deutsch, 2015c)

The impact of the influencing factors on PME is expressed as the change in the average PME (over all the grid sizes):

- i) The average PME decreases more than twofold with increasing the variogram range from one sample spacing to 10.
- ii) The average PME increases twofold with increasing the nugget effect contribution from 0.1 to 0.5.
- iii) Using block discretization does not influence the average PME.
- iv) The average PME for log-normal data distribution is slightly higher than for the normally distributed data.

Practical recommendations for a better grade control and achieving the least possible PME are the following:

- i) The GSS ratio should be in the range from 0.25 to 0.40 (grid size is 25-40 percent of the sample spacing).

ii) The GSS ratio should not exceed 0.5. After this point the incremental error starts growing rapidly.

3.4 Limitations

The reference distributions are synthetic. Real reference distributions of grades were not available. Even though the real geology is rarely so ideal, the synthetic distributions are a good way to determine general trends.

There are a small number of the influencing factors. Many different experiment repetitions have been considered for different input parameters. Still, more influencing factors may be added and the final conclusions can be refined.

Despite the limitations, the recommendations made here address the problem of a reasonable grid size in a practical manner. An example using real data is described in Chapter 7.

Chapter 4

Simulation versus Estimation

4.1 The Concept of Utility in Grade Control

Grade control requires predictions of all grade variables that influence the economic consequences of the grade control decisions. The number of sampled locations is always limited and there is some uncertainty in the grade predictions.

Estimation methods have evolved during the last decades. Mining engineers and geologists used to employ the simplest approaches such as nearest neighbor (NN) or the method of averaging grade within polygons. Kriging was formulated to account for correlations between data and provide the best possible estimates (SK or OK). Kriging and the inverse distance (ID) methods make the predictions using a weighted average of the available data. They provide smoother estimates and are good for revealing geologic trends (Rossi & Deutsch, 2014). Because of this smoothness, Kriging and ID estimates are not always suitable for the determination of geological resources. These methods for the characterization of deposits are deterministic because they produce a single estimate for each unsampled location. They do not directly quantify uncertainty.

A common practice at mines is to estimate the variables of interest sep-

arately using kriging (Teck Cominco Alaska Inc., 2009; Dimitrakopoulos & Godoy, 2014; Verly, 2005). Then, these estimates undergo some post-processing for defining the destinations for mined material. These deterministic methods become less effective when the decision is dependent on the non-linear recovery functions; especially, when several variables are involved. All the variables must be considered together with their variability to ensure the optimal economic decision. Cokriging might be used for modeling several variables at once. Unfortunately, cokriging estimates are also deterministic.

If a grade control decision is wrong, there is some particular loss; if it is correct, there is a profit. It is difficult to check if the estimates were right or wrong after the blasted rocks are excavated. The effectiveness of quality control can be measured only on a larger scale when the production reports are summarized. The purpose of grade control is to maximize profit or minimize loss.

Utility functions could be used to express the profit a company obtains from mining ore. In the simplest case, a utility function would be expressed as follows:

$$Utility(\mathbf{u}) = z(\mathbf{u}) \times r(z(\mathbf{u})) \times price - c_m(\mathbf{u}) - c_p(\mathbf{u}) \quad (4.1)$$

where \mathbf{u} is the location; $Utility(\mathbf{u})$ is the profit or loss value at a location \mathbf{u} ; $z(\mathbf{u})$ is the grade at the location \mathbf{u} ; $r(z(\mathbf{u}))$ is the recovery at the location \mathbf{u} ; $price$ is the value of one unit of the final product; $c_m(\mathbf{u})$ and $c_p(\mathbf{u})$ are the costs of mining and processing ore respectively.

The utility function can be depicted as a line (see Figure 4.1) or some more complex function in other circumstances. In this case the utility is determined by the equation of this line ($f(x) = kx + b$).

When several variables are considered, the total utility at a location comprises the utilities of multiple components. They can be positive or negative (penalties) depending on their roles in the recovery process. The total utility

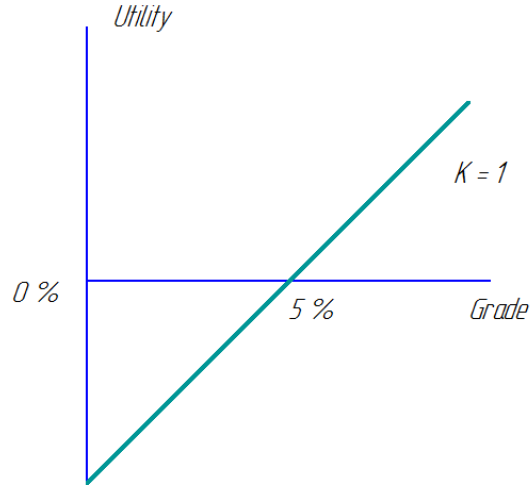


Figure 4.1: A simple utility function

at a location may be expressed as follows:

$$Total\ utility(\mathbf{u}) = U_1(\mathbf{u}) + U_2(\mathbf{u}) + U_3(\mathbf{u}) - P_1(\mathbf{u}) \quad (4.2)$$

where *Total utility* (\mathbf{u}) is the profit or loss obtained at the location \mathbf{u} ; $U_{1-3}(\mathbf{u})$ are some three utility functions; $P_1(\mathbf{u})$ is a penalty function. The variables may interact with each other, that is, a combination of two variables could lead to more penalty.

The above Equations 4.1 and 4.2 express the profit (if the total utility is positive) or the loss (if the total utility is negative) for each location. The grade control procedure should choose the decision dependent on the maximum utility. The total utility can be optimized by using conditional simulation.

4.2 Decision Making Using Uncertainty

The main characteristics and features of grade control decision making by means of simulation are the following:

- i) Simulation reproduces uncertainty, histograms, variograms and multivariate relationships.

- ii) A single realization cannot be used for decision making.
- iii) The decision should be based on multiple realizations and the profit/penalty function optimization.
- iv) The decision should be based either on the maximum profit or minimum loss.
- v) Simulation uses multiple realizations and is able to incorporate multiple variables to account for uncertainty in profit.

Loss functions are another way to illustrate the consequences of grade control decisions (Isaaks, 1991). They represent the penalties associated with the grade control decisions. The simplest types of loss functions are the quadratic and absolute penalty to error. As both these loss functions are symmetric, the decision is penalized equally for both underestimation and overestimation. In reality, the underestimation and overestimation decisions incur different losses. Some simple asymmetric linear loss functions are shown in Figure 4.2.

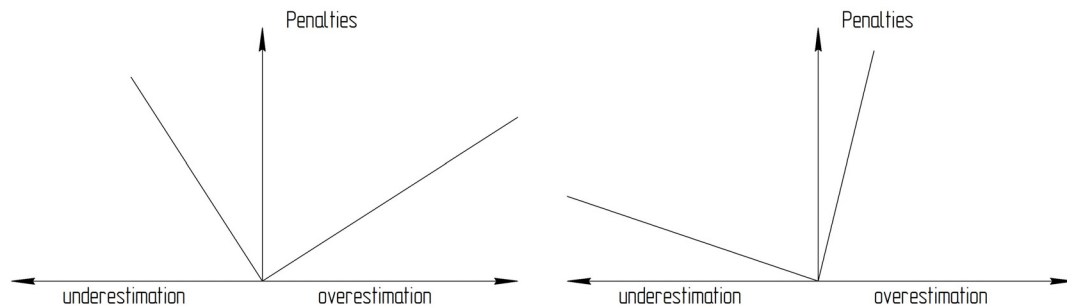


Figure 4.2: Asymmetric loss functions

Loss functions can be treated for any number of possible decisions. In the case of many decisions, the loss functions are similar to the ones in Figure 4.2. There is any number of possible decisions. The x axis can be discretized at any step, and the consequences of each decision can be calculated. The discretization of the axis x is illustrated in Figure 4.3. Each blue tick is a probable decision. All the ticks comprise the range of possible decisions.

There are a number of existing maximum profit/minimum grade control methods based on conditional simulation. All the methods are using the same

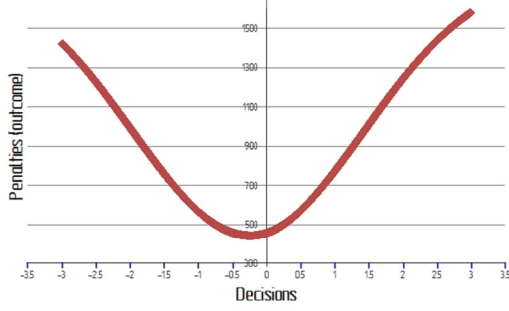


Figure 4.3: Range of possible decisions

principle of optimizing the grade control decisions. A short outline is provided in Chapter 2. The method used in this thesis is based on the minimum loss and similar to the one developed by Isaaks (1991); but the way to assign penalties is different. It uses coefficients for the risk aversion and lost opportunity cost similar to the method developed by Glacken (1996). The coefficients are always non-zero and dependent on the shape of the loss function.

The original minimum loss method expressed by Isaaks (1991) in mathematical notation.

The loss function for the ore decision:

$$g(z) = \begin{cases} -c_m - (prz - c_m - c_p), & z \leq z_c; \\ (prz - c_m - c_p) - (prz - c_m - c_p), & z > z_c; \end{cases} \quad (4.3)$$

where $g(z)$ is a loss function; c_m is the cost of mining for ore and waste; c_p is the cost of processing metal; p is the price of metal; r is the metal recovery; z is the grade of metal; z_c is the cutoff grade, $z_c = c_p/pr$.

The expectation of the loss under the ore decision is expressed as follows:

$$Loss|ore = E[g(Z)] = E[i(Z, z_c) \times (-prZ + c_p)] \quad (4.4)$$

where Z is a random variable; $i(z, z_c)$ is 0 if the estimate is ore and 1 if the estimate is waste.

The loss function for the waste decision:

$$g(z) = \begin{cases} (-c_m) - (-c_m), & z \leq z_c; \\ (prz - c_m - c_p) - (-c_m), & z > z_c; \end{cases} \quad (4.5)$$

The expectation of the loss under the waste decision is expressed as follows:

$$Loss|waste = E[g(Z)] = E[(1 - i(Z, z_c)) \times (prZ - c_p)] \quad (4.6)$$

The decision is penalized only if it is incorrect. There is no profit or loss, if the decision is correct.

Simulation provides any number of equiprobable realizations that could be considered as possible truth values. The decision bringing the least of loss on average is chosen. In the case of the quadratic loss function, the optimal decision is the mean of all the simulation values. For the asymmetric loss functions, the optimal decision will be shifted depending on the asymmetry.

Two cases are considered in this thesis: ore and waste. There is no a fundamental difference in the methodology if more than two destinations are considered. The optimal grade control decision brings a minimum amount of penalties. In mathematical notation, the two decisions case is expressed below.

The loss function for the ore decision:

$$g(z) = \begin{cases} (z_c - z) \times b_2, & z \leq z_c; \\ 0, & z > z_c; \end{cases} \quad (4.7)$$

where b_2 is the penalty coefficient for overestimation decisions.

The expectation of the loss under the ore decision is expressed as follows:

$$Loss|ore = E[g(Z)] = E[i(Z, z_c) \times (z_c - Z) \times b_2] \quad (4.8)$$

The loss function for the waste decision:

$$g(z) = \begin{cases} 0, & z \leq z_c; \\ (z - z_c) \times b_1, & z > z_c; \end{cases} \quad (4.9)$$

where b_1 is the penalty coefficient for underestimation decisions.

The expectation of the loss under the waste decision is expressed as follows:

$$Loss|waste = E[g(Z)] = E[(1 - i(Z, z_c)) \times (Z - z_c) \times b_1] \quad (4.10)$$

The cutoff grade splits the two decisions and determines the amount of penalties. The cutoff loss function for the two grade control decisions case is illustrated in Figure 4.4.

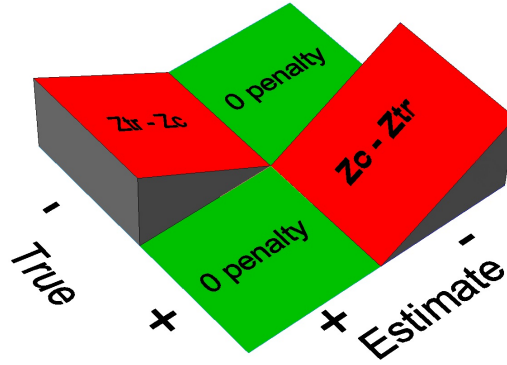


Figure 4.4: Two grade control decisions case loss function

The extension to the many decision case is performed in a similar fashion: the expected loss is calculated in all cases and the decision with the least loss is chosen.

4.3 Profitability of Estimation Versus Simulation

A numerical experiment is conducted to assess the effectiveness of estimation versus simulation in grade control. The experiment consists of 2 basic cases: many grade control decisions case and two grade control decisions case. Similar to previous numerical experiment, a synthetic reference distribution is built, sampled and then estimated. The reference distribution (or the truth) is a single unconditional realization. The parameters of the reference distribution are the following: i) the resolution is 1×1 nodes, ii) the variogram is omni-directional with a range of 12 nodes, iii) the variogram model is spherical with one nested structure, iv) the nugget effect contribution is 0.1. The truth distribution is constructed in 2-D. The experiment is repeated for normal and log-normal distributions of reference data. In order to decrease the computational time, the size of the theoretical mine bench is chosen smaller than the one in Chapter 3. It does not influence the results of the experiment as all the parameters for simulation and estimation are reduced as well.

The main steps of the experiment:

- i) Simulate 2500 nodes of the truth distribution on 1×1 nodes grid.
- ii) Sample the truth on 5×5 nodes grid.
- iii) Construct estimates with ID, NN, SK, OK, and simulation (SIM) on 3×3 nodes grid.
- iv) Re-grid the estimates to 1×1 nodes resolution.
- v) Compare the truth value and the estimate values at each node.
- vi) Repeat the above procedure 100 times for the stability in the results.
- vii) Repeat all the previous steps for two basic cases.
- viii) Repeat all the above steps with the normal and log-normal distributions of the truth
- ix) Check a series of different loss functions.

x) Summarize results.

The results of the experiment are presented in Tables 4.1-4.4 and Figure 4.5. The tables contain the losses for each estimation method and simulation. The numbers under the 'Loss function' headers define the shape of loss functions. For example, '30-30' means that it is a symmetric absolute loss function with the angles of inclination equal to 30 degrees for both underestimation and overestimation sides. '50-30' is an asymmetric linear loss function with the angle of inclination for the underestimation part equal to 50 degrees, and the angle of inclination for the overestimation part equal to 30 degrees.

In the tables, there are also total losses for all the methods under each loss function. These losses are obtained after comparison with the true value and an estimate at each node. The penalty is zero if the decision is correct; the penalty depends on the magnitude of the error if the decision is incorrect.

Summary Tables 4.1-4.4 are below. A paper on the research is in Vasylchuk and Deutsch (2015a).

Table 4.1: Effectiveness of ore/waste selection for the case with many grade control decisions and normal distribution of data (Vasylchuk & Deutsch, 2015a)

Methods	Loss functions											Average
	80-30	70-30	60-30	50-30	40-30	30-30	30-40	30-50	30-60	30-70	30-80	
NN	5335.5	2849.6	1983.5	1522.2	1220.9	997.2	1225.4	1532.8	2003.4	2886.8	5422.6	2452.7
ID	4469.2	2389.2	1664.7	1278.7	1026.6	839.4	1032.6	1292.8	1691.3	2439.3	4586.4	2064.5
OK	4405.6	2354.6	1640.1	1259.4	1010.8	826.3	1016.1	1271.9	1663.4	2398.5	4508.4	2032.3
SK	4348.4	2321.6	1615.6	1239.5	993.8	811.4	996.7	1246.4	1628.5	2346.0	4405.4	1995.8
SIM	1871.7	1528.6	1309.4	1133.7	975.8	816.0	974.4	1131.7	1307.6	1526.0	1869.4	1313.1

Table 4.2: Effectiveness of ore/waste selection for the case with many grade control decisions and and log-normal distribution of data (Vasylchuk & Deutsch, 2015a)

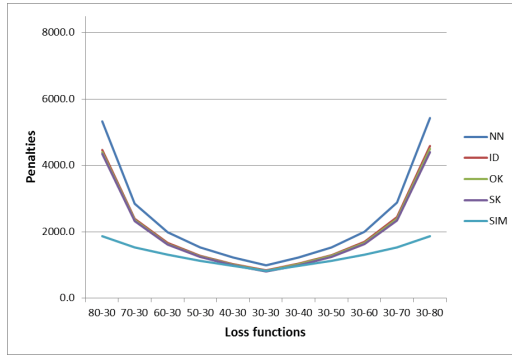
Methods	Loss functions											Average
	80-30	70-30	60-30	50-30	40-30	30-30	30-40	30-50	30-60	30-70	30-80	
NN	4435.9	2369.0	1649.0	1265.4	1014.9	828.9	1018.6	1274.0	1665.1	2399.3	4506.7	2038.8
ID	3832.9	2048.3	1426.5	1095.4	879.0	718.4	883.4	1105.6	1445.9	2084.6	3917.9	1767.1
OK	3800.9	2030.8	1414.1	1085.6	871.1	711.8	875.1	1095.0	1431.7	2063.8	3878.2	1750.7
SK	3764.0	1932.1	1396.3	1070.4	857.6	699.6	858.6	1072.7	1400.6	2016.2	3783.1	1713.8
SIM	2344.9	1669.7	1371.5	1060.7	856.3	670.0	750.3	821.3	893.6	973.7	1077.6	1135.4

Table 4.3: Effectiveness of ore/waste selection for the case with two grade control decisions and normal distribution of data (Vasylchuk & Deutsch, 2015a)

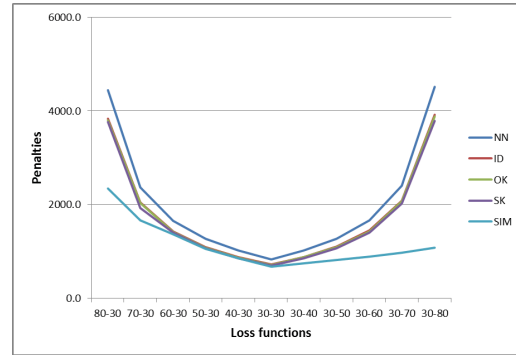
Methods	Loss functions											Average
	80-30	70-30	60-30	50-30	40-30	30-30	30-40	30-50	30-60	30-70	30-80	
NN	1199.3	641.6	447.3	343.7	276.1	229.1	278.1	348.4	456.1	658.2	1238.2	556.0
ID	949.3	509.9	356.9	275.4	222.1	182.6	225.8	283.9	373.0	540.3	1020.3	449.0
OK	920.0	493.1	344.4	265.1	213.4	175.0	215.8	270.9	355.1	513.3	967.4	430.3
SK	895.9	479.8	334.9	257.6	207.2	169.8	209.3	262.4	343.9	496.8	935.6	417.6
SIM	365.6	308.0	269.4	236.6	205.5	172.0	205.5	238.5	275.6	319.0	390.4	271.5

Table 4.4: Effectiveness of ore/waste selection for the case with two grade control decisions and log-normal distribution of data (Vasylchuk & Deutsch, 2015a)

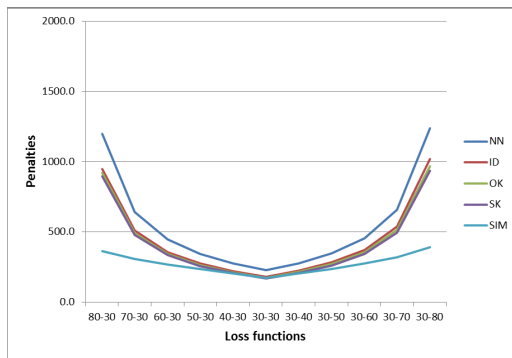
Methods	Loss functions											Average
	80-30	70-30	60-30	50-30	40-30	30-30	30-40	30-50	30-60	30-70	30-80	
NN	1217.5	625.6	419.4	309.6	237.8	184.6	215.0	255.9	318.6	436.2	773.8	454.0
ID	851.9	449.8	309.7	235.1	186.4	150.2	182.0	225.0	290.7	414.0	768.1	369.3
OK	835.4	440.5	303.0	229.7	181.8	146.3	177.0	218.5	281.9	401.0	742.8	359.8
SK	828.0	435.0	298.1	225.2	177.6	142.2	171.3	210.5	270.4	383.0	706.2	349.8
SIM	311.7	261.5	225.9	194.7	168.0	139.6	167.1	195.6	223.8	264.5	319.5	224.7



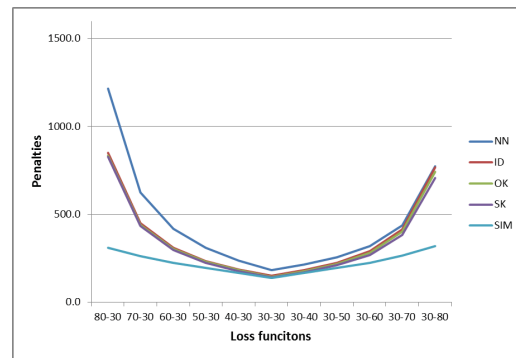
(a) Many grade control decisions (normal distribution)



(b) Many grade control decisions (log-normal distribution)



(c) Two grade control decisions (normal distribution)



(d) Two grade control decisions (log-normal distribution)

Figure 4.5: Penalties for estimation and simulation (Vasylichuk & Deutsch, 2015a)

A graphical representation of the information contained in Tables 4.1-4.4 is in Figure 4.5. It is seen from the graphs that simulation incurs the least amount of penalties on average and for every particular loss function. It is observed in all four cases. The shapes of the graph lines also show that the effectiveness of simulation increases when the overestimation and underestimation errors are penalized asymmetrically.

4.4 Limitations and Recommendations

The experiment is synthetic and, therefore, the results show an ideal case. Nevertheless, the conditions of a real life grade control process are preserved.

The goal is to define the most profitable way for ore/waste classification.

Grade control is performed only for one variable in the example. As a result, the loss functions are simplistic. Usually, grade control involves more variables. In this case, the loss functions would be more complex. However, involving more variables will, most likely, make the difference between simulation and the deterministic methods even bigger.

Conclusions:

i) Simulation incurs the least penalty/loss in all the cases presented in the experiment.

ii) Nearest neighborhood and inverse distance methods showed the worst results in many cases and may be considered as the least suitable methods for the short-term grade control.

iii) Simple and ordinary kriging showed very similar results and are the best deterministic methods for the short-term grade control.

iv) The more asymmetric the loss functions become, the more difference between deterministic estimation and simulation. The author assumes that the more complex loss function is, the more unsuitable deterministic estimation becomes for grade control.

v) The difference between simulation and deterministic estimation is slightly higher for log-normal distribution of grades, which is more realistic. It may indicate that simulation can be even more beneficial for real life grade control.

v) All mining sites have their unique geology. Mining companies may use different approaches for treating ore and obtaining the final product. Author recommends using simulation, which is proven to be the most flexible method able to address any unique mining and economic conditions.

vi) A lack of robustness of simulation highlighted in this chapter appeared to be not a big problem. Simulation outperformed deterministic practically in all the cases. Theoretically, grade control decisions can be even more improved using more simulation realizations. This, however, requires more computational

time.

Simulation is expected to work in circumstances that are completely stationary, multi-Gaussian and with the exact correct input histogram and variogram. In the situations where this is not true, ordinary kriging might perform slightly better than simulation and simple kriging.

More research should help to establish guidelines for using simulation for different applications and different mining conditions. Currently, it is believed that it is worth additional effort to set up simulation for the situations with asymmetric penalizing underestimation and overestimation errors. Simulation is also beneficial for modeling multivariate relationships between many variables involved in the technological process, especially when these relationships are complex.

Chapter 5

Background of the Blast Movement Problem

Before excavation, rocks should be fragmented by drilling and blasting. Blastholes are made throughout the mine bench and filled with explosive. Blastholes (BH) are situated on a rectangular or staggered pattern to evenly distribute the energy of explosive inside the bench volume. Plan views of rectangular and staggered drilling patterns are in Figure 5.1. The BH are usually bored slightly below the elevation of bench bottom (subdrill) to ensure fragmentation in the lower part of the bench. The upper portion of the BH is filled up with inert material (stemming) to prevent fly rock.

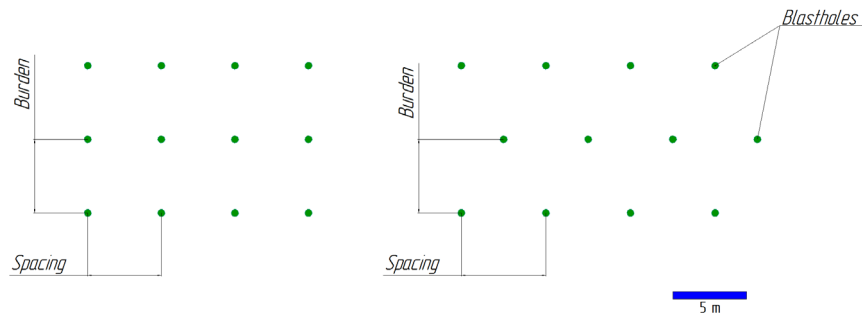


Figure 5.1: A schematic illustration of rectangular (left) and staggered (right) drilling patterns

The column of charge is usually initiated at the bottom of BH by a primer.

The primer can be a dynamite cartridge or packaged emulsion explosive. Bottom initiation is used to allow detonation uninterruptedly going along the column of charge. Detonation causes an instantaneous chemical reaction in the explosive. It follows the front of detonation releasing heat and detonation gases. The detonation gases create a shock pressure on the walls of the BH. This initial impulse creates a zone of plastic deformation. The energy of the shock wave decreases going through the rock mass and turns into a stress wave traveling with the velocity of sound for the particular medium. The velocity of detonation for emulsion explosives is usually from 3500 to 6000 m/s. The higher the velocity of detonation the faster the gases are released and, consequently, the higher the impact on the walls of BH. This initial impulse also creates cracks going radially from BH. After the stress wave has reached a free face, it is reflected from it as a tensile wave. The tensile strength of rocks is much lower than the compression strength. Therefore, the rocks are deemed to be destroyed mostly by the reflected waves. Blasting movement of rocks is performed by the gases going inside the radial cracks and expanding them (Figure 5.2). More information on detonation theory, the stress and reflected waves created by blasting in rocks can be found in Persson et al. (1993, pp. 87-143) and Field and Ladegaard-Pedersen (1971).

The free face of the mine bench can be any surface which is not confined by intact or previously blasted rocks. The blasted rocks move in the direction of the nearest free surface after the blast initiation. For example, if a mine bench is completely confined from all the sides, the rocks tend to move upward. If the blasted rocks are layered or split by principal systems of faults, the surfaces of the layers can also serve as free faces (Shapurin & Eschenko, 1970).

Mutual behavior of stress and reflected waves in rocks can be more complex if there are multiple free faces, rock types, and the systems of faults.

Blasting at mines is performed using short-time delays between blastholes. The sequencing of blasts significantly impacts blast movement. Usually, blasted

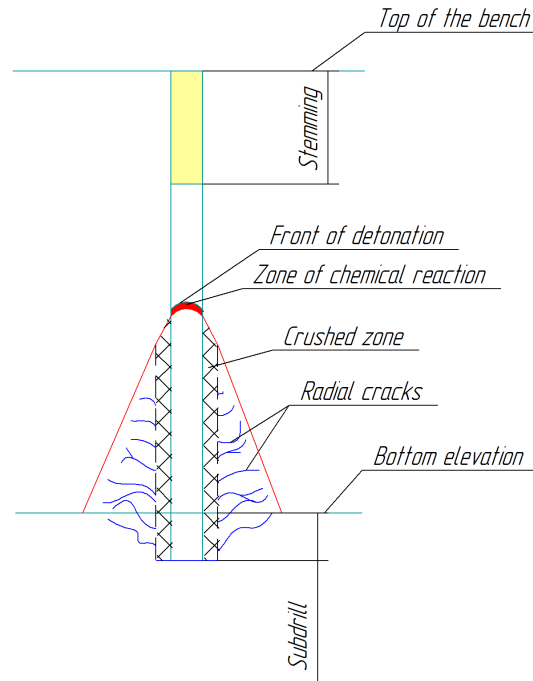


Figure 5.2: A schematic illustration of the detonation wave passing through the column of charge. Image is adapted from Bender (1999, p. 6)

rocks move in the direction perpendicular to timing contours if there is no free face close to blastholes (Thornton, 2009a).

Geology, topographic surfaces, fracturing, sequencing of firing, properties of explosive, powder factor, drilling pattern, and the design of BH, among other aspects, should be taken into consideration to theoretically model the blast movement of grades.

5.1 Accounting for Blast Movement in Grade Control

The primary concern of grade control is to reduce dilution and ore losses. Accounting for blast movement in turn is an important part of grade control.

The simplest approach to excavate blasted rocks selectively involves using different visual methods (markers) for defining the direction of blast move-

ment. Usually, it requires using additional drillholes. The markers are placed inside the drillholes and their coordinates are surveyed before and after blasting (Taylor, 1995). After dig limits are defined, colored tape and stakes with flags are often used to delimit ore/waste zones on the muckpile surface.

There were several attempts to theoretically model the blast heave and the shape of the post-blast muckpile. A 2-D kinematic model is proposed to model the muckpile formation in Yang et al. (1989). Due to simplicity, the model is easy calibrated to field data. A semi-empirical model for blast movement calculation is in Leite et al. (2014). Some solutions for modeling the 2-D and 3-D motion of rocks are proposed in Preece et al. (1997) and Tordoir et al. (2009). The Distinct Motion Code (DMC) from Preece et al. (1997) is further developed by the authors and now allows processing millions of discrete particles to model dilution in 3-D (Preece et al., 2015).

Another modern way to decrease dilution and ore losses is measuring blast movement directly. Blast Movement Monitors (BMM) are described in Chapter 2. Reportedly, the BMM system provides a precise and cost-effective way to measure blast-induced displacement of grades (Yennamani, 2010). The system uses disposable transmitters, which are put into dedicated blastholes. That is, special drillholes should be drilled to certain depths (Yennamani, Aguirre, & Mousset-Jones, 2011) to measure the blast movement of rocks at different elevations. The accuracy of BMM's measurements is from 0.1 to 0.2 m and dependent on the depth of a transmitter. Some BMM transmitters are not found during reading their post-blast coordinates due to damage or a significant depth (Yennamani et al., 2011). BMM systems have been used in multiple case studies (Yennamani, 2010; Thornton et al., 2005; Engmann et al., 2013; Fitzgerald, York, Cooke, & Thornton, 2011) and provide new knowledge on the processes occurring during blasting. A summary of these findings is given below (Thornton, 2009a):

- i) During a free-faced blast, the lower part of mine bench moves more than

the upper part. The horizontal displacement is commonly from 5 to 15 m (La Rosa & Thornton, 2011; Thornton, 2009a). A free face during blast follows a classical D-shape outline. Therefore, using visual markers close to the surface of pre-blast mine bench does not show the actual movement. In the case of confined blasting, the blasted rocks move preferentially upward.

ii) Post-blast swell is uniform for the entire muckpile.

iii) Blast movement is almost perpendicular to timing contours. In Figure 5.3, the theoretical movement of rocks is shown by blue arrows.

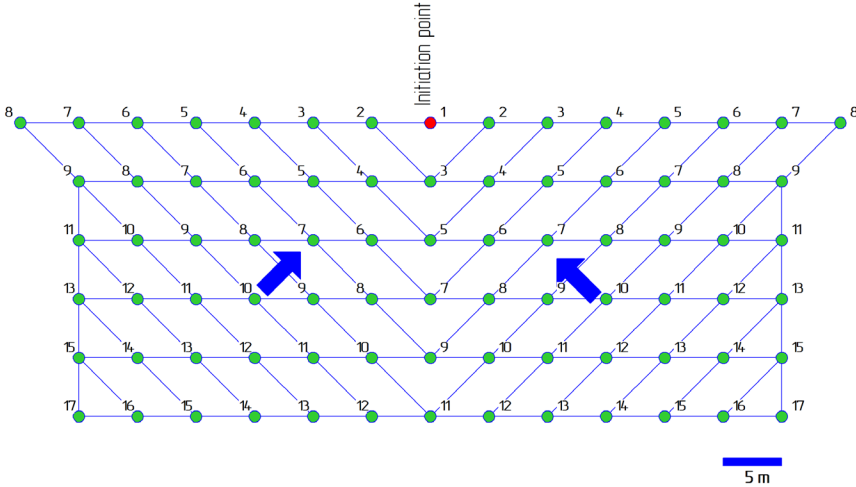


Figure 5.3: A schematic movement of rocks for the V-cut firing sequence. Image is adapted from Konya and Walter (1991, p. 160)

iv) The blast movement of rocks along the timing centerline is chaotic. Therefore, echelon blasting is preferable for grade control.

v) The mine bench height does not have a significant influence on the horizontal displacement.

vi) The back of mine bench is a special case for blasting. The rocks on the top of mine bench do not move forward but instead fall down into the void left after the top and middle level rocks moved forward. A so called 'power trough' is formed.

5.2 Common Problems for Blast Movement Measurement

Ore and waste zones are delimited manually or by computer means based on grades from blasthole samples before the blast. The pre-blast dig limit lines are then modified onto the post-blast 3-D geometry.

The current blast movement measurement approach has two main drawbacks related to grade control:

i) There is a limited amount of transmitters and, therefore, the data on the new positions of grades. For example, only six transmitters were used for the blast movement measurements in Yennamani et al. (2011) during one of a series of blasts. It may provide enough data to change positions and shape of the pre-blast dig limits, but more samples may be required to model the entire post-blast geology of mine bench. The issues related to the dig limits grade control paradigm are discussed in Chapters 6 and 7.

ii) It is not clear how the sparse blast movement vectors are used to address a diverse topography of the post-blast muckpile, that is, the post-blast geometry. It is difficult to match the pre- and post-blast topographies of the mine bench, even if the blast movement vectors are known. Drawing the dig limit lines at some complex muckpile surface may be challenging.

These two issues above are addressed in Isaaks, Barr, and Handayani (n.d.). The program presented there uses pre- and post-blast topographic surfaces for creating 3-D models of the mine bench before and after blasting. Both models are discretized at high resolution. The post-blast grid size is obtained by multiplying the cubed root of the swell factor to the pre-blast grid size. Data obtained from the BMM system are used to calculate the vectors of displacement for each single block of the pre-blast model. A series of BMM measurements provide means and standard deviations of horizontal displacements for different heights of the mine bench. Then, the horizontal displacement for each

pre-blast unit is randomly drawn from an appropriate normal distribution of horizontal displacements. The directions of blast movement vectors for each unit of the pre-blast model are calculated perpendicular to timing contours. Thus, each block of the pre-blast model obtains a unique movement vector and the distance of displacement. Having all the displacement vectors, it becomes possible to account for the collisions of particles and internal dilution.

The displacement data are used to find new locations of each pre-blast block and, consequently, re-define initial dig limits.

5.3 Calculating Approximate Blast Movement

This thesis provides another solution to the blast movement problem in grade control. The approach utilizes a principle similar to Isaaks, Barr, and Handayani (n.d.) in terms of using pre- and post-blast topographies for the construction of pre- and post-blast 3-D models. As practice shows, direct theoretical modeling of blasts is a complex task. Nevertheless, a reliable grade control practice requires accounting for blast movement. Some reliable input data should be used to find probable post-blast positions of grades.

Unfortunately, the behavior of blasted rocks may be different even in presumably similar conditions due to physical properties of rocks, fracturing, shapes and numbers of free faces, among other aspects. Blasting engineers do not have a full knowledge of the deposit or the technological parameters and performance of blast initiating systems. For example, there are always errors in the delays of non-electric blast initiating systems (Lusk et al., 2013).

The most reliable source of information for blast movement assessment is topography. Pre- and post-blast topographic surfaces are usually stored as digital elevation models. Therefore, the shapes and volumes of pre- and post-blast 3-D models are known. The challenge is defining how pre-blast blocks with assigned grades should be mapped into the post-blast geometry. The shapes of

the 3-D models can be very different and the mapping should be performed in 3-D space.

A program for predicting blast movement (*bmov*) has been developed using a simple principle (Vasylchuk & Deutsch, 2015b): the more a unit of the pre-blast model of mine bench is confined before blasting, the more it will be confined afterwards. The pre- and post-blast topographies may be discretized at any resolution. Having a bottom bench elevation, it is straightforward to obtain discretized pre- and post-blast 3-D models of a mine bench.

Blocks of the pre-blast 3-D model are associated with blocks of the post-blast 3-D model using their relative positions inside the models. The relative position (position index) of a block inside the 3-D model is defined as the summation of distances from the center of this block to the edges of the model in three orthogonal directions. These distances are calculated in the North (y), East (x), and vertical (z) directions for each particular block at a location \mathbf{u} within the 3-D model. The spacial orientations of the pre- and post-blast 3-D models should be aligned with one of the three main orthogonal directions. As the boundaries of the pre- and post-blast 3-D models are defined by the pre- and post-blast polygons and topographic surfaces submitted by the user, we always know where the edges of each model are in any direction. For example, the vertical distance for some block of the pre-blast model is calculated as the difference between the elevation of this particular block at the location \mathbf{u} and the surface elevation. The same procedure is done for the two of remaining directions, as we know the coordinates of each block in the North and East directions and coordinates of the edges of the models in these directions as well. The position indices of all the the blocks of the pre-and post-blast 3-D models are calculated according to the expression below:

$$Position\ index\ (\mathbf{u}) = Dist_x(\mathbf{u}) + Dist_y(\mathbf{u}) + Dist_z(\mathbf{u}) \quad (5.1)$$

where $Dist_x(\mathbf{u})$, $Dist_y(\mathbf{u})$, $Dist_z(\mathbf{u})$ are the distances to the edges in the three orthogonal directions at each particular location \mathbf{u} of the pre- and post-blast 3-D models.

The principle of mapping the pre-blast grades onto the post-blast muckpile is illustrated in Figure 5.4. The grades assigned to the pre-blast blocks are translated to the post-blast blocks with respect to their position index values. The pre- and post-blast models should be aligned along the x or y coordinate and with the burden and spacing in the horizontal plane. The first point, for which the distances to the edges of the models are calculated, is indicated in Figure 5.4. It is the lower left corner of the 3-D model. For this particular point in this particular model, the distances in the North, East, and vertical directions are the largest. It is obvious that the block at the starting point is situated at the maximum possible distance from the the edges of the model in any of the three directions. The distances to the edges for each subsequent block are calculated as their coordinates are read by the program according to the GSLIB conventions.

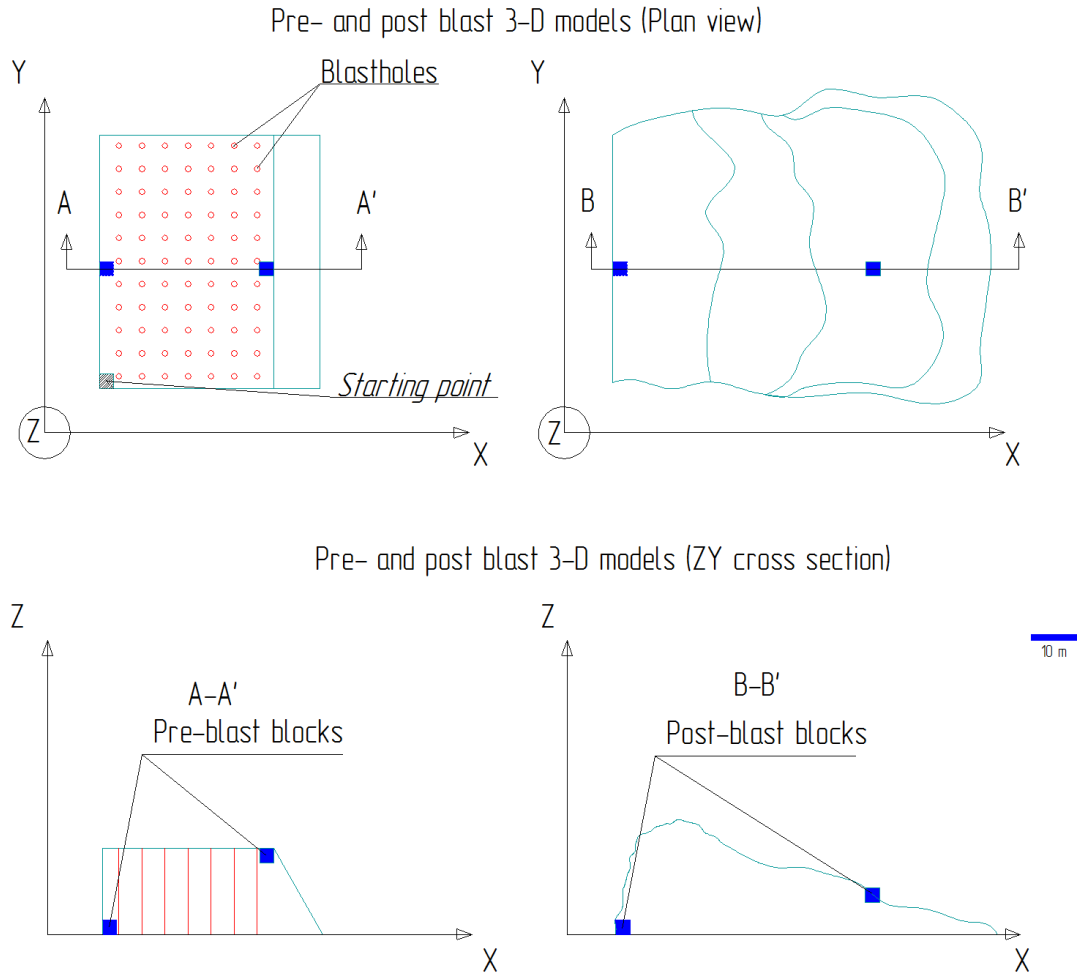


Figure 5.4: A schematic illustration of the mapping principle of *bmov*

The input data for *bmov* include:

- i) Pre- and post-blast topographic surfaces. An example is in Appendix 1.
- ii) Pre- and post-blast polygons outlining the pre-blast mine bench and the post-blast muckpile respectively. The polygons should also be stored in ASCII-format text files. The files should only contain the coordinates of the vertices. The first vertex should be repeated as the last vertex in order to 'close' the polygon.
- iii) Bottom bench elevation for creating 3-D models should be defined by user. It should be 1 m less than the lowest elevation coordinate value in the pre-blast topographic file.

v) Discretization constant (the grid size of topographic surfaces).

vi) A matching number to fit the pre- and post blast models (this parameter is explained below).

The reader can refer to Appendix 1 for an example of the parameter file to *bmov*.

The main steps of the *bmov* program are the following (Vasylichuk & Deutsch, 2015b):

i) Create pre- and post-blast 3-D models of rock that was blasted. Topographic surfaces of pre- and post-blast areas are used to create the models. The resultant models are discretized at a user defined grid size.

ii) Create pre- and post-blast 3-D bench models. The program automatically crops the topographic surfaces using the pre- and post-blast polygons. The models represent the mine bench before and after blasting. The grid size is the same as for the 3-D area models.

iii) Change the pre-blast grid to match the post-blast geometry and volume. The directions of displacement of grades are automatically determined. Resultant post-blast 3-D models have volumes defined solely by the post-blast topographic surfaces and polygons. The model's grid size is increased in each direction based on displacement. The grid size of the post-blast 3-D model could be decreased as well. For example, the elevation of a post-blast muckpile can be lower than the elevation of a pre-blast mine bench model due to a significant spread of rocks during blasting. It uses the ratios between pre- and post-blast dimensions for defining the post-blast grid. For example, a pre-blast width of a mine bench is 50 meters, length 70 meters, and height 15 meters, initial grid sizes for both models are 1 m. After blasting, a post-blast maximum width of the muckpile is 65 meters, maximum length 70 meters and maximum height 17 meters. The ratio between pre- and post-blast widths is $65/50 = 1.3$; the ratio between pre- and post-blast lengths is $70/70=1.0$; the ratio between pre- and post-blast heights is $17/15=1.13$. This means the pre-blast grid should

be expanded in two directions (the 'width' direction and the 'height' direction) as the third is unchanged (the 'length' direction). The 'expansion' of the pre-blast model is performed by changing (decreasing or increasing) the grid size in all the three principal directions. For our example above, the grid size in the 'width' direction tends to be increased from 1 to 1.3 and in the 'height' direction from 1 to 1.13. The exact ratios are not always achieved depending on the complexities of the geometries of the pre- and post-blast models. The program aims to achieve the fit of the nodes in both models changing the initial grid size. As a result of changing the grid size, we receive new grid dimensions for the post-blast model in our example: $1.3 \times 1.0 \times 1.13 \text{ m}^3$.

The change of the pre-blast grid size is performed gradually. Increasing or reducing the grid size in one direction honors increasing or reducing the grid size in other directions. It is done by adding a small number to the pre-blast grid size. The small number is by default 0.0001 and is re-calculated for each direction if it changes. For instance, if the height and width ratios are as calculated above, the small number for the width of the post-blast muckpile is re-calculated as follows: $(1.3-1)/(1.13-1) \times d = 0.00025$, where d is the initial small number. The d value for the height remains 0.0001. As a result, the width grid size increases faster than the height grid size.

iv) Calculate the position index values of each block of the pre- and post-blast 3-D models for further manipulations.

v) Assign input grades data to the pre-blast 3-D model. The program considers simulation or estimation input.

vi) Map the input data on the post-blast 3-D model using the position index value of each block. A grade of the pre-blast block with the largest position index values is attached to a correspondent block of the post-blast model with the largest position index value. This process is performed for each block of the post-blast 3-D model. In practice, multiple blocks with equal position index values might occur. The program uses an additional restriction using the pre-

and post-blast coordinates of each block of both models. The program uses a loop though all the pre-blast blocks and assigns the pre-blast grade to the post-blast block if the condition below is true. The process is repeated for each post-blast block.

$$\begin{aligned}
& \textit{Post-blast block}_i \leftarrow \textit{pre-blast grade}_j \quad \textit{if} \quad \textit{abs}(x_i^{\textit{post-blast}} - x_j^{\textit{pre-blast}}) \\
& + \textit{abs}(y_i^{\textit{post-blast}} - y_j^{\textit{pre-blast}}) + \textit{abs}(z_i^{\textit{post-blast}} - z_j^{\textit{pre-blast}}) \\
& + \textit{abs}(\textit{Position index}_i^{\textit{post-blast}} - \textit{Position index}_j^{\textit{pre-blast}}) = \textit{Minimum}
\end{aligned} \tag{5.2}$$

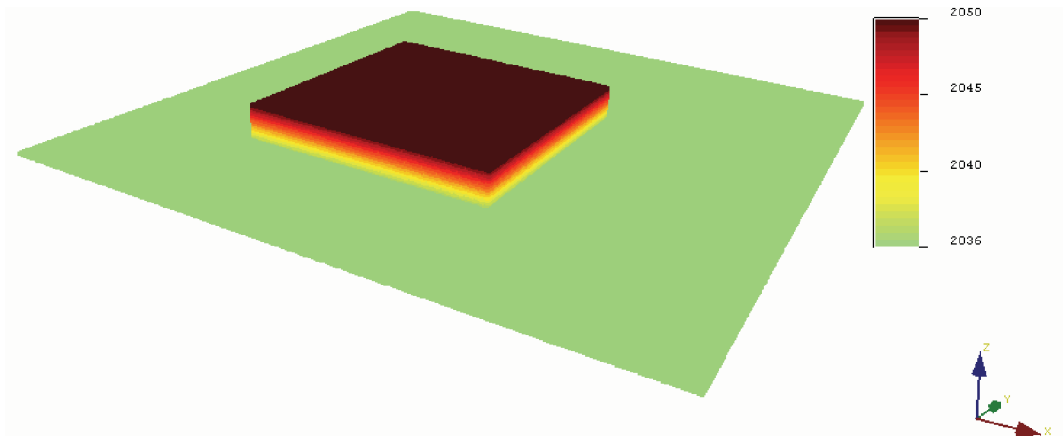
where $x_i^{\textit{post-blast}}$ and $x_j^{\textit{pre-blast}}$ are the x coordinates of the pre- and post-blast blocks of the 3-D models; $y_i^{\textit{post-blast}}$ and $y_j^{\textit{pre-blast}}$ are the y coordinates of the pre- and post-blast blocks of the 3-D models; $z_i^{\textit{post-blast}}$ and $z_j^{\textit{pre-blast}}$ are the z coordinates of the pre- and post-blast blocks of the 3-D models; $\textit{Position index}_j^{\textit{pre-blast}}$ and $\textit{Position index}_i^{\textit{post-blast}}$ are the position index values of the pre- and post-blast blocks of the 3-D models.

5.4 Examples of Blast Movement Modeling

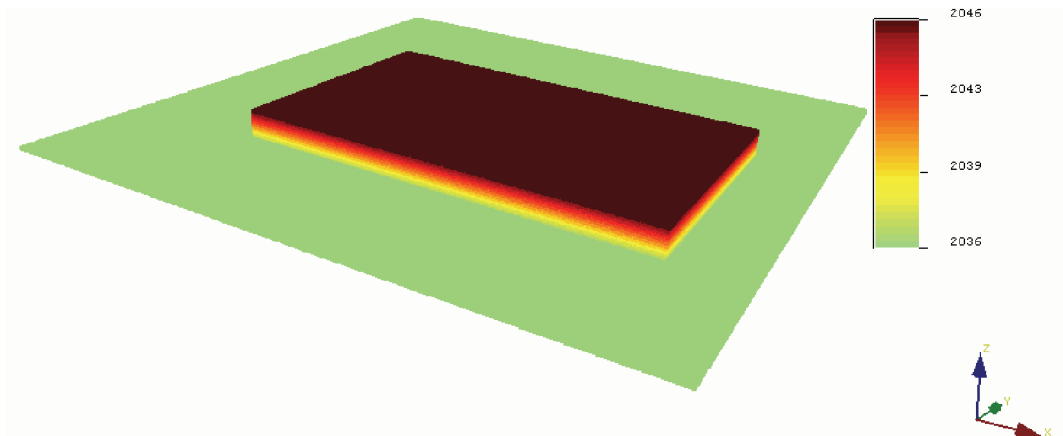
The program's work is shown on three simple examples and one realistic example are shown. The program distinguishes three principle directions for blast movement calculations. By default, the East direction is the x axis; the North direction is the y axis; the height is expressed as the z axis (it complies with GSLIB conventions). The rocks can move in any direction along these 3 axes: positive or negative. The main direction of blast movement should be aligned with one of orthogonal axes (either x or y). Three simple examples represent 3 different cases: i) the pre-blast model expands along the x axis, remains the same along the y axis and contracts along the z axis, ii) the pre-blast model expands along the x and y axes, but contracts along the z axis, iii) the pre-blast model expands along the z axis, but remains the same along the x and y axes. In other words, these three examples represent the cases when the

pre-blast mine bench is confined in one direction, unconfined in any direction and confined in two directions respectively.

For the first simple example, the discretization constant is 1.0 m and the bottom bench elevation is 2035.0 m. Topographic surface files represent 250×250 m² (nodes²) pre- and post-blast areas: the coordinates in the North direction (the y axis) change from 10500 to 10150 m; the coordinates in the East direction (the x axis) change from 26000 to 26250 m. The pre- and post-blast 3-D models of mine surfaces are shown in Figure 5.5. The pre-blast mine bench for the first example is a rectangular parallelepiped ($100 \times 100 \times 15$ m³). As a result of blasting, the pre-blast volume (150 000 m³) is expected to increase 1.3 times to 195 000 m³. If the height reduces to 12 m, the post-blast parallelepiped should have the following dimensions: $163 \times 100 \times 12$ m³ (195600 m³ \approx 195 000 m³, which is close enough for our case).



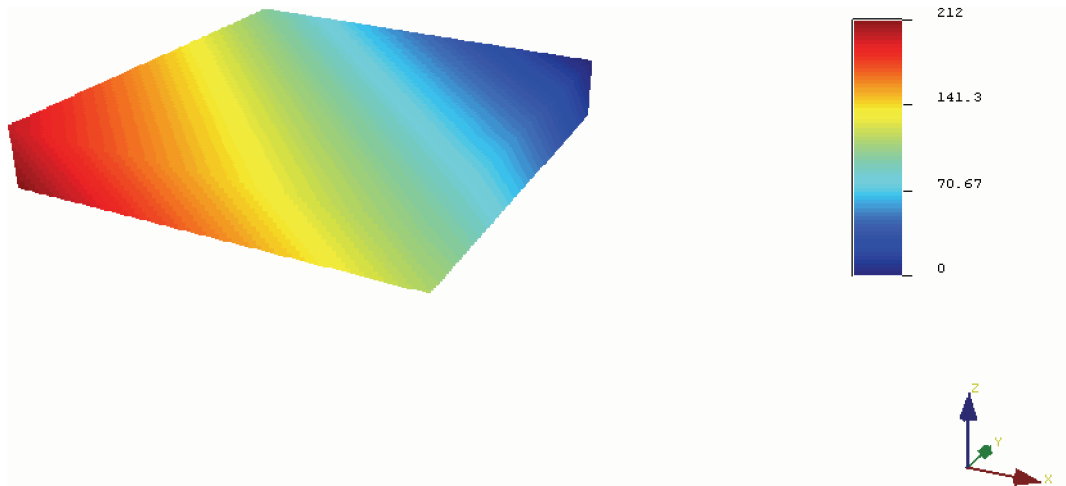
(a) Pre-blast model



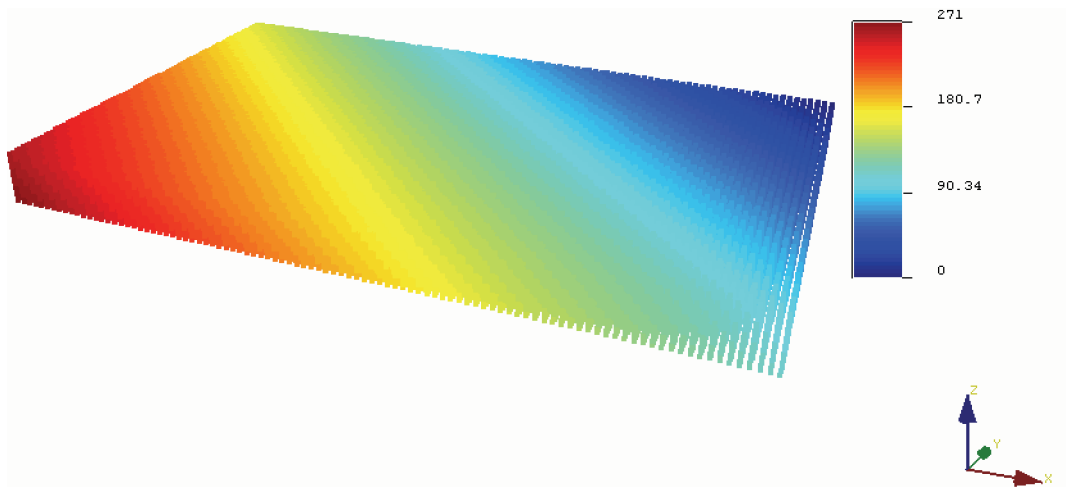
(b) Post-blast model

Figure 5.5: 3-D models of mine area before and after blasting (first simple example)

The pre- and post-blast 3-D models with the illustration of position index values are in Figure 5.6. The color is changing from red to blue with decreasing the position index value.



(a) Pre-blast model



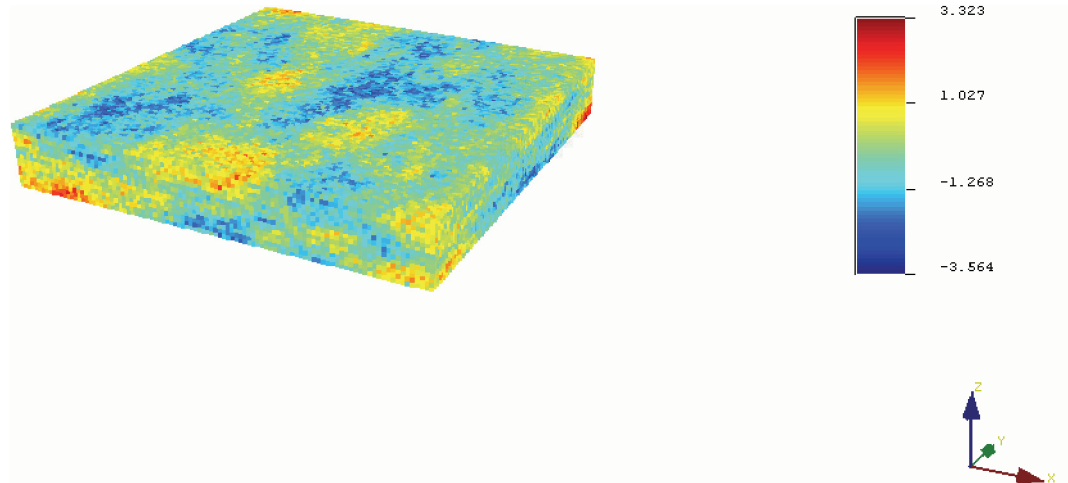
(b) Post-blast model

Figure 5.6: 3-D models colored according to the position index value (first simple example)

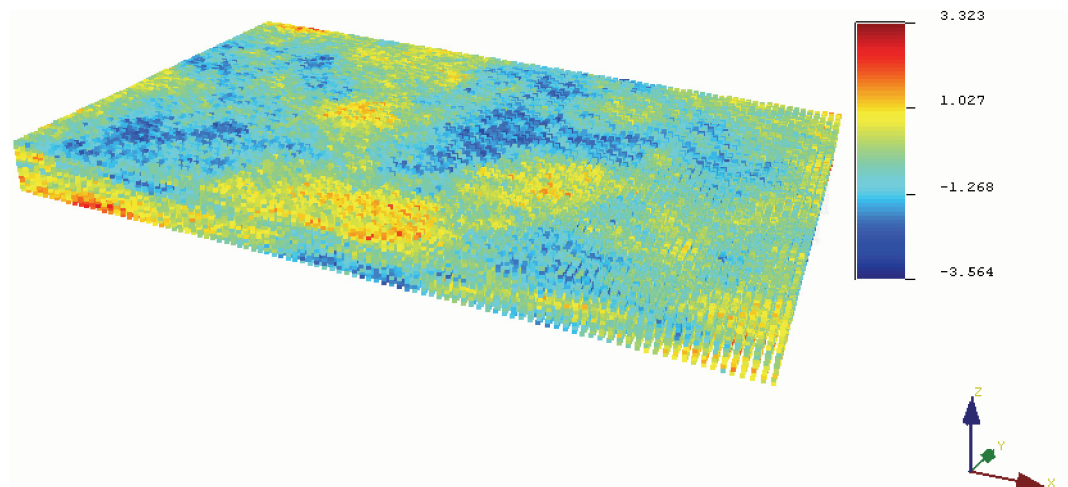
A matching number is a parameter controlling the fit of two models. The simpler the pre- and post-blast geometries, the smaller the matching number is needed. In the case of the first simple example, the matching number can be as small as 0. The geometry of the pre- and post-blast models in Figures 5.6 is very simple: one model can be easily converted to another just by altering the grid size. If the 3-D geometry is more complex, the process of choosing an appropriate matching number is iterative. The closer the match, the less

information is lost for grade control.

In the final step, the pre-blast grades are mapped on the post-blast 3-D model of muckpile. The pre- and post-blast 3-D muckpiles with assigned grades are illustrated in Figure 5.7. The grades are obtained from an unconditional *sgsim* realization. Geological structure is preserved. The topography of mine surface in this simple example is ideal.



(a) Pre-blast model

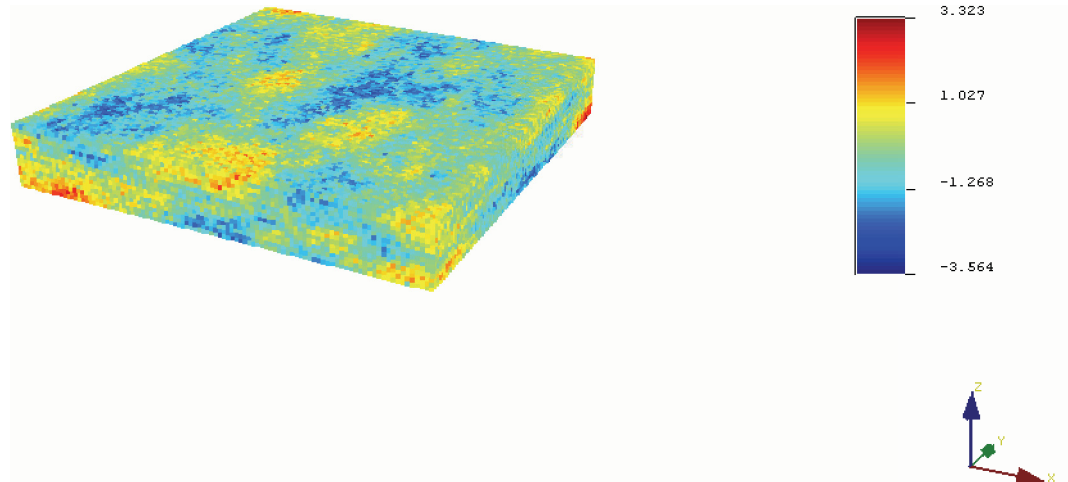


(b) Post-blast model

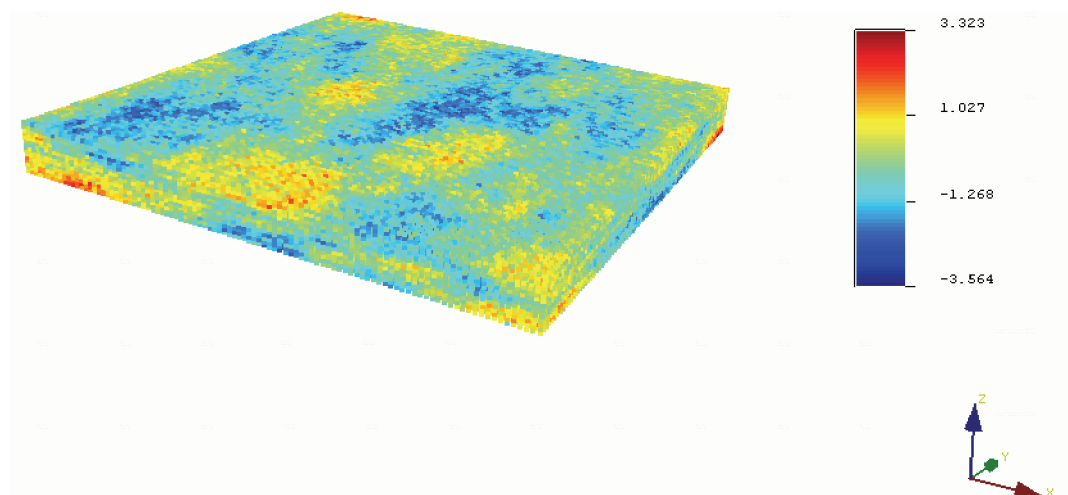
Figure 5.7: 3-D models with assigned grades (first simple example)

The second simple example represents a less common pattern of blast movement when a mine bench is expanding along the x and y axes during blasting.

The pre- and post-blast volumes are preserved (accounting for the swell factor of approximately 1.3) similar to the first example. The dimensions of the pre- and post-blast models are $100 \times 100 \times 15 \text{ m}^3$ and $127 \times 127 \times 12 \text{ m}^3$ respectively. *Bmov* automatically determines that the pre-blast grid should be increased along the x and y axes and decreased along the z axis. The pre- and post-blast 3-D models with assigned grades are in Figure 5.8.



(a) Pre-blast model

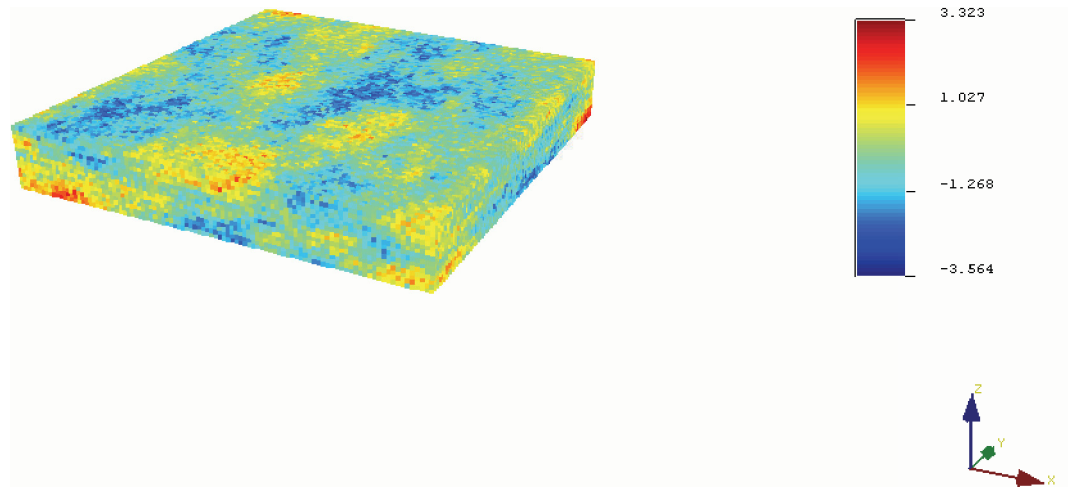


(b) Post-blast model

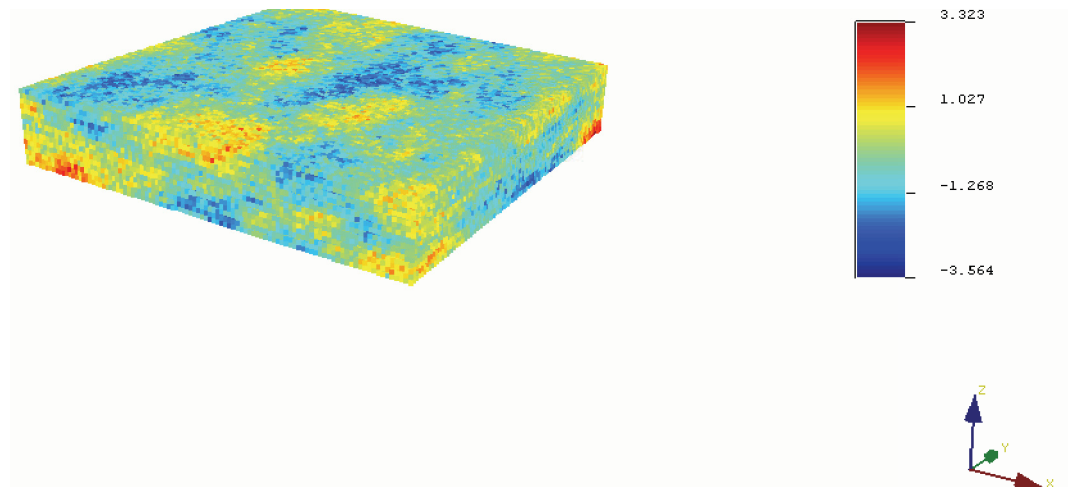
Figure 5.8: 3-D models with assigned grades (second simple example)

The third simple example represents the case when the mine bench is confined from all the sides. It can be surrounded either by intact rocks or previ-

ously blasted material. The only free face in this situation is the top of the bench. Therefore, the rocks do not have any other direction to move but up. Again, the directions of blast movement are completely governed by the pre- and post-blast topographies of the mine area. The dimensions of the pre- and post-blast models are $100 \times 100 \times 15 \text{ m}^3$ and $100 \times 100 \times 19 \text{ m}^3$ respectively. The swell factor is 1.27. The pre- and post-blast 3-D models with assigned grades are in Figure 5.9.



(a) Pre-blast model

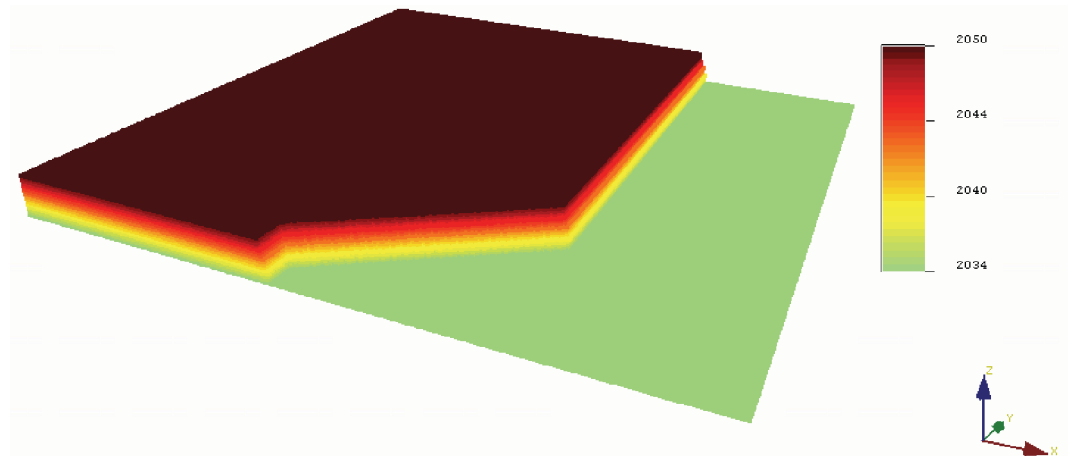


(b) Post-blast model

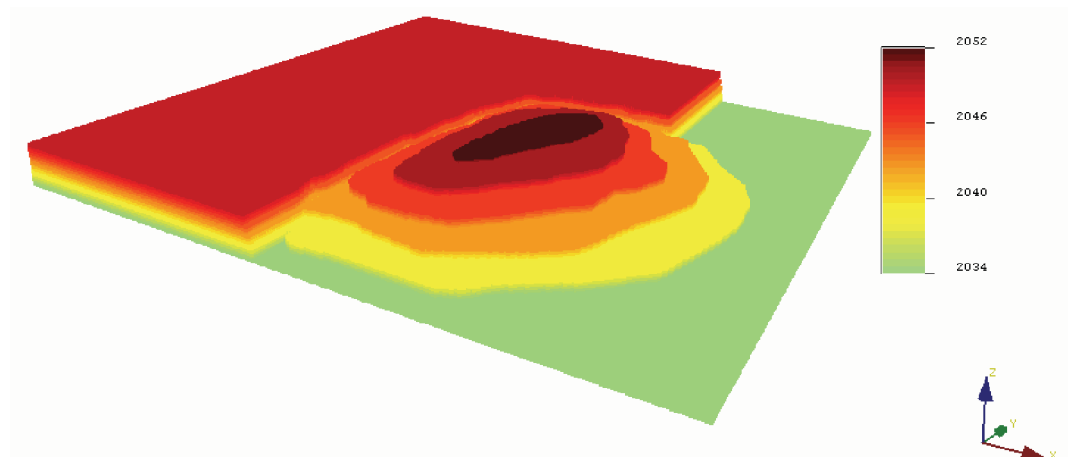
Figure 5.9: 3-D models with assigned grades (third simple example)

The last example represents a case with more complex pre- and post-blast

topographies. The topographic files are artificially developed. This example illustrates a very common situation when blasted rocks move preferentially in the direction of the free face (East). Due to the swell factor of approximately 1.3, a post-blast heave is slightly higher than the top elevation of the pre-blast mine bench. The pre- and post-blast 3-D models of the mine area are illustrated in Figure 5.10. The areas with the same elevations are colored identically.



(a) Pre-blast model



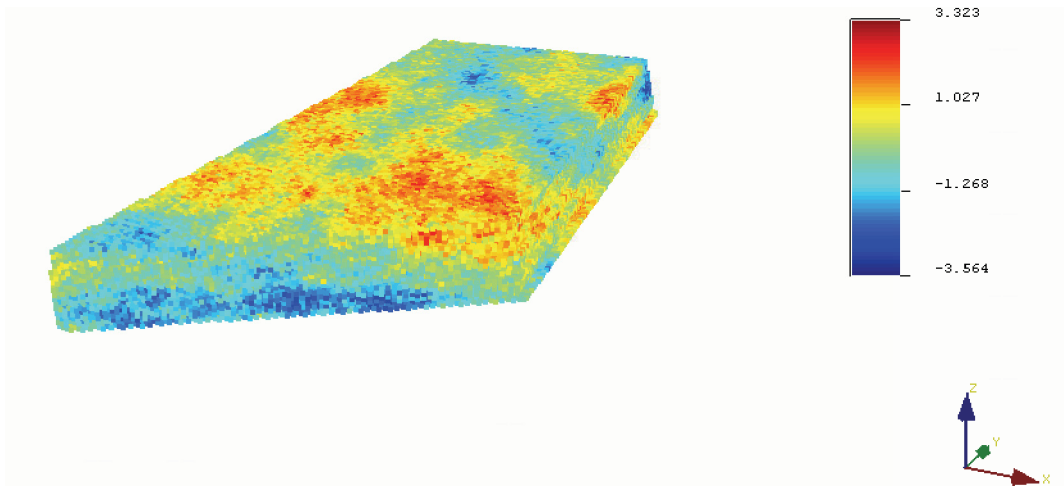
(b) Post-blast model

Figure 5.10: 3-D models representing the mine area before and after blasting (more complex example)

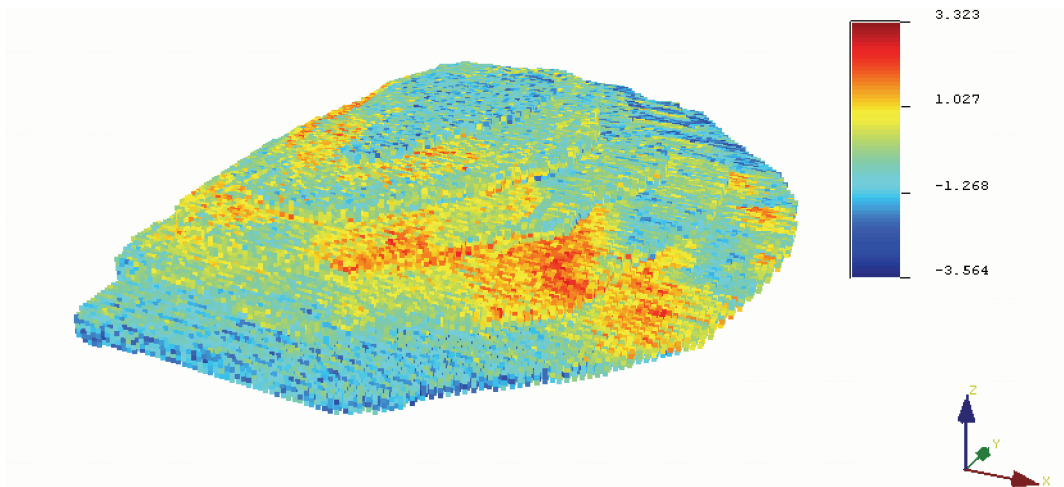
Due to complexity of the pre- and post-blast mine bench configurations, their dimensions are calculated as rectangular boxes. The pre- and post-blast

models are inscribed inside these boxes. It is done only to calculate the ratios between pre- and post-blast dimensions similar to the simple examples. For the simple examples, the dimensions of these boxes coincide with the actual dimensions of the 3-D pre- and post-blast models. The dimensions of the pre- and post-blast rectangular boxes for the last example are $79 \times 165 \times 16 \text{ m}^3$ and $125 \times 163 \times 19 \text{ m}^3$ respectively. The discretization constant is 1 m. An initial number of blocks is displayed on the screen. The initial numbers of blocks for the pre- and post blast models are 147 313 and 188 087 accordingly. The program increases the grid in the East direction and achieves a satisfactory match for the pre- and post-blast 3-D models: 147 313 versus 147 306. Even though the pre- and post-blast geometries are complex, only 7 units of information are lost.

It should be mentioned that the number of blocks is not equal to the volume of models. It is determined solely by topography. Therefore, the volumes are always correct. The pre- and post-blast 3-D models of the mine bench with assigned grades for this example are in Figure 5.11. The bottom views of the same 3-D models are in Figure 5.12.

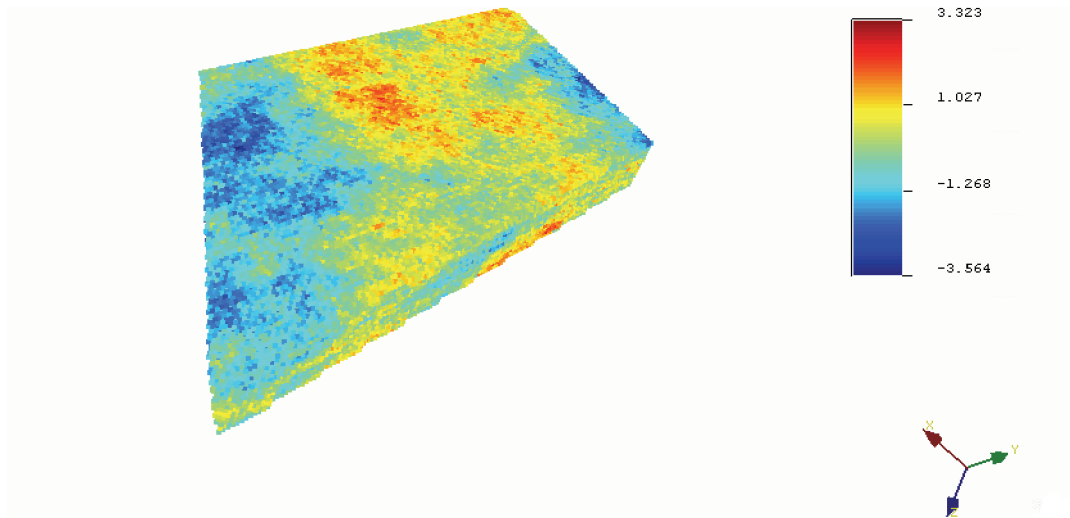


(a) Pre-blast model

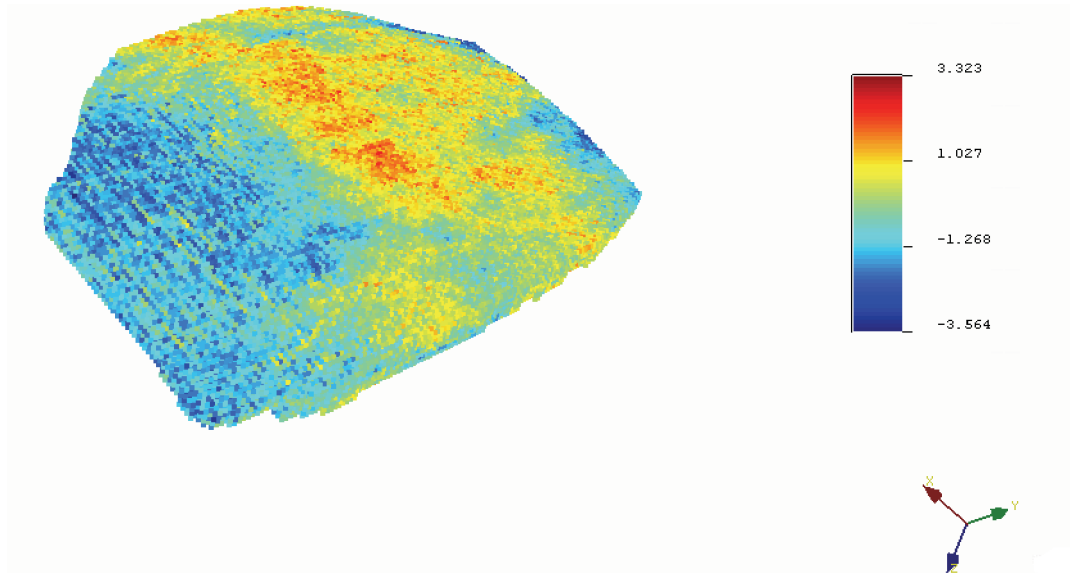


(b) Post-blast model

Figure 5.11: 3-D models with assigned grades (more complex example, top view)



(a) Pre-blast model



(b) Post-blast model

Figure 5.12: 3-D models with assigned grades (more complex example, bottom view)

Due to complex configuration of both models, the blast movement pattern is not so obvious as for the simple examples. Nevertheless, the general principle is the same: the grades are assigned to the post-blast blocks with respect to their position index values and coordinates. Pre-blast high valued and low valued grades appear in the correspondent places of the post-blast 3-D model. It can be mentioned looking in Figures 5.11 and 5.12 that the pre-blast geological

continuity is largely preserved for the post-blast muckpile.

5.5 Conclusions

A current version of *bmov* is not an ultimate blast movement program. It only shows the basic principle of work. The idea is to use the current template and adjust it to conditions of a particular mine. In principle, other influencing and constraining factors can be incorporated. The concept is that the numerical mapping scheme of pre- to post-blast locations would be changed as additional data becomes available. The main conclusions on the blast movement assessment:

i) The blast movement issue in grade control is addressed. A new program for approximate blast movement prediction is developed.

ii) The estimation of the blast movement of grades with *bmov* consider direct measurements, but would in the future if that data were available.

iii) A simple principle of mapping pre-blast grades onto the post-blast 3-D model according to their relative positions inside 3-D models is used: the more a unit of a pre-blast mine bench is confined before blasting, the more it will be confined after blasting. The displacement of grades during blasting is defined by topographic data.

iv) The program accounts for the blast movement in different directions. It is achieved by changing the post-blast grid size according to post-blast topography.

v) Only pre- and post-blast topographic surface files and digitized polygons are required.

vi) The mapping function of *bmov* is flexible. Additional data would be incorporated in the future to refine the coordinates of displaced grades.

The current version of the program is just a starting point. Real data should be used for tuning the program. A function to account for direct blast

movement measurement data should be embedded in the code. The firing sequence of blastholes and other considerations will be important in practice.

Chapter 6

Truck-By-Truck Selection

6.1 Motivation

Short-term grade control is an ongoing process in open pit mines. A destination must be chosen for all mined material at the time of excavation. Errors in grade control decisions mean a direct loss of profit. In a simple case, a cutoff grade is a basis for making these decisions: if the grade of mined material exceeds the cutoff value then, it is ore; otherwise, it is waste. Depending on different treatment options and geology, multiple destinations for mined material are possible: plant, stockpile, leach pad, waste dump, etc. The major reasons for misclassification errors include: i) unreasonable estimation parameters of grade control models, ii) inappropriate estimation methods, iii) not accounting for blast movement of grades, and iv) imprecise delimitation of ore/waste zones using large or unmineable dig limit polygons.

Many developments in grade control have been aimed at improving dig limits for better selection of grades (Isaaks, Barr, & Handayani, n.d.; Thornton et al., 2005; Engmann et al., 2013; La Rosa & Thornton, 2011; Norrena & Deutsch, 2001; Norrena, 2007; Isaaks, Treloar, & Elenbaas, n.d.). Unfortunately, the dig limits approach is inflexible. That is, the grade control decisions must be made for large areas (polygons) at a mine bench not considering that

each truck moves a relatively small volume. Using polygons, often defining tens or even hundreds of thousands of tonnes, does not permit precise selectivity of grades. Major sources of misclassification for grade control with dig limits are the following: i) internal dilution and ore losses, ii) misclassification errors on the edges of the polygons, iii) blast-induced displacement of rocks (Thornton, 2009a), iv) ignoring equipment constraints, and v) using large polygons.

The truck-by-truck method (TBT) implies making decisions based on expected profit or loss of each truck load. The grade control decisions are made before mining. However, the technological parameters and constraints of the excavating equipment are accounted for in decision making. That is, the profit of each scoop of a shovel or an excavator is considered. The TBT method should be used with a robust dispatching system and accurate position information on the equipment and for blast movement.

In Wilde and Deutsch (2007b) and Wilde and Deutsch (2007a), a Feasibility Grade Control method (FGC) is used for prediction of recoverable reserves on the feasibility stage of a mine life using a truck-by-truck basis. The maximum profit principle is used for defining ore/waste indicators of each mining unit. Each mining unit, in turn, consists of several blocks nominally corresponding to scoops of the excavating equipment. The method accounts for the shape of mining units and the direction of mining. A simulated annealing procedure is used to optimize the geometrical parameters of the mining units and maximize the total profit of a reserve model. The method offers a way to mimic grade control at the feasibility stage to more accurately predict recoverable reserves.

This truck-by-truck idea can be used to improve short-term planning at the moment of grade control. More data are available at this stage, which allow establishing reliable simulation models. Simulation allows constructing unbiased and precise predictions that are appropriate for correct profit estimations. Appropriate scale for profit calculations must consider the mining equipment and other site specific conditions. The best selectivity in open pit mines is a

truck load. The selectivity of such a the truck-by-truck scheme is demonstrated below.

6.2 The Importance of a Flexible Grade Control

Data from an existing grade control study are used to analyze probable errors in the classification of mined material (Vasylichuk & Deutsch, 2015d). Data are originally obtained from a copper-molybdenum Ujina open-pit in Chile, which is operated by Compani Minera Dona Ines de Collahuasi (CMDIC). A case study is described in Rossi and Deutsch (2014, pp. 231-234). It is an example of a complicated grade control task with 12 probable destinations for mined material. Several grade control methods are used to classify the mined material of the bench 4270 with dimensions $250.0 \times 187.6 \text{ m}^3$. Two actual deterministic estimates are analyzed to understand how different they might be. The estimates are obtained using Break Even Indicator Method (BEI) (Douglas, Rossi, & Parker, 1994) and the inverse distance cubed method (ID).

Figure 6.1 represents the same bench 4270 estimated by the ID and BEI methods. Figure 6.2 illustrates the ID estimate (dashed lines) superimposed on the BEI estimate. The height of the bench is assumed 15.0 m. The numbers at each polygon indicate their volumes. Different colors of the models indicate different directions for mined material. Even visually, it is evident than both estimation methods classify some parts of the bench differently. Both these estimates might be used for an actual short-term grade control procedure at the mine. The discrepancies in classification between these two methods can be defined.

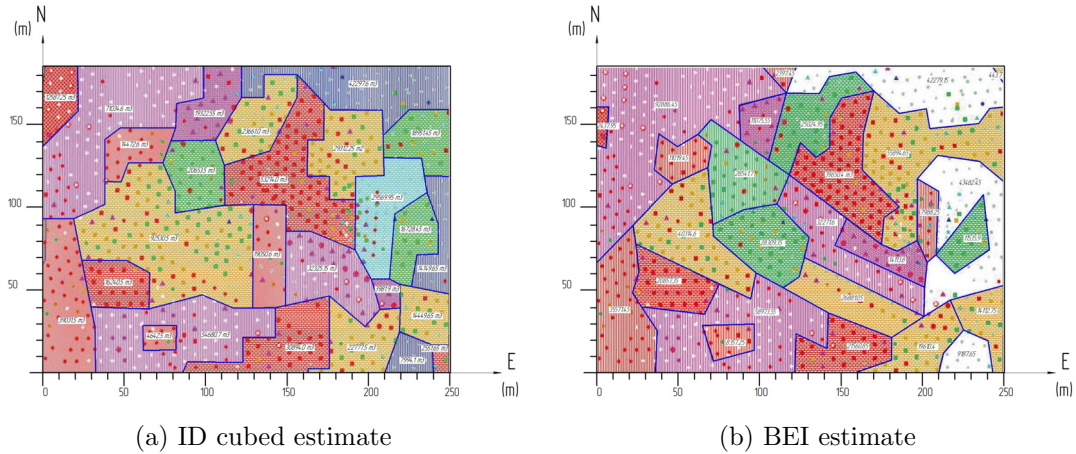


Figure 6.1: Bench 4270 estimated by ID cubed and BEI method. The image is taken from Rossi and Deutsch (2014, pp. 232-233)

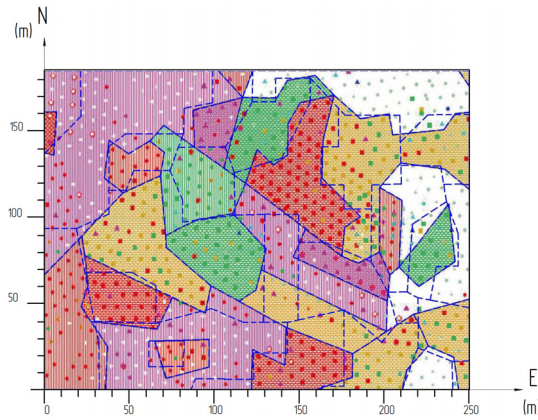


Figure 6.2: The ID cubed estimate (dashed lines) superimposed onto the BEI estimate. The image is taken from Rossi and Deutsch (2014, p. 233)

Simple calculations allow determining a total volume of the mine bench: $250 \times 187.6 \times 15 = 703\,500 \text{ m}^3$. Figure 6.2 shows the areas where grade control polygons from two models mismatch. There are two cases: i) the mismatch of ore types is not taken into account, and only the outlines of polygons are compared (first case), ii) the mismatch of ore types is considered (second case). Green areas in Figure 6.3 represent the parts of the mine bench where the grade panels of two models match in shape (first case) or in both shape and the type of ore (second case), and red areas represent the places where the mismatch

OCCURS.

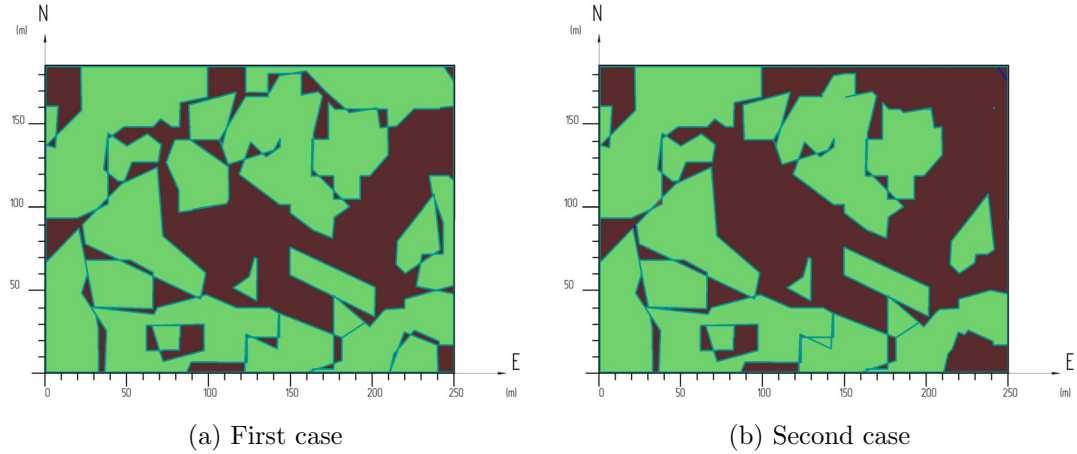


Figure 6.3: Bench 4270 with green areas representing the parts where two estimates coincide and brown areas where they do not

The percentages of mismatch of the polygons are calculated and presented in Table 6.1 along with other information.

Table 6.1: Comparison of two estimation methods

Summary items	First case	Second case
Total volume(bcm)	703 500	703 500
Total volume of match (bcm)	466 052	389 982
Total volume of mismatch (bcm)	237 448	313 518
The percentage of mismatch	33.75%	44.56%

According to mining-technology.com (n.d.), the blasted rock mass at Colahuasi copper mine is being hauled by Komatsu 830 with the payload equal to 221.6 tonnes and heaped capacity of 147 lcm (Komatsu, n.d.). Assuming the swell factor of 1.3, the total volume of loose rocks is $703\,500\text{ m}^3 \times 1.3 = 914\,550\text{ lcm}$. The total number of truck operating cycles is calculated as: $914\,550/147 \approx 6221$ cycles by volume. Nevertheless, assuming the density of 2 700

kg/m^3 for intact rock, one truck is not able to carry this amount of the mined material ($703\,500\text{ m}^3 / 6221\text{ cycles} = 113\text{m}^3 \times 2\,700\text{ kg} = 305\text{ tonnes}$). The number of truck cycles is restricted by the tonnage instead of volume leading to: $(703\,500\text{ m}^3 \times 2\,700) / 221.6\text{ tonnes} = 8569\text{ cycles}$.

The calculations above allow illustrating the selectivity of the TBT approach compared to dig limits polygons. Bench 4270 can be discretized by units representing one truck load. The units are square in shape with dimensions: $46900\text{ m}^2 / 8569\text{ cycles} = \sqrt{5.47\text{m}^2} = 2.3\text{ m}$. Bench 4270 is discretized by $2.3 \times 2.3\text{ m}^2$ units is in Figure 6.4.

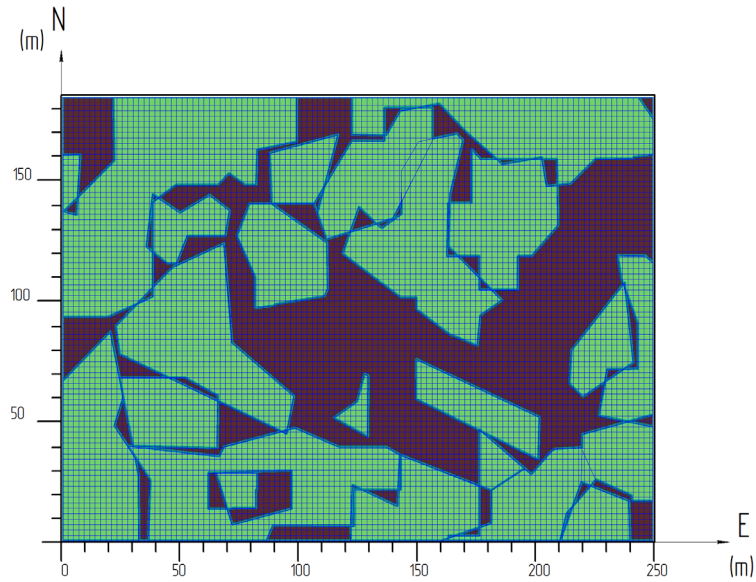


Figure 6.4: Bench 4270 is discretized by units representing one truck load

It is obvious that the truck-based unit represents much smaller area than any of the dig limit polygons in Figure 6.3. Therefore, the truck-based units are prospectively much more selective than the dig limits. The TBT method allows decision making at the smallest scale available. The next step is to account for the shape of truck-based units and adapt making grade control decisions based on maximum profit or minimum loss. The benefits of the truck-by-truck approach would only be realized by a precise blast movement model and precise knowledge of the rock being mined.

6.3 Choice of truck-based units

A small numerical experiment is constructed to check the relationship between the size of a truck-based unit and the total profit of a mine bench. It is reasonable to use the dimensions of the mine bench and the truck-based units from the previous section of the chapter as a starting point. The idea is to check how the total profit of the bench changes for the truck-based units with the dimensions from $2.3 \times 2.3 \text{ m}^2$ to $40 \times 40 \text{ m}^2$ and compare it to the profit obtained using dig limits. The expected profit in this case is used with the TBT method instead of the expected loss (Equations 4.7-4.10 in Chapter 4). It is the same in principle; instead of assigning a loss when a grade control decision is incorrect, a profit is assigned when the decision is correct. Both methods work the same in terms of giving more priority to a certain decision when coefficients are used for adjusting penalty or profit. The coefficients b_1 and b_2 from Equations 4.7-4.10 in Chapter 4 serve for this purpose. The coefficients could be replaced with functions to represent more complex relationships. For this small experiment, the priority is to 'restrict' overestimation decisions. It is done to model a situation when a mining company cares more about sending waste rock to the plant than losing ore. Grade control decisions are shifted to underestimation in this case. In order to tune simulation to this task, the profit for correct ore grade control decisions is reduced twice in comparison with the profit from correct waste decisions.

Two cases are considered: i) a case with big and simple polygons and a low nugget effect, ii) a case with complex and erratic polygons and a higher nugget effect. The idea of the case with big polygons is to represent a mine bench that is easy to delimit to ore and waste zones. The traditional polygonal approach is expected to perform effectively, and the selectivity of grades is expected to be very high. A reference model for this case is constructed using the following parameters: i) the variogram is omni-directional with the range of 150 m ,

ii) the variogram model is spherical with one nested structure, iii) the nugget effect contribution is 0.05. It is illustrated in Figure 6.5. Brown areas and green areas represent ore and waste zones respectively. Ore/waste delimitation for a reference variable is performed using a cutoff grade of 0.

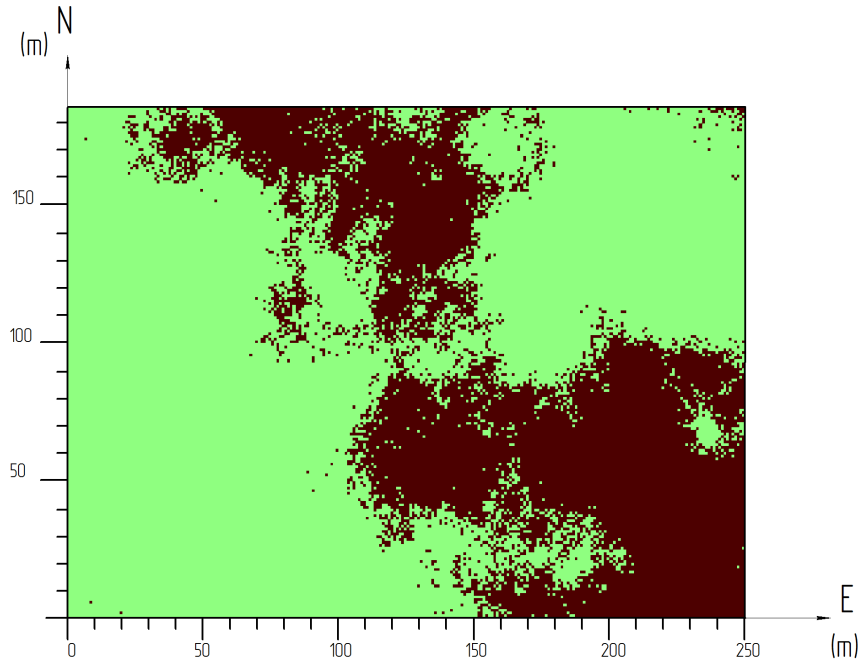


Figure 6.5: Reference model for simple grade control case

The idea of the second case is to represent a more complex grade control situation. The geological structure of the deposit is constructed erratic with ore and waste zones mixing with each other. A reference model for this case is constructed using the following parameters: i) the variogram is omni-directional with the range of 25 m , ii) the variogram model is spherical with one nested structure, iii) the nugget effect contribution is 0.2. The model is illustrated in Figure 6.6.

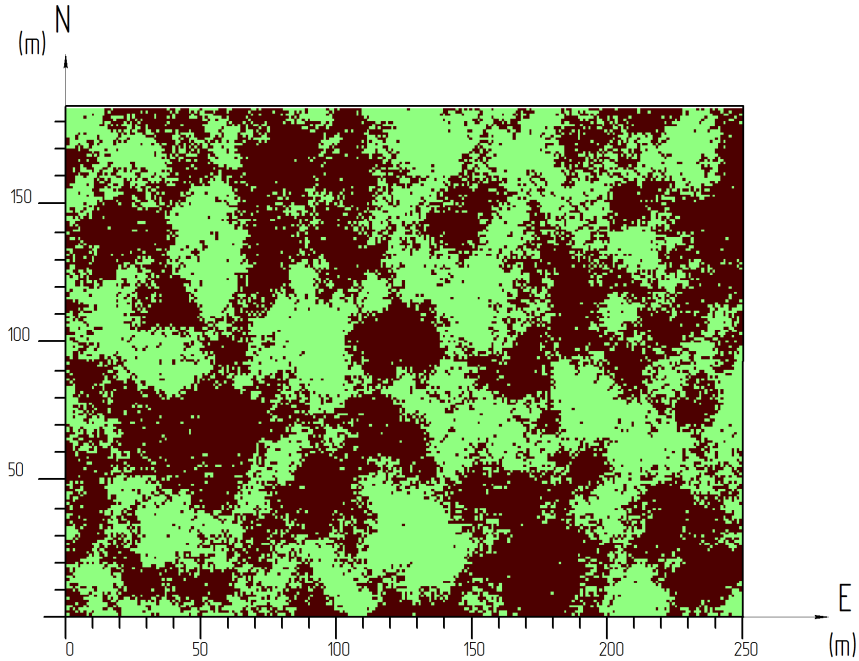


Figure 6.6: Reference model for complex grade control case

Dig limits for both cases are drawn using ordinary kriging estimates at a reasonable resolution. Then, the ore/waste indicator maps, obtained using dig limit polygons, are assessed and the profit from this type of estimation is calculated. The mine benches with dig limits are also mined using trucks and the excavating equipment. Therefore, the total profit is also calculated inside the truck-based units with dimensions from $2.3 \times 2.3 \text{ m}^2$ to $40 \times 40 \text{ m}^2$. Of course, the truck-based units more than $7 \times 7 \text{ m}^2$ are unrealistic but they are used for comparison. The ore/waste indicators inside each truck-based unit are calculated. A unit is assigned ore when the probability of being ore is more than 50 percent, and waste otherwise. The ore/waste maps for the two grade control cases are in Figure 6.7

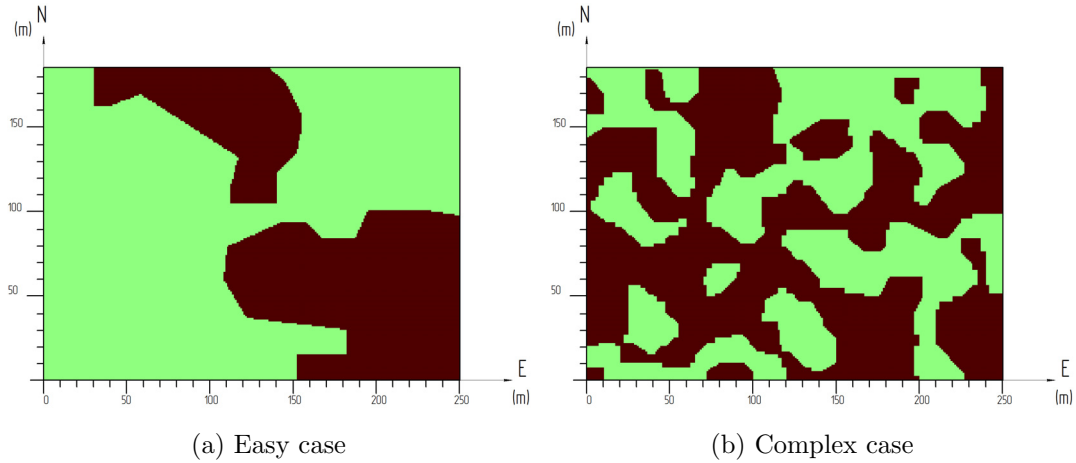


Figure 6.7: Ore/waste maps for two grade control cases

The main steps of the experiment are the following:

- i) Construct the reference distribution at $1 \times 1 \times 15$ m³ resolution.
- ii) Sample the reference distribution at $10 \times 10 \times 15$ m³ resolution.
- iii) Estimate and simulate the area of interest at $2.5 \times 2.5 \times 15$ m³ resolution using ordinary kriging (OK) and sequential Gaussian simulation (SGS) respectively. SGS is used to obtain 100 realizations for the calculation of profit.
- iv) Regrid estimates to the resolution of the reference models.
- v) Construct the TBT and dig limits ore/waste maps for the truck-based units with dimensions from 2.3×2.3 m² to 40×40 m². A random offset of 4 meters from modeled position is assigned to each unit to simulate poor navigation and poor knowledge of the precise bucket location.
- vi) Compare the reference ore/waste map with the TBT and dig limits ore/waste maps and assign profit for each grade control decision.
- vii) Repeat the above steps for both grade control cases.
- viii) Compare the performance of the two grade control methods.

The TBT method produces ore/waste estimates delimited by the truck-based units. Final dig limits ore/waste maps are also delimited by truck-based units, but they are obtained from the dig limits ore/waste maps. The examples of these ore/waste maps for the simple and complex grade control

cases are in Figure 6.8. The dimensions of the truck-based units for these maps are $2.3 \times 2.3 \text{ m}^2$. Due to a significant random offset of 4 meters from modeled positions, some errors occur in the classification of mined material.

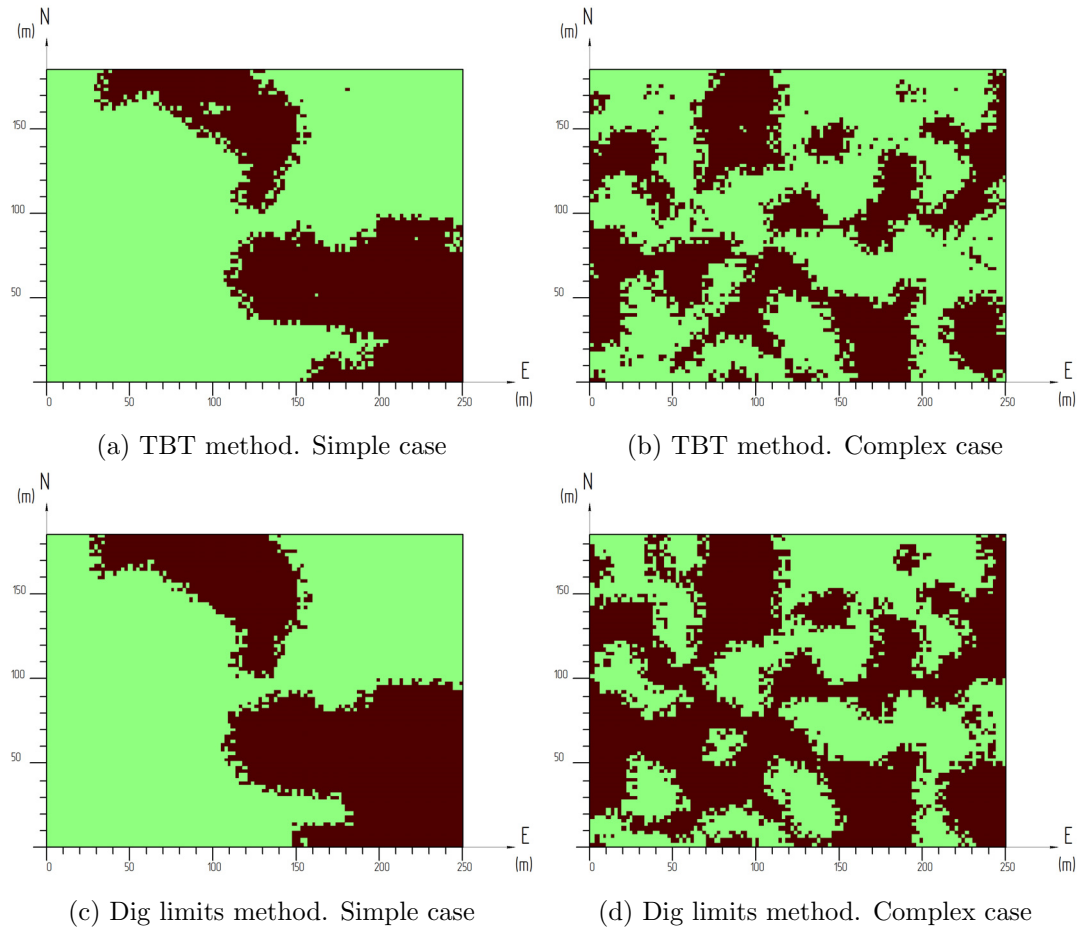
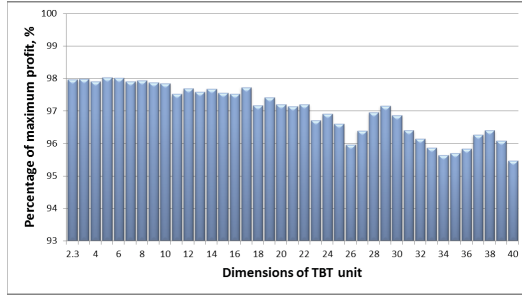
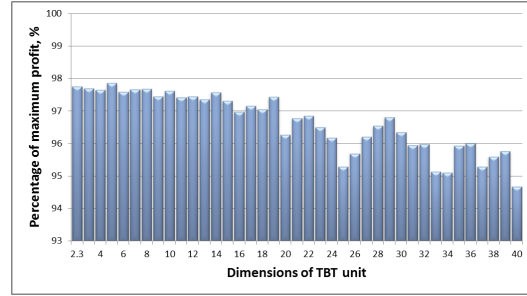


Figure 6.8: Ore/waste for two grade control methods

The effectiveness of each grade control method for both cases is calculated as the percentage of the maximum possible profit. The maximum profit is achieved for a perfect selection of mined material when each portion of the material is sent in a correct destination. Figures 6.9 and 6.10 illustrate the performance of the TBT and dig limits grade control methods for both grade control cases.

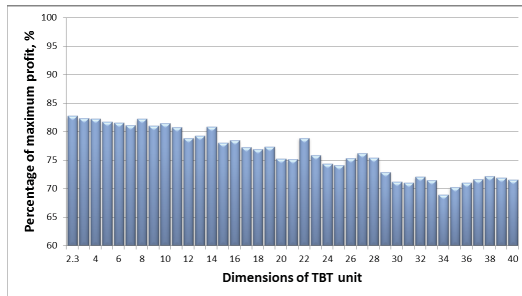


(a) TBT method

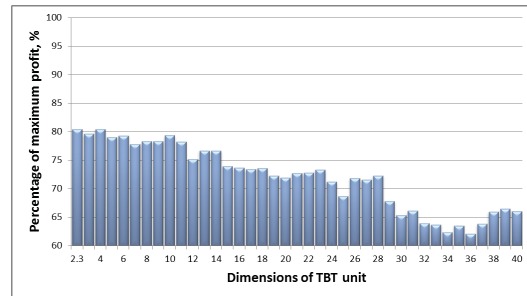


(b) Dig limits method

Figure 6.9: Percentage of maximum profit across the range of TBT sizes for simple grade control case



(a) TBT method

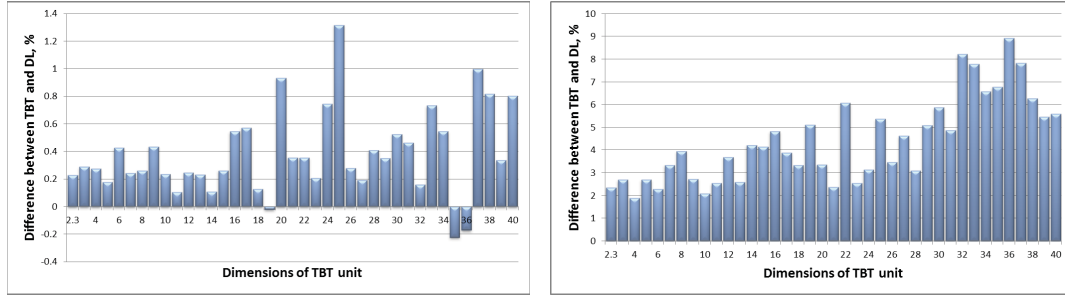


(b) Dig limits method

Figure 6.10: Percentage of maximum profit across the range of TBT sizes for complex grade control case

As expected, both grade control methods perform well in the straightforward grade control situation with just two big ore zones. The TBT and dig limits methods reach 98.03 and 97.85 percent of maximum profit respectively. For both methods, the most optimal size of the truck-based units is $5 \times 5 \text{ m}^2$. The effectiveness of both methods is lower for the complex grade control case. The TBT method reaches 82.72 percent of the maximum profit for this bench while the dig limits method reaches 80.39 percent. The optimal sizes of the truck-based units are $2.3 \times 2.3 \text{ m}^2$ and $4 \times 4 \text{ m}^2$ for the TBT and dig limits methods respectively.

The bar charts in Figure 6.11 show the difference in performance of the TBT and DL methods for the simple and complex cases with respect to profit.



(a) Simple case

(b) Complex case

Figure 6.11: Difference with respect to profit between two grade control methods for both grade control cases

Figure 6.11 illustrates that the effectiveness of the TBT over the dig limits method increases with the increase in the size of the TBT units. The difference is generally much more significant for the complex grade control case. It reaches up to 8-9 percent for some large sizes of the TBT units. The dig limits approach shows a slightly better performance (0.02-0.22 percent) for some three large TBT sizes. The TBT still performs better than the dig limits method on average over all the TBT unit sizes for both grade control cases.

6.4 Conclusions and Limitations

This chapter advocates the truck-by-truck (TBT) method of selection versus polygonal dig limits. Synthetic examples are used to compare the performance of the traditional grade control method with dig limits and the proposed TBT method. Two grade control cases represent real life grade control situations with simple and complex geological settings of the mine benches. The results of the experiment allow concluding the following

- i) The TBT method outperforms the traditional grade control method for both simple and complex grade control situations.
- ii) The difference between two methods is higher for the complex grade control situation.

iii) The average improvement of the TBT method is 4.4 percent with respect to the maximum profit for the complex grade control case and 0.38 percent for the simple grade control case.

iii) The optimal size of the truck-based units is smaller for the complex grade control cases with erratic geological settings. For simple grade control cases with well-defined and few ore/waste zones, larger selection units are preferable.

iv) The TBT method is compatible with simulation. Grade control decisions could be obtained using multiple realizations and complex expected profit calculations

The synthetic examples above do not fully represent the challenges of grade control at mines. The complexity of grade control cases in the experiment is only controlled by different geological settings. Only one variable and a very simple profit calculation principle are used. The parameters of the reference distributions are known and used for qualitative estimation and simulation. Different situation could occur if several variables were involved with complex non-linear relationships. The TBT method is expected to perform better in such situations due to the properties of simulation. Nevertheless, the results above represent possible advantages of using the TBT method instead of the dig limits approach.

Chapter 7

Red Dog Case Study

7.1 Purpose

This chapter presents a new workflow for short-term grade control in open pit mines. Four major aspects of the new grade control procedure comprise a new paradigm providing better estimates in terms of expected profit for each unsampled location: (1) a reasonable resolution for grade control models is defined, (2) simulation is used for making grade control decisions based on economic factors, (3) the impact of the blast movement of grades on short-term grade control is evaluated and addressed, and (4) final grade control decisions are based on the expected profit of each truck load. All the aspects outlined above help to better define final destinations of mined material (plant, waste dump, leach pad, etc.).

A case study is constructed to show the main steps of the new grade control procedure. An existing grade control practice is compared to the new paradigm using real data and a series of assumptions. The structure of the case study consists of the following main steps:

- i) Construct a reference distribution.
- ii) Define a reasonable grid size range for short-term grade control models.
- iii) Compare the effectiveness of estimation versus simulation for short-term

grade control.

iv) Compare the effectiveness of measuring blast movement versus using pre-blast dig limits onto post-blast muckpile surface.

v) Compare the truck-by-truck (TBT) ore/waste selection versus dig limits approach (DL).

vi) Assess the impact of sampling and dispatching errors on grade control and the performance of TBT and DL.

All the parts of the case study represent the elements of the new short-term grade control workflow. Dispatching and sampling errors are incorporated and taken into account. A real life grade control procedure would not involve the construction of reference distributions; it is done only for having a basis for comparison. All the aspects of the new grade control procedure are separate. It means each aspect of the this procedure is possible to use individually depending on needs of a mine. For example, a company may have a blast movement measuring or modeling system, which is properly calibrated and precise. In this case, the data from an existing blast movement system could be incorporated into the new workflow.

The TBT approach presented in this thesis allows better selectivity on the stage of excavation. It could be fitted to an existing grade control practice. A reasonable grid size allows decreasing ore/waste misclassification without spending additional costs and working hours. Simulation allows accounting for complex relationships between different variables involved in grade control. These are only some of the examples of using the new short-term grade control paradigm. The author aims to show that the existing grade control procedure is not ultimate and may be improved.

The case study is fashioned after some data from Red Dog Mine; however, this was done independently of the operator and is meant to show the developments of this thesis. Actual application to the mine and other site-specific economic and mining considerations would be required for definitive conclu-

sions.

7.2 Background

The Red Dog mine is located in an isolated area 150 km from Kotzebue, Alaska, USA. It is one of the world's biggest producers of Zinc. It also produces a significant amount of Lead and Silver (Teck Cominco Alaska Inc., 2009). The mine is partially owned by a Canadian metals and mining company Teck Resources Limited.

The Red Dog mineral resources consist of three main deposits suitable for a surface mining method: 1) Main open pit, ii) Aqqaluk deposit, and iii) Qanaiyaq deposit. There are also two deposits adjacent to the Main open pit: Paalaaq (a deeper zone of Aqqaluk deposit) and Anarraaq (Teck Cominco Alaska Inc., 2009). They are situated deeper below the surface than the three main deposits and, therefore, might be economically mined only by underground mining method.

All the deposits were originally a single formation. This original formation was then divided by tectonic forces into separate parts. The Red Dog deposit consists of three ore-bearing rock types: silica, barite rock, and sulphide rock. The main part of the Red Dog deposit consists of four structural plates: upper, median, lower, sub-lower plate (Teck Cominco Alaska Inc., 2009). More information on the geological formation of the Red Dog deposit can be found in Teck Cominco Alaska Inc. (2009) and Moore, Young, Modene, and Plahuta (1986).

For this case study, only some production data from the Main open pit are used. The idea is to simulate the short-time grade control procedure on an example of one mine bench.

Available Data of Grade Control

For the main deposit, there are four variables important for metallurgical

recovery: Zn, Pb, Fe, Ba. Siliceous ore type accounts for 70 percent of the Main deposit's reserves. The Fe content in the siliceous ore influences its metallurgical recovery. The higher the content of iron, the lower the recovery of Zn. Another influencing factor is the content of Ba (Teck Cominco Alaska Inc., 2009). The Red Dog mine developed a recovery formula that is used for calculating recovery.

The actual Red Dog recovery formula is not used for this case study. Some approximate utility functions are assigned to each of the four main elements according to stockpile blending criteria (constraints) established by the company (Teck Cominco Alaska Inc., 2009):

$$\begin{aligned} \text{Zn/Fe} &\geq 2.5 \\ \text{Zn/Pb} &\geq 3.5 \\ \text{Ba} &\leq 10 \% \\ \text{Total Organic Carbon} &\leq 0.65 \% \\ \text{Weathered Ore} &\leq 5 \% \end{aligned}$$

Only the first three criteria are used for ore/waste delimitation. Additionally, a minimum Zn criteria is added: the content of Zn should not be less than 5 % ($\text{Zn} \geq 5 \%$). Totally, these four constraints are used for constructing a reference ore/waste indicator map. The utility and penalty functions representing an influence of each constraint on final profit are in Figure 7.1.

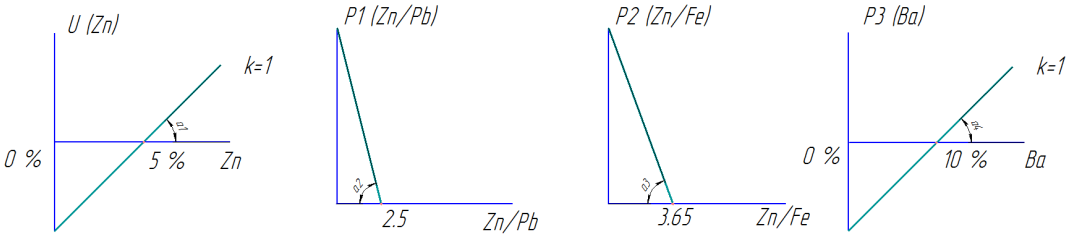


Figure 7.1: A schematic illustration of stockpile constraints at Red Dog

7.3 Construction of Reference Distribution

Long- and short-term grade control models at the Main Red Dog open pit are constructed using Ordinary Kriging (OK) interpolation. Each variable of interest is modeled separately using available drillhole (DH), reverse circulation (RC) and blasthole data (BH). Only DH and RC data are used for the long-term models. For the short-term models, closely spaced BH data are also used (Teck Cominco Alaska Inc., 2009). Existing short-term models are constructed at 25'×25'×25' resolution. BH assays provide information on the content of SPb, but it is not used for this case study. The BH data are on 14'×14' grid.

The reference ore/waste map is constructed using BH assay data of four main elements and the stockpile blending criteria provided above. A single realization of *sgsim* conditional to the BH data is used to construct reference models for each variable. The forward normal score transformation is performed using *ppmt* program (Barnett et al., 2014; Barnett, 2015). It allows preserving multivariate relationships between variables. Simulation is then performed for each variable separately. Back-transformation is performed using *ppmt_b* program. The standard normal score transformation is applied to the BH data prior the PPMT transformation using *n_score* program (Deutsch & Journel, 1998). It is done to improve reproducing univariate statistics for all the variables. This approach is proposed in (Barnett, 2015).

Back-transformed variables reproduce multivariate relationships in data. Accurate modeling of these relationships could be very important for ore/waste delimitation, as the metallurgical recovery of Zn at Red Dog is dependent on the content of multiple variables. A deterministic method is not suitable for such a complex modeling task.

Ore/waste indicators are used to compare a conventional and the new grade control procedures. Grade control models are converted to ore (1) or waste (0) indicators at each location. Each location is then compared to a reference

model, which is also expressed as the ore/waste indicators. Final reference ore/waste indicator maps reflect all the univariate and multivariate relationships between data in order to mimic the reality. Constructing the reference distribution is a very important procedure and consists of the following steps:

- i) Choose a mine bench for the case study.
- ii) Decluster data if needed. This procedure is not required for the current case study, as the data are situated on a regular grid.
- iii) Calculate variograms of original data for estimation.
- iv) Perform the standard normal score transformation of each variable separately.
- v) Calculate variograms of standard normal score data.
- vi) PPMT-transform all four variables at once.
- vii) Perform simulation for each variable separately using normal score variograms. It is done to improve the reproduction of variograms in resultant simulated models (Barnett, 2015).
- viii) Back-transform the simulated models in a reverse order: PPMT back-transformation, then NS back-transformation.
- ix) Validate the reference model.
- x) Combine all four simulated variables into one ore/waste indicator map using the stockpile blending criteria.

Bench 20177 (further 'bench') on the bottom of the Main Pit is chosen for the case study. The bench contains ore and waste zones, which are relatively easy to delimit manually. The bench consists of 193 blastholes situated on a staggered pattern with grid dimensions of 14'×14'. The dimensions of the bench are 252'×134'×25'. BH maps colored according to the content of four main chemical elements are in Figure 7.2.

Declustering

Declustering is a procedure for obtaining representative first order statistics of a set of data. It is necessary when data are situated irregularly throughout

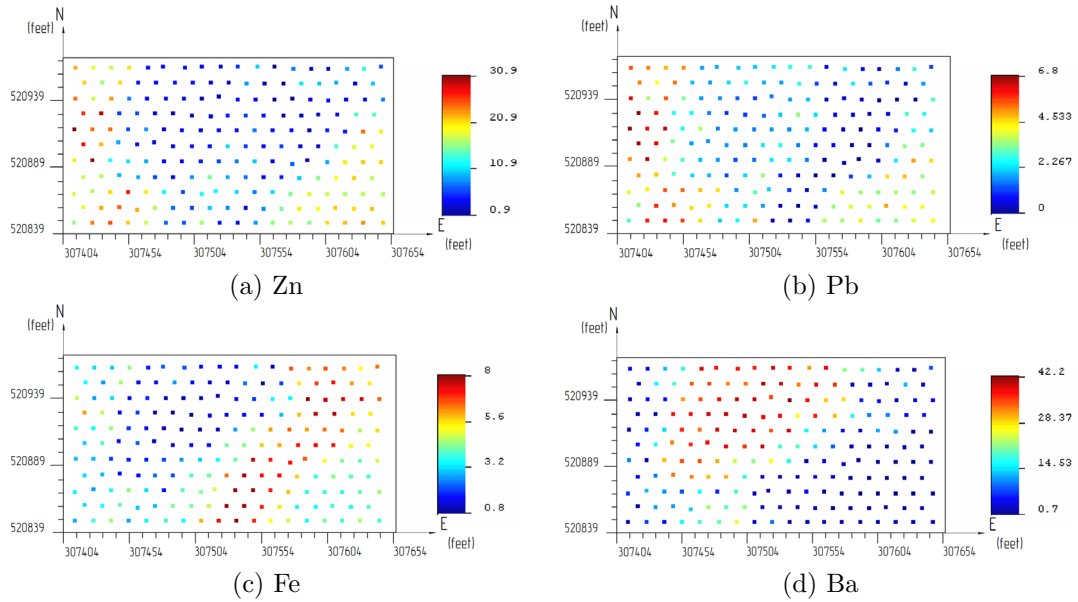


Figure 7.2: Mine Bench 20177 with BH colored according to contents of each variable

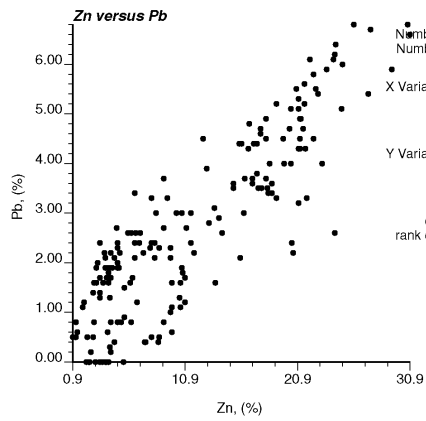
an area of interest. In this case, each sample might represent different areas and, as a result, receive a higher or lower weight in the resultant statistics. The BH at the bench are bored at a regular staggered pattern. Therefore, each sample out of 193 has approximately the same weight; declustering is not needed.

Normal score and PPMT forward transformation of data

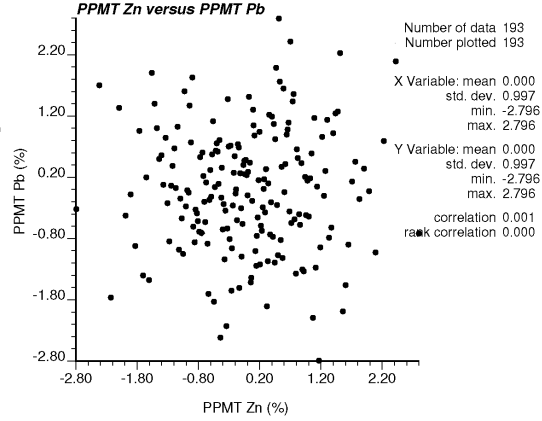
NS transformation of the data prior to PPMT transformation helps to reproduce univariate statistics in resultant simulated models. After NS transformation, the data are normally distributed with the mean of 0 and variance of 1 (standard normal distribution). A function to enforce simulated data to be standard Gaussian is included in the PPMT back-transformation program. This step is performed because the reproduction of histograms can be compromised for simulated models after PPMT back-transformation. The simulated data are then back-transformed to original values using normal score back-transformation program.

As mentioned before, the PPMT normal score transformation of all four

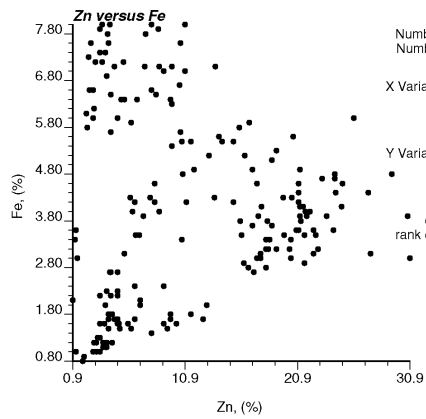
variables is performed using *ppmt* program (Barnett, 2015). The bi-variate scatter plots of normalized variables show practically zero correlation. Using the first NS transformation ensures the reproduction of both univariate and multivariate statistics. The comparison of the scatter plots of original and PPMT-transformed variables is in Figure 7.3.



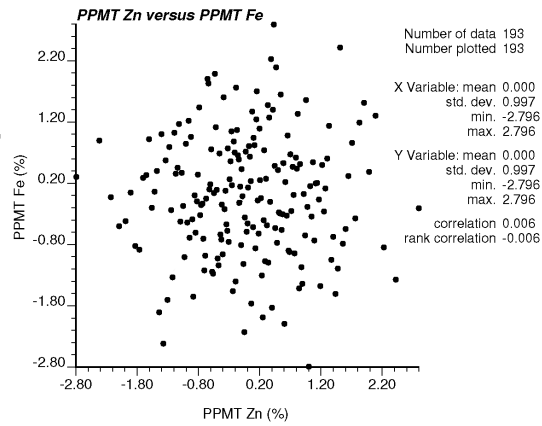
(a) Original Zn-Pb



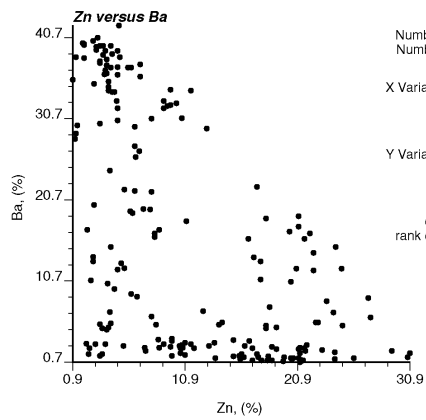
(b) PPMT Zn-Pb



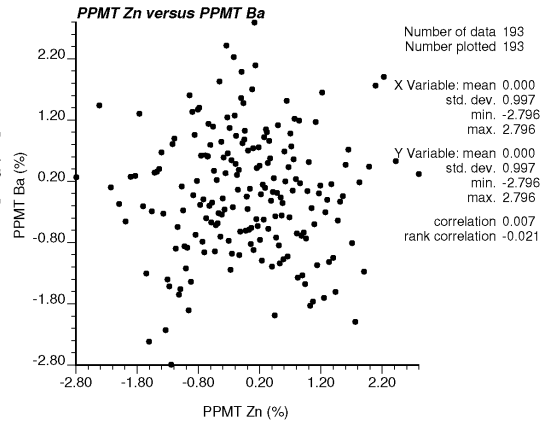
(c) Original Zn-Fe



(d) PPMT Zn-Fe



(e) Original Zn-Ba



(f) PPMT Zn-Ba

Figure 7.3: Comparison of bi-variate plots of original and PPMT transformed variables

Variogram calculation and modeling

Variogram is a common tool for characterizing spatial continuity. The BH samples do not provide information on vertical variability. Therefore, the variograms are calculated only in the horizontal plan in 2 principal directions. For regular patterns, variograms in major and minor directions of continuity are usually calculated along the rows of BH. In the case of staggered pattern, it is also reasonable to consider the directions N45E and N135E. Tolerance parameters for lag distances in this case should be reasonably increased. All the variables are normal score transformed before calculating variograms. The variograms of standard normal score data are used instead of variograms of the PPMT-transformed data. The PPMT-transformed data are forced to be uncorrelated at $h=0$ distance. It may cause a loss of continuity and difficulties during fitting a variogram model (Barnett, 2015). The NS variograms for the four variables are shown in Figure 7.4.

Sgsim is used to obtain the reference models of all four PPMT variables. NS values are then back-transformed using transformation tables of each variable and *ppmt_b*. Output simulation models are shown in Figure 7.5.

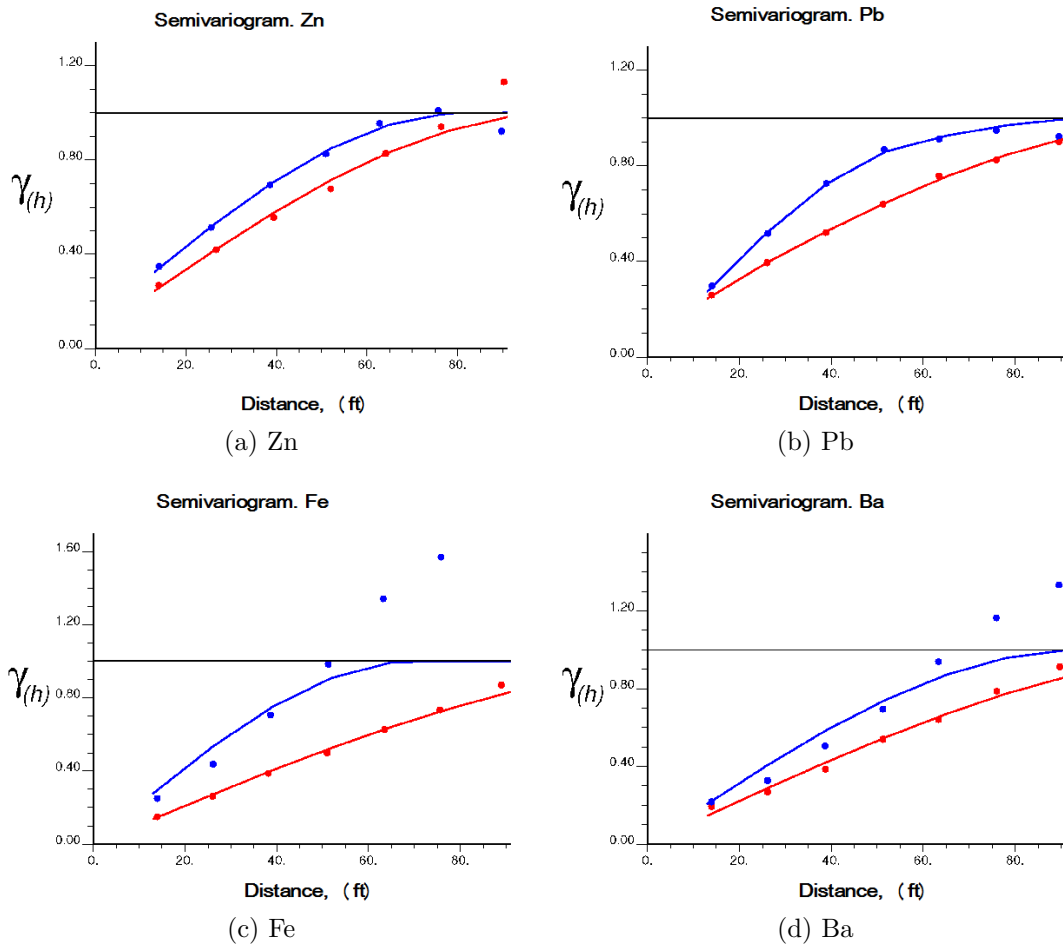


Figure 7.4: Variogram models for all four variables in normal scores

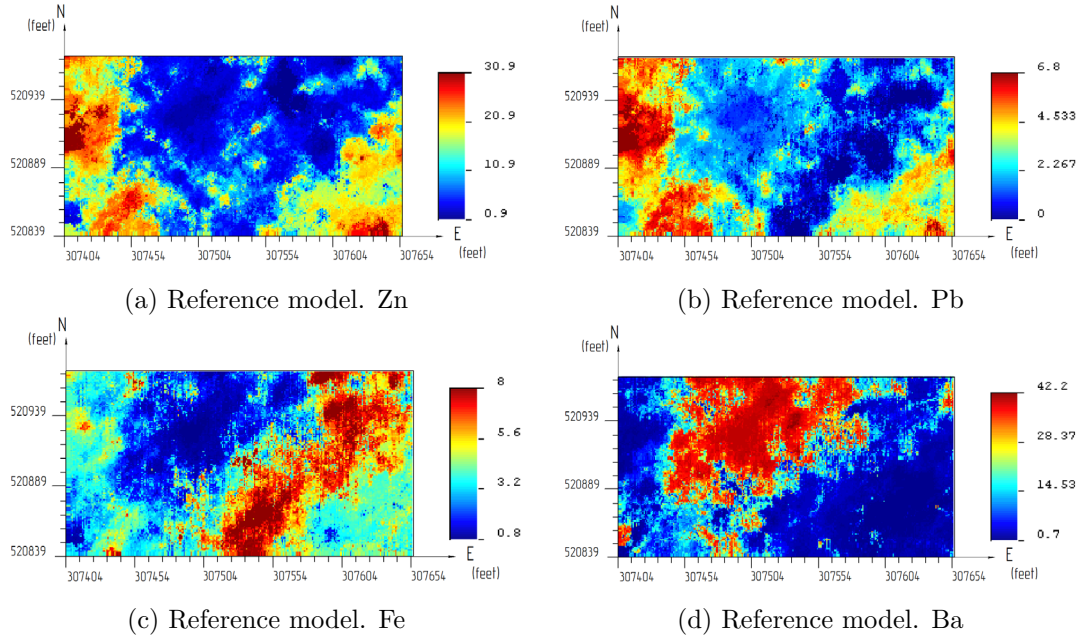


Figure 7.5: Simulated reference models for all four variables

Data reproduction

Distributions of original BH and simulated data after back-transformation are compared using Q-Q probability plots. 100 realizations of simulated data are checked. Values corresponding to the same quantiles of two distributions are plotted against each other. The closer a point to a 45 degrees line at a Q-Q plot, the better data reproduction is. The Q-Q plots for each variable are in Figure 7.6. They show a good data reproduction for all four variables.

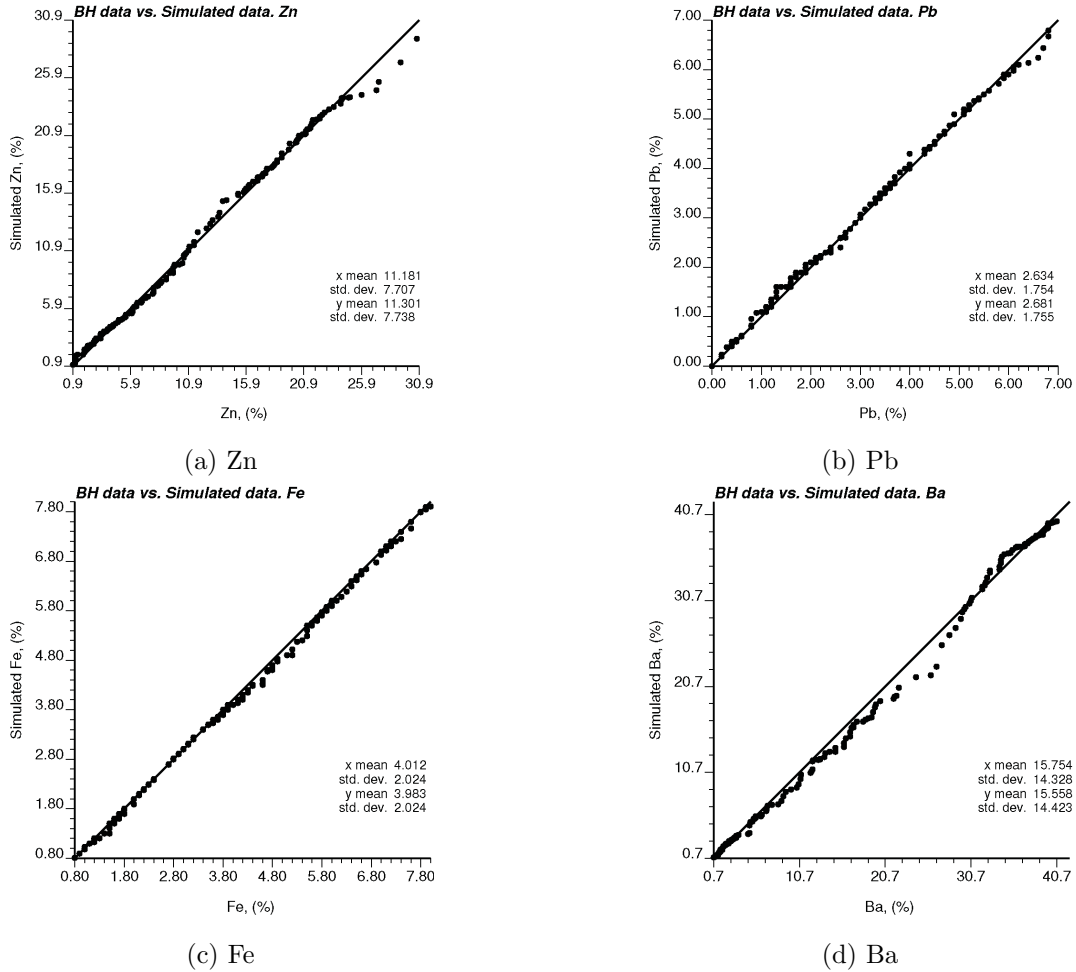
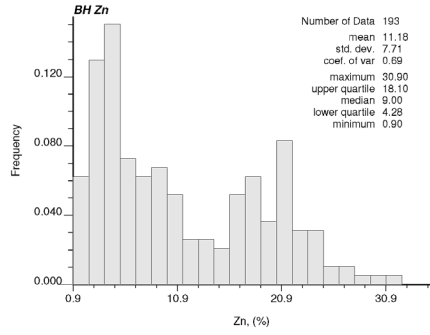


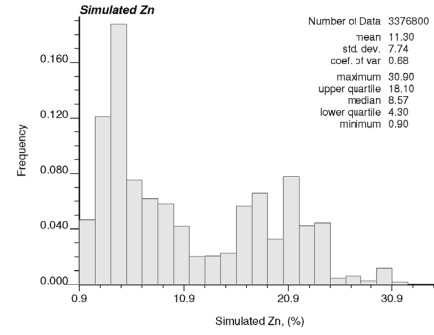
Figure 7.6: Q-Q plots between original and simulated data for all four variables

Histogram reproduction

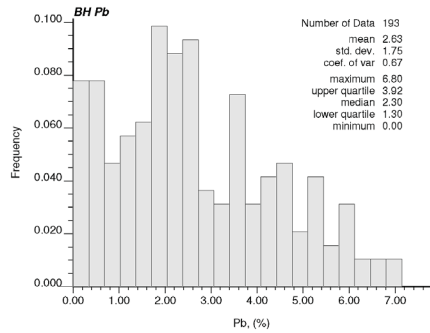
The reproduction of the histogram shape as well as mean and variance of the original data are important checks. The means and standard deviations of simulated values should be similar to the means and standard deviations of the original BH data with some insignificant fluctuations. The shapes of histograms should also be close. The check is performed over 100 simulation realizations. In Figure 7.7, the histograms of BH data are plotted against the histograms of simulated data of all four variables. Overall, the shapes of histograms and accompanying statistics are reproduced reasonably good.



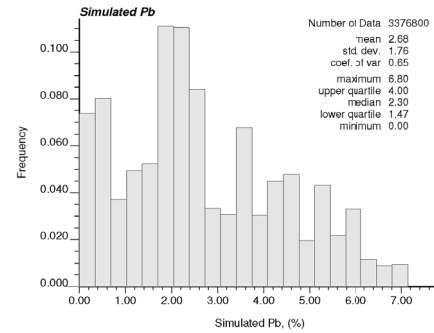
(a) Histogram. BH Zn



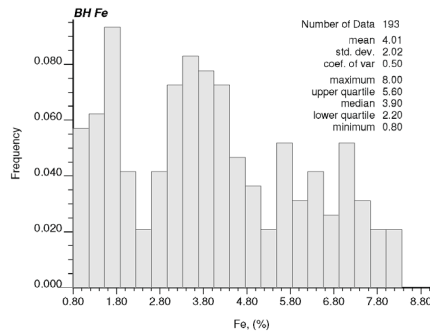
(b) Histogram. Simulated Zn



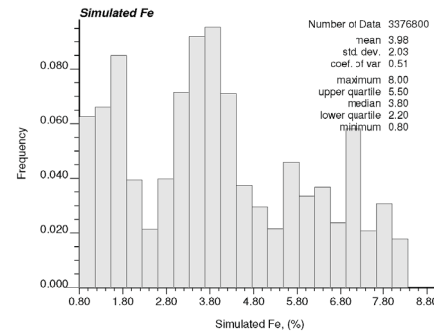
(c) Histogram. BH Pb



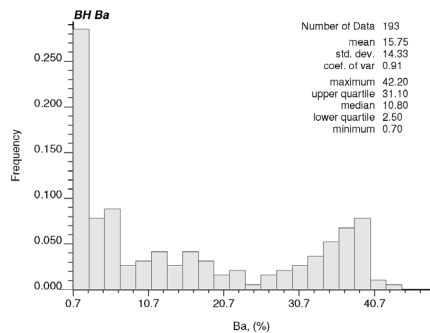
(d) Histogram. Simulated Pb



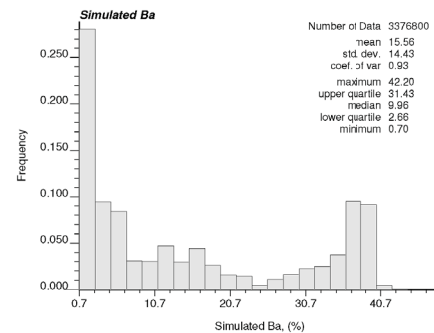
(e) Histogram. BH Fe



(f) Histogram. Simulated Fe



(g) Histogram. BH Ba



(h) Histogram. Simulated Ba

Figure 7.7: Comparison of histograms of original and simulated data for all four variables

Variogram reproduction

Some statistical fluctuations are expected. The variograms of ten simulated realizations are compared to the NS variograms (Figure 7.8). The major and minor directions of continuity of the NS variograms are represented by purple and green point respectively. The major and minor directions of continuity of the variograms of the simulated realizations are represented by red and blues dashed lines respectively. Each pair of the green and blue dashed lines corresponds to one simulated realization. It is clear from the figure that the NS variograms are reproduced very good.

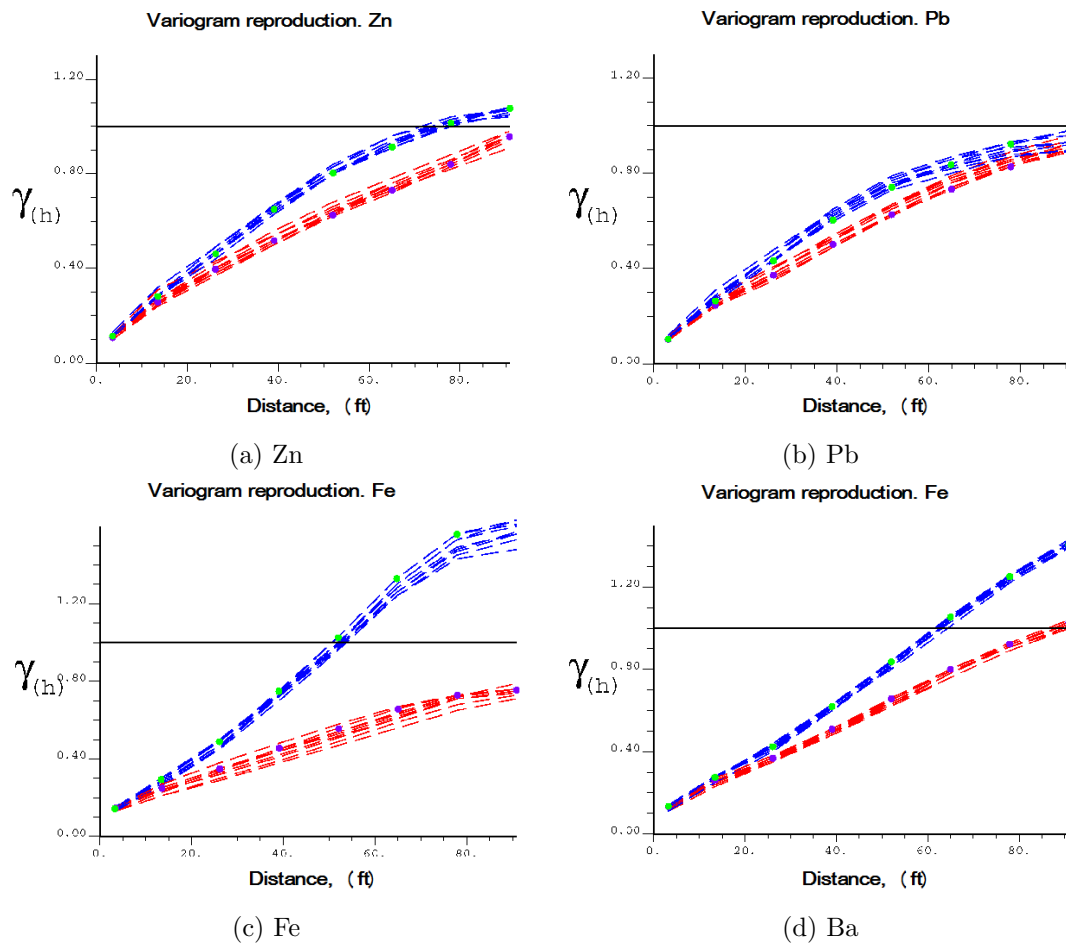
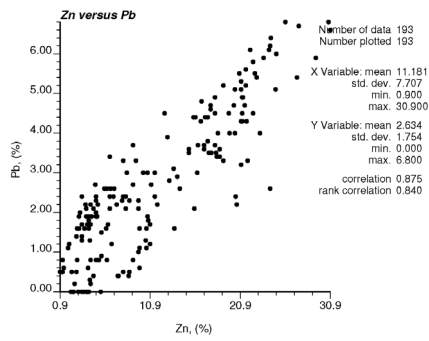


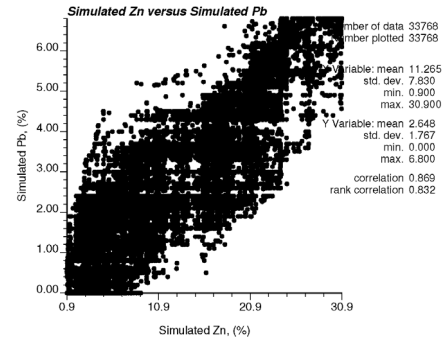
Figure 7.8: Variogram reproduction for all four variables

Reproduction of bivariate relationships

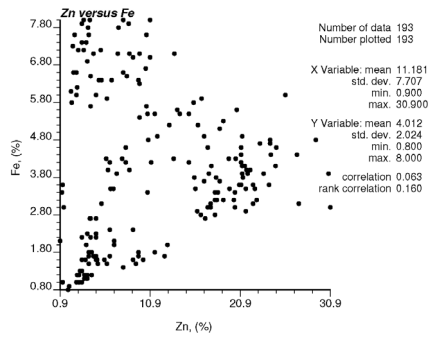
After simulated models are back-transformed to original units, bivariate relationships between data are checked. One of the advantages of simulation over estimation is the ability to reproduce bivariate statistics between all variables along with univariate. In this particular case study, the recovery of Zn is dependent on the content of other chemical elements and the relationships between them. For example, the stockpile blending criterion $\text{Zn}/\text{Pb} \geq 2.5$ indicates that it is not desirable for grade control to ignore the bivariate relationships between Zinc and Lead. According to the stockpile blending criteria, it is important for the simulated models to reproduce univariate statistics for Zn and Ba as well as Zn-Pb and Zn-Fe bivariate relationships. Of course, all the bivariate and univariate statistics could be important for grade control decisions and should be addressed in the resultant simulated models. The most important bivariate relationships between Zn, Pb, and Ba are illustrated in Figure 7.9. The scatter plots of the BH data are shown against the scatter plots of simulated data. Overall, the bivariate relationships between the variables of interest are reproduced in the simulated models.



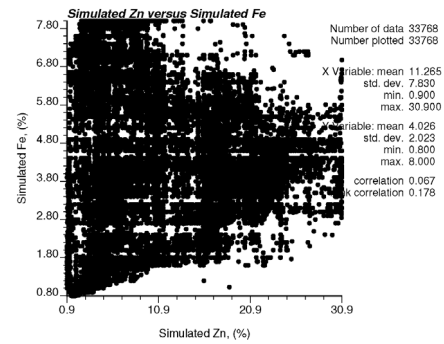
(a) BH Zn-Pb



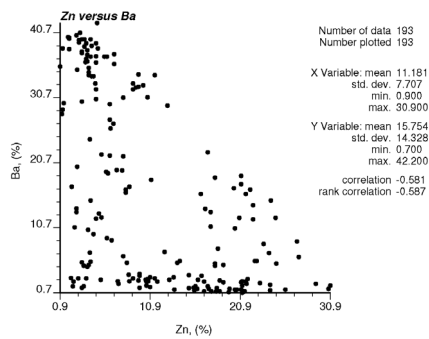
(b) Simulated Zn-Pb



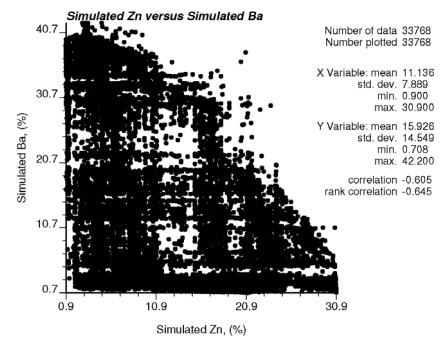
(c) BH Zn-Fe



(d) Simulated Zn-Fe



(e) BH Zn-Ba



(f) Simulated Zn-Ba

Figure 7.9: Bi-plots of data in original units versus bi-plots of simulated data

After the reference model is validated, all four simulated models are merged in one ore/waste indicator map according to the stockpile blending criteria mentioned above. The stockpile blending criteria illustrated in Figure 7.1 are

coded inside a small Fortran code as follows:

$$U(Zn(\mathbf{u})) = \begin{cases} 0, & Zn(\mathbf{u}) < 5 (\%); \\ \tan a_1 \times Zn(\mathbf{u}) - 5 (\%), & Zn(\mathbf{u}) \geq 5 (\%); \end{cases} \quad (7.1)$$

where $U(Zn(\mathbf{u}))$ is the utility function of Zn; a_1 is the angle of inclination of the $U(Zn)$ line from Figure 7.1; $Zn(\mathbf{u})$ is the grade of Zn at a location \mathbf{u} .

$$P1(Zn/Pb(\mathbf{u})) = \begin{cases} 0, & Zn/Pb(\mathbf{u}) \geq 2.5; \\ \tan a_2 \times (2.5 - Zn/Pb(\mathbf{u})), & Zn/Pb(\mathbf{u}) < 2.5; \end{cases} \quad (7.2)$$

where $P1(Zn/Pb(\mathbf{u}))$ is the penalty function for not complying with the first stockpile blending criterion; a_2 is the angle of inclination of the $P1(Zn/Pb)$ line from Figure 7.1; $Zn/Pb(\mathbf{u})$ is the value of the stockpile blending constraint at the location \mathbf{u} .

$$P2(Zn/Fe(\mathbf{u})) = \begin{cases} 0, & Zn/Fe(\mathbf{u}) \geq 3.65; \\ \tan a_3 \times (3.65 - Zn/Fe(\mathbf{u})), & Zn/Fe(\mathbf{u}) < 3.65; \end{cases} \quad (7.3)$$

where $P2(Zn/Fe(\mathbf{u}))$ is the penalty function for not complying with the second stockpile blending criterion; a_3 is the angle of inclination of the $P2(Zn/Fe(\mathbf{u}))$ line from Figure 7.1; $Zn/Fe(\mathbf{u})$ is the value of the stockpile blending constraint at the location \mathbf{u} .

$$P3(Ba(\mathbf{u})) = \begin{cases} 0, & Ba(\mathbf{u}) < 10 (\%); \\ \tan a_4 \times (Ba(\mathbf{u}) - 10 (\%)), & Ba(\mathbf{u}) \geq 10 (\%); \end{cases} \quad (7.4)$$

where $P3(Ba(\mathbf{u}))$ is the penalty function for not complying with the third stockpile blending criterion; a_4 is the angle of inclination of the $P3(Ba)$ line from Figure 7.1; $Ba(\mathbf{u})$ is the grade of Ba at the location \mathbf{u} .

The total utility function is expressed as follows:

$$T. \text{ utility}(\mathbf{u})|decision = U(Zn(\mathbf{u})) - P1(Zn/Pb(\mathbf{u})) - P2(Zn/Fe(\mathbf{u})) - P3(Ba(\mathbf{u})) \quad (7.5)$$

where $T. \text{ utility}(\mathbf{u})|decision$ is the total utility or loss at a location \mathbf{u} given a grade control decision. These functions and parameters are illustrative, but not what Red Dog Mine considers.

The reference map is illustrated in Figure 7.10. This reference is used throughout the case study for comparison and further manipulations.

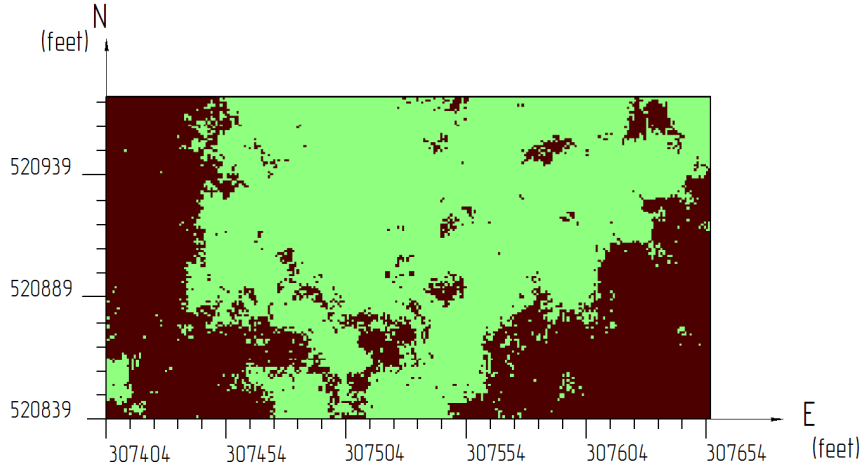


Figure 7.10: Reference ore/waste map for the Red Dog case study

7.4 Optimal Grid Size

As mentioned above, the short-term grade control models at Red Dog mine are constructed using ordinary kriging (OK) at $25' \times 25' \times 25'$ resolution. The variograms in original units are calculated and modeled for using with OK. According to the information from Teck Cominco Alaska Inc. (2009), the OK kriging interpolation is performed in 2 passes separately for each variable. The first pass is performed using $100' \times 100' \times 60'$ search ellipses and from 3 to 7 sample data. The second pass is performed using a two times smaller search

of $50' \times 50' \times 30'$ and from 4 to 7 sample data. This 2 pass-technique is used for conducting short-term grade control models at the Red Dog mine.

The purpose of this section is defining a reasonable kriging grid size for a particular Red Dog mine bench. The procedure consists of the following steps:

- i) Calculate and model the variograms of original data.
- ii) Perform the 2-pass kriging interpolation at different grid sizes in the range of 0.1-1.9 of sample spacing (14 feet) or 1-25 feet.
- iii) Re-grid estimates to the resolution of the reference model.
- iv) Apply stockpile blending criteria to OK estimates to obtain ore/waste indicator maps.
- v) Compare the estimates to the reference model at each node.
- vi) Summarize results.

Examples of the ore/waste indicator maps obtained using OK are in Figure 7.11.

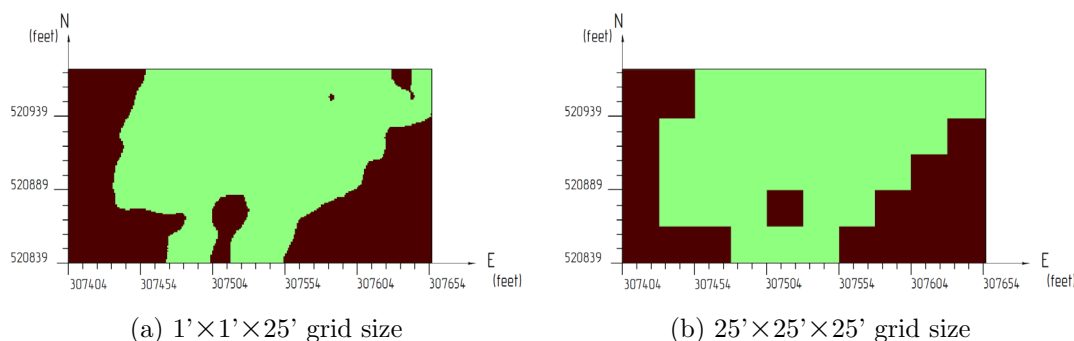
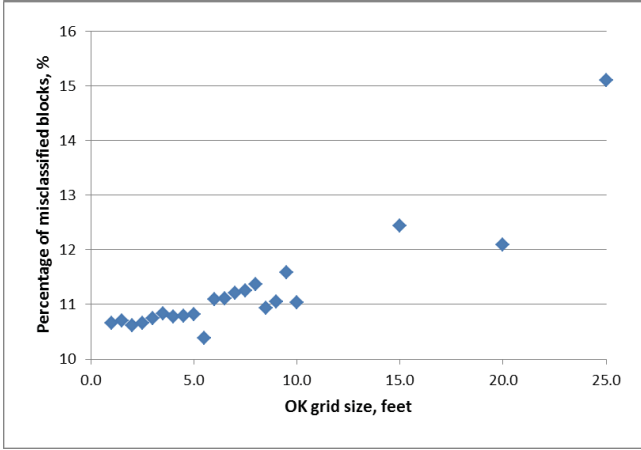


Figure 7.11: Ordinary kriging ore/waste indicator maps

Even looking at these two maps, it is possible to say that the coarser grid is losing some information. For instance, the ore zone at the top right corner is misclassified. The effectiveness of estimation at different grid sizes is summarized in Table 7.1. The percentage of misclassified blocks for the reasonable range of grid sizes (10-50 % of the BH sample spacing) varies from 10.3 to 11.2 % of all the blocks of the mine bench. The reasonable range of grid sizes can be reduced to 10-40 % of the sample spacing for this case study. Looking at

a graph in Figure 7.12, it is possible to confirm that after exceeding a threshold of 0.39 for GSS ($5.5' \times 5.5'$ grid size), the percentage of misclassified blocks increases (Chapter 3).



(a) $1' \times 1' \times 25'$ grid size

Figure 7.12: Percentage of misclassified blocks for different grid sizes (Red Dog case study)

Table 7.1: Effectiveness of ore/waste classification at different grid sizes for the Red Dog mine

Grid size, feet	1.0	1.5	2.0	2.5	3.0	3.5	4.0	4.5	5.0	5.5	6.0	6.5	7.0	7.5	8.0	8.5	9.0	9.5	10.0	15.0	20.0	25.0
Kriging grid size/sample spacing ratio (GSS)	0.07	0.11	0.14	0.18	0.21	0.25	0.29	0.32	0.36	0.39	0.43	0.46	0.50	0.54	0.57	0.61	0.64	0.68	0.71	1.07	1.43	1.79
Number of misclassified blocks	3601	3615	3585	3598	3631	3663	3637	3645	3653	3506	3747	3750	3783	3804	3841	3692	3733	3912	3729	4199	4081	5102
Percentage of misclassified blocks, %	10.66	10.71	10.61	10.66	10.75	10.84	10.77	10.79	10.82	10.38	11.09	11.11	11.21	11.26	11.37	10.94	11.05	11.58	11.04	12.44	12.09	15.11

Conclusions

The data from Table 7.1 and 7.12 show that with increasing the GSS ratio the percentage of misclassified blocks consistently increases. Overall, the graph in Figure 7.12 resembles the shape of the curve from Figure 6 in Chapter 3. The incremental error from Chapter 3 is just a residual of some initial percentage of misclassified blocks. The experimental points at Figure 7.12 are sparse because they are not averaged over many realizations as in Chapter 3.

According to the data from Table 7.1 and Figure 7.12, the reasonable grid

size for grade control models is in the range from 1'×1'×25' to 5.5'×5.5'×25'. It corresponds to the GSS ratio in the range from 0.1 to 0.4.

The average percentage of misclassification in the optimal range of grid sizes is 4.4 % less on average than the percentage of misclassification for the reported 25' block size.

7.5 Estimation Versus Simulation

Multiple realizations are used for developing grade control ore/waste indicator maps. The stockpile blending criteria are incorporated in calculations in a similar manner as in Equations 7.1-7.4. The only difference is that the final ore/waste classification is made according to an expected total utility value. It is obtained from 100 realizations. The expected total utility can be expressed as follows:

$$\begin{aligned} \text{Expected utility}^l(\mathbf{u})|decision &= \frac{1}{L} \sum_{l=1}^L (U(Zn^l(\mathbf{u})) - P1(Zn/Pb^l(\mathbf{u})) \\ &\quad - P2(Zn/Fe^l(\mathbf{u})) - P3(Ba^l(\mathbf{u}))) \end{aligned} \quad (7.6)$$

where $\text{Expected utility}^l(\mathbf{u})|decision$ is the expected profit or loss obtained at a model's location \mathbf{u} in a realization l given a grade control decision; L is a total number of realizations; $U(Zn^l(\mathbf{u}))$ is the utility of Zn at the location \mathbf{u} in the realization l given the grade control decision; $P1(Zn/Pb^l(\mathbf{u}))$ is the penalty for not complying with the first stockpile blending criterion at the location \mathbf{u} in the realization l given the grade control decision; $P2(Zn/Fe^l(\mathbf{u}))$ is the penalty for not complying with the second stockpile blending criterion at the location \mathbf{u} in the realization l given the grade control decision; $P3(Ba^l(\mathbf{u}))$ is the penalty for not complying with the third stockpile blending criterion at the location \mathbf{u} in the realization l given the grade control decision.

Estimation and simulation models are constructed at the same resolution.

The previous section provides recommendations on the reasonable grid size for the current mine bench. The reasonable resolution for grade control models is chosen to be $3' \times 3' \times 25'$. The construction of grade control models at this grid size does not require extensive computational time and theoretically provides a minimum amount of misclassification. In order to compare the effectiveness of estimation and simulation for short-term grade control, the following steps are performed:

- i) Define a grid size for estimation and simulation.
- ii) Perform estimation using ordinary kriging.
- iii) Re-grid the models of each variable to the resolution of the reference distribution.
- iv) Obtain estimation ore/waste indicator maps using Equation 7.5 at each location.
- v) Simulate 100 realizations for each variable.
- vi) Re-grid the models of all the variables and all the realizations to the reference resolution.
- vii) Obtain simulation ore/waste maps using Equation 7.6.
- viii) Compare simulation and estimation ore/waste maps to the reference model at each location.

Estimation and simulation ore/waste indicator maps at $3' \times 3' \times 25'$ resolution are provided in Figure 7.13.

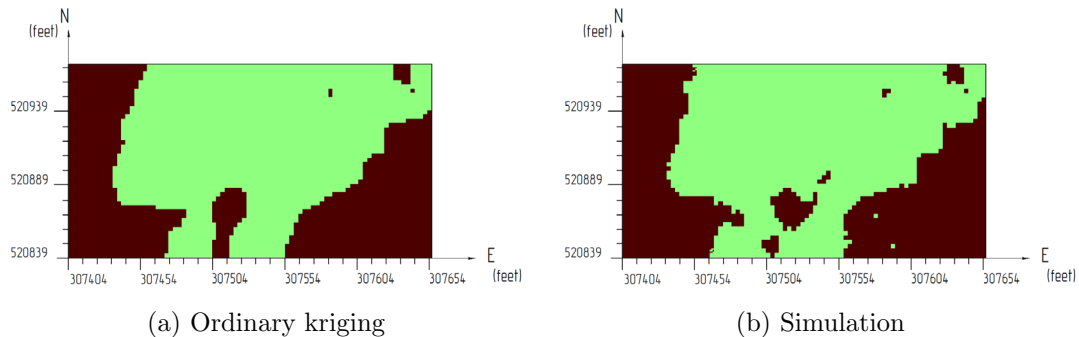


Figure 7.13: Ore/waste indicator maps at $3' \times 3' \times 25'$ resolution

Conclusions and discussion

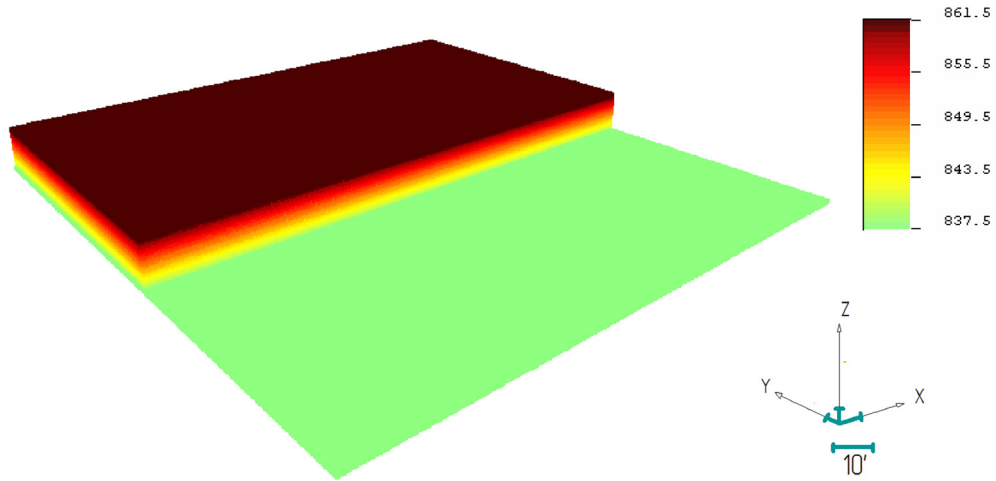
Simulation provides more selective and precise grade control models. Simulation and estimation produced 9.86 % and 10.75 % of misclassified blocks respectively. The difference between methods is 0.89 % or 7 513 ft³ more mined material sent in the correct destination.

The amount of loss and dilution is not discriminated for this case study. The utility functions in Figure 7.1 are chosen arbitrarily. Therefore, they may incorrectly reflect the penalties for processing waste or losing ore.

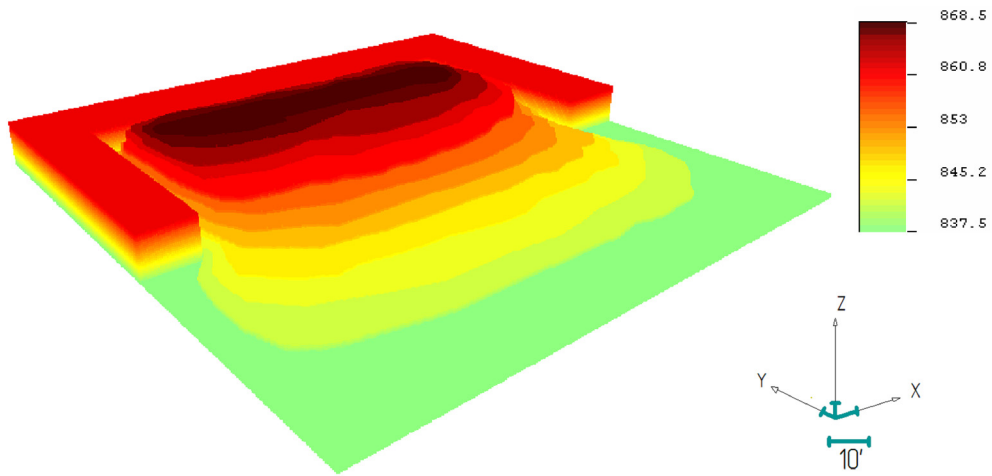
7.6 Blast Movement

The blast movement program (*bmov*) is used for this part of the case study to approximately assess the influence of the displacement of grades during blasting on the effectiveness of short-term grade control. An OK kriging ore/waste indicator map at the resolution of 25'×25'×25' is used as a reference estimate. The available BH data provide elevations of each blasthole's collar. These data can be used to create a pre-blast topographic surface needed as an input to *bmov*. The elevation values are interpolated using inverse distance method in order to get a gridded surface file. The dimensions of the mine bench define a pre-blast polygon. The mine bench is aligned with the Y axis. It has 2 free faces: in the South and the vertical directions. This causes the movement of rocks during blasting preferentially along the Y axis in the South direction and upward.

The post-blast topographic surface is created artificially. The synthetic post-blast geometry aims to mimic a real post-blast muckpile. The spread of rocks is assumed to be significant with the swell factor of approximately 1.35. A post-blast polygon outlines the post-blast muckpile. The pre- and post-blast topographic surfaces are illustrated in Figure 7.14.



(a) Pre-blast



(b) Post-blast

Figure 7.14: Topographic surfaces for Bench 20177

The purpose of this part is comparing a model obtained using the dig limits approach with the output model of *bmov*. Thus, some post-blast 3-D model with the dig limits translated onto it should be constructed. A Fortran code is developed to transfer pre-blast dig limits onto the post-blast muck pile surface. This grade control dig limits model is also constructed in 3-D.

After the *bmov* and dig limits models are obtained, it is possible to compare ore/waste indicators at all locations. The models are constructed at the same resolution.

The workflow of this part of the case study can be summarized as follows:

i) Obtain pre- and post-blast topographic surfaces and polygons.

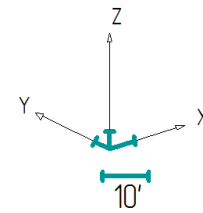
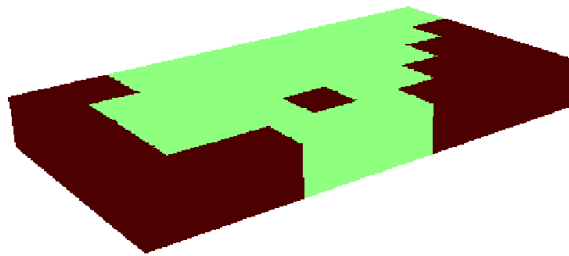
ii) Use *bmov* to obtain the pre- and post-blast 3-D models.

iii) Construct a 3-D model for the dig limits case.

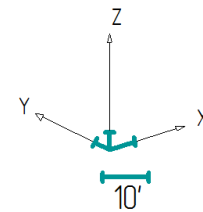
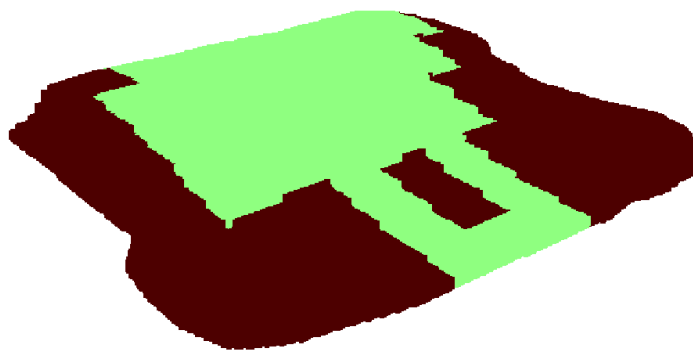
iv) Compare the output post-blast models at each location at 1'×1'×1' resolution and assess a percentage of mismatch.

v) Summarize results

The pre-blast reference estimate and the post-blast muckpile with dig limits are shown in Figure 7.15.



(a) Pre-blast



(b) Post-blast

Figure 7.15: 3-D models for the dig limits case

The *bmov* output model is in Figure 7.16.

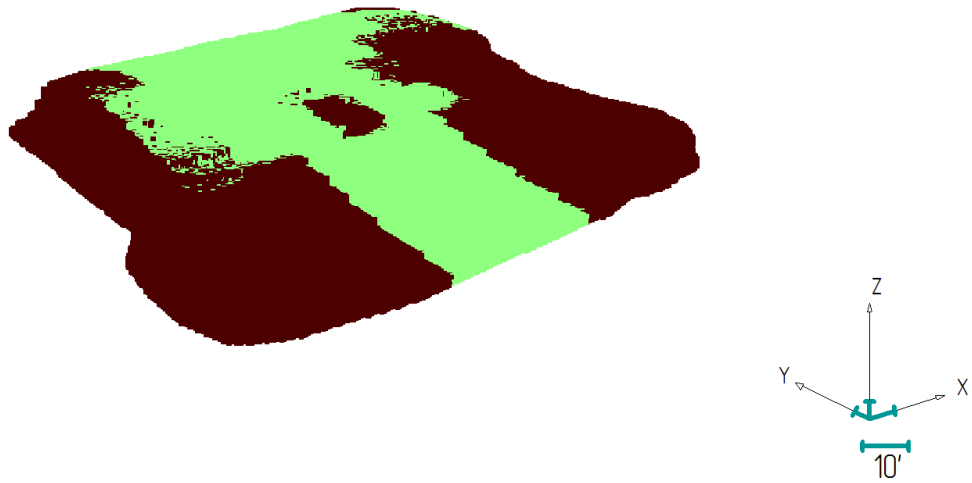


Figure 7.16: The output of BMOV

Bmov achieved a satisfactory fit of nodes between the pre- and post-blast models: 844 200 versus 844 175. The mismatch between two 3-D grade control models is 44.3 % out of all the nodes. Such a significant difference is mostly due to incorrect ore/waste volumes of the post-blast dig limits model. Accounting for the swell factor of 1.35, the difference between the ore volumes is 17.1 %; the difference between the waste volumes is 9.1 %. Another factor is the manual transformation of the shapes of the pre-blast dig limits onto the post-blast muckpile surface.

The pre-blast 3-D model with dig limits evidently shows more ideal picture when the dig limit lines are translated at the post-blast muckpile directly. Nevertheless, it is challenging to match the ore/waste volumes of the pre- and post-blast models; manual matching the volumes of the polygons could be an iterative and time consuming process.

The *bmov* model is built using the pre- and post-blast topographic surfaces. It accounts for the details of the post-blast geometry. The ore/waste volumes of the post-blast 3-D model are correct because they are automatically transferred from pre-blast 3-D model. The synthetic post-blast topographic surface cannot provide the correct blast movement model. It only shows the approximation

of *bmov*. The post-blast model in Figure 7.16 shows some artifacts at the top of the muckpile. They could appear due to a non-optimal artificial post-blast topography or due to using *bmov* without tuning to real mine's conditions. Therefore, a real life blast movement pattern could be different. It is not known, for example, how far a small ore zone at the middle of the mine bench should be moved. Additional data could help to correct the blast movement pattern.

It would be necessary to further adjust *bmov* to the real conditions of blasting at Red Dog. The current example serves only as an illustration of the blast movement assessment procedure.

7.7 Truck-by-Truck Selection

Dig limit lines or polygons are drawn manually or using computer-aid design (CAD) programs. The dig limits may be adjusted to the outlines of ore and waste zones with respect to equipment limitations or some expected profit calculations. Usually, practitioners tend to use geometrically simple polygons without acute angles to delimit different types of mined rocks. Small zones of waste material inside ore polygons are usually disregarded as well as small ore zones inside waste polygons. Once the dig limit polygons are obtained, they are approximately translated onto the post-blast muckpile. An example of such a translation is in Figure 7.15.

The biggest disadvantage of the dig limits (DL) approach is using manual limits. Chapter 3 reviews new approaches for adjusting dig limits to post-blast 3-D muckpile using blast measurements (Isaaks, Treloar, & Elenbaas, n.d.) and pre- and post-blast 3-D models. Dig limits are expressed as coordinates onto the surfaces of these 3-D models. Following digitized dig limits at the post-blast surface of the mine bench by excavating equipment requires a precise GPS dispatching system.

Having such a GPS system allows changing the way grade control decisions are made. It is not expedient to make decisions for big polygons. The decisions should be made for a smaller amount of mined material. The smallest amount of rocks that is possible to extract selectively is one truck load. Therefore short-term grade control decisions should be made based on this minimum amount of mined material and the way it is excavated. That is, the sequence and shape of each scoop should be modeled throughout all the mine bench. A profit from several scoops should be averaged for a truck load.

A theoretical experiment has been conducted to compare the DL and TBT methods. An ore/waste indicator map for the dig limits case is developed using an OK estimate at $3' \times 3' \times 25'$ resolution. It is used for defining destinations for each truck load. It is done by calculating the probability of being ore for each truck-based unit. After the mine bench is delimited by the truck-based units, it is checked against the reference ore/waste indicator map. For the TBT method, no dig limits are needed. Grade control decision are made using the total profit of each scoop over 100 realizations. This part of the case study includes the following steps:

- i) Choose the equipment for excavating and hauling mined material.
- ii) Determine geometrical shapes and the sequences of scoops for each piece of the excavating equipment.
- iii) Delimit the mine bench to ore and waste zones manually for the dig limits case and obtain a digitized dig limits map.
- iv) Delimit the mine bench by truck-based units using the TBT and dig limits approaches.
- v) Compare the resultant ore/waste maps to the reference ore/waste indicator map at $1' \times 1' \times 25'$ resolution.
- vi) Check different types of the excavating equipment.
- vii) Incorporate random offsets to the positioning of scoops in the course of excavation (dispatching errors).

viii) Check the influence of sampling errors on the performance of both methods.

ix) Summarize the results of the TBT- and dig limits-based selection for both methods and all types of equipment.

Three types of the excavating equipment are compared for this case study: Caterpillar 992G front loader, Caterpillar 6018 hydraulic excavator and P&H 1900AL electric rope shovel. The Red Dog mine actually uses Caterpillar 992G loaders and Caterpillar 777D haul trucks (Teck Resources Limited, n.d.). Each piece of excavating equipment in combination with the Caterpillar 777D haul truck constitutes a unique selection scheme. Equipment specifications are taken from Caterpillar (n.d.-b), Caterpillar (n.d.-a), Caterpillar (n.d.), Joy Global (n.d.) and Red Dog documentation Teck Resources Limited (n.d.). Some of assumptions include (Teck Resources Limited, n.d.): i) swell factor is 1.3, ii) the bulk density of rocks is 12.25 ft³, and iii) CAT777d payload is 83.6 tonnes/load. Important parameters are summarized in Table 7.2.

Table 7.2: Technological parameters of equipment related to the TBT selection

	Bucket volume, ft ³	Bucket fill factor	Dimensions of cut, ft ³	Number of passes
Caterpillar 992G	335.48	1	15.82×0.8×25	4
Caterpillar 6018	301.8	0.85	3.5×3.5×25	4
P&H 1900AL	315.9	0.83	3×3×25	4

The ore/waste map with hand drawn digitized polygons for the dig limits case is in Figure 7.17. These ore/waste indicators are then used to calculate the probabilities of being ore inside the truck-based units.

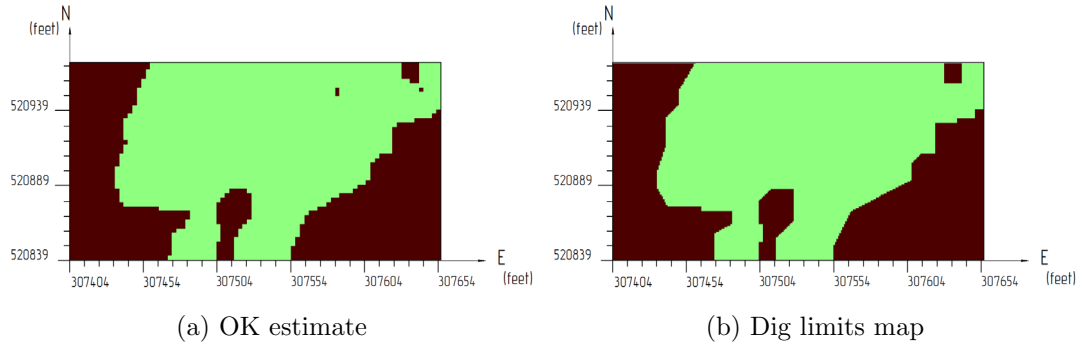


Figure 7.17: Ore/waste indicator map with digitized dig limits for the selection of ore

The dimensions of cuts in Table 7.2 define geometrical parameters of each scoop for each type of the excavating equipment with some reasonable approximations. Several scoops comprise a truck load. The reference ore/waste map is delimited by the truck-based units for each type of the excavating equipment, as it is shown in Figure 7.18.

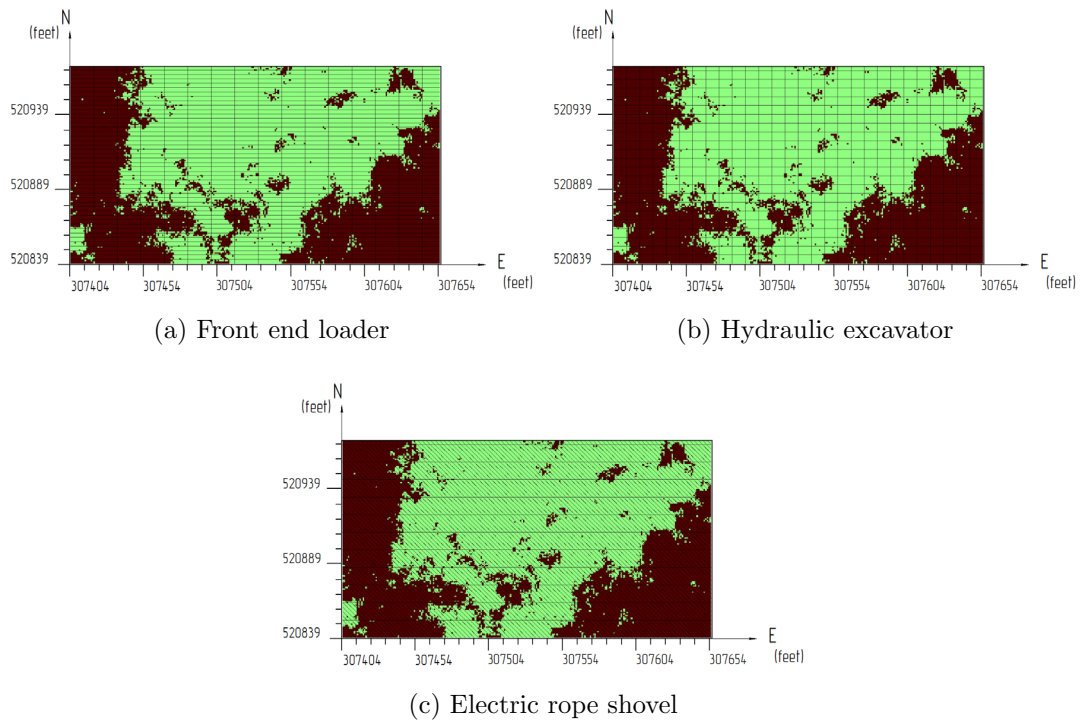


Figure 7.18: Reference ore/waste indicator maps discretized by the units equal to one truck load

Dispatching errors

In a real life excavation process, some random offsets from designed positions could occur. A precise dispatching system is very important for the TBT method. It should be mentioned that accurate navigation is very important for advanced dig limits methods as well; it is used to follow optimized and complex dig limits lines.

A random offset is added to each scoop of the excavating equipment to assess the influence of imprecise navigation. Schematically, the directions of possible offsets are illustrated in Figure 7.19 for each type of excavating equipment.

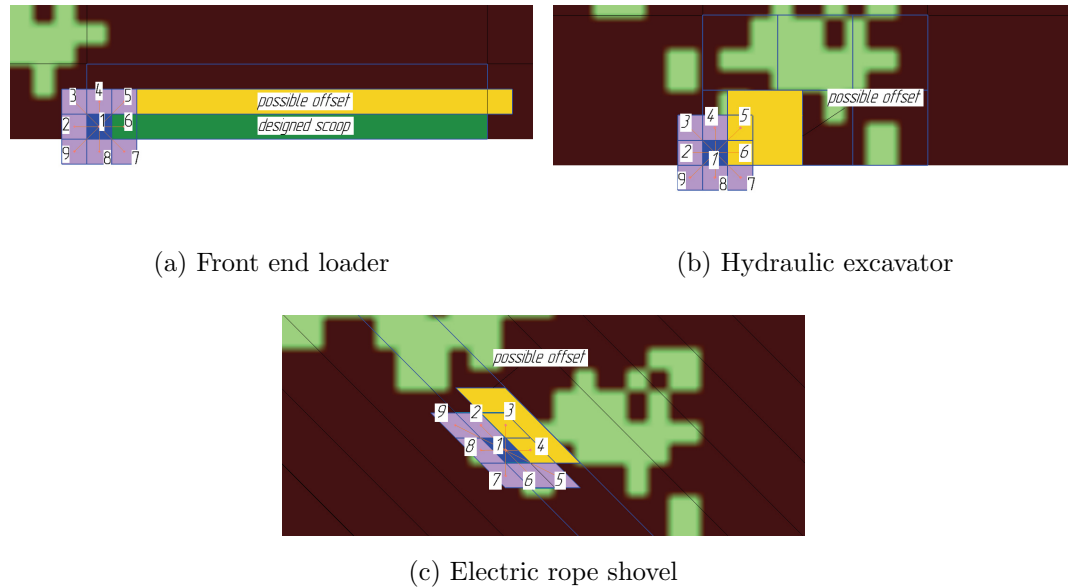


Figure 7.19: Possible directions of displacement from modeled positions for each type of excavating equipment

Some precautions are set inside the code 'performing' excavation. They prohibit the scoops from overlapping and digging material already excavated. These preventive measures may be described as follows: i) the origin of each scoop (blue color in Figure 7.19) cannot go beyond the boundaries of the mine bench (Figure 7.20), ii) the scoops cannot overlap in both horizontal and vertical directions in order not to account for the same data multiple times. For example, if the origin of a scoop is shifted to the direction 5, the next scoop in

the line cannot shift in the directions 3 or 4. (Figure 7.21). The directions 9, 8, and 7 are possible only if there is a material there to excavate. In practice, the plan would not consider navigation errors; it would consider the best possible positioning and best possible decision. Nevertheless, this approach allows checking how navigation errors influence the quality of ore/waste selection.

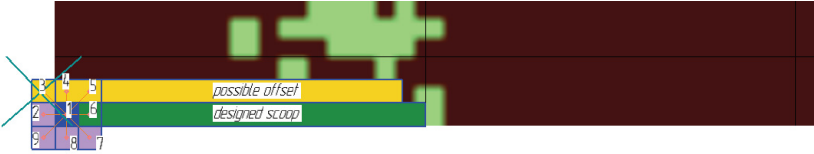


Figure 7.20: A mine block boundary constraint

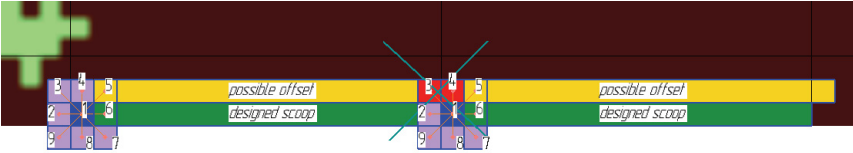


Figure 7.21: An overlap constraint

Decision making

Grade control decisions are based on each truck load unit. A profit is calculated within each truck unit over 100 realizations similar to the simulation grade control method. The profit inside all the truck units is calculated using the formula below.

$$\begin{aligned}
 \text{Expected utility}^l(\mathbf{b})|\text{decision} &= \frac{1}{L} \frac{1}{B} \sum_{l=1}^L \sum_{b=1}^B (U(Zn^l(\mathbf{b})) - P1(Zn/Pb^l(\mathbf{b})) \\
 &\quad - P2(Zn/Fe^l(\mathbf{b})) - P3(Ba^l(\mathbf{b})))
 \end{aligned}
 \tag{7.7}$$

where $\text{Expected utility}^l(\mathbf{b})|\text{decision}$ is the expected profit or loss obtained

from a truck unit with an origin \mathbf{b} in a realization l given a grade control decision; B is the number of blocks inside the truck unit with the origin \mathbf{b} ; L is a total number of realizations; $U(Zn^l(\mathbf{b}))$ is the utility of Zn obtained from the truck unit with the origin \mathbf{b} in the realization l given the grade control decision; $P1(Zn/Pb^l(\mathbf{b}))$ is the penalty for not complying with the first stockpile blending criterion obtained from the truck unit with the origin \mathbf{b} in the realization l given the grade control decision; $P2(Zn/Fe^l(\mathbf{b}))$ is the penalty for not complying with the second stockpile blending criterion obtained from the truck unit with the origin \mathbf{b} in the realization l given the grade control decision; $P3(Ba^l(\mathbf{b}))$ is the penalty for not complying with the third stockpile blending criterion obtained from the truck unit with the origin \mathbf{b} in the realization l given the grade control decision.

The effectiveness of the ore/waste selection for the TBT and DL methods with dispatching errors is calculated as follows:

i) Each scoop of the excavating equipment is randomly shifted from its project position (Figure 7.19).

ii) A number of blocks inside each scoop is counted and an expected profit over 100 realizations is calculated. The expected profit from each shifted scoop is considered to represent a random error.

iii) The profits of all scoops inside one truck selective unit are averaged and a final profit value is assigned to each truck unit. For example, the profits from 6 scoops in Figure 7.20 (b) are averaged inside one truck unit (outlined by blue color).

iv) The influence of the offsets from 1 to 4 feet are checked for each type of excavating equipment.

v) The results are averaged over 100 realizations. With change of a seed number of a random number generator, the direction of offsets are changed for each scoop.

v) The process is performed for TBT and DL approaches.

Sampling errors

The idea is to check how random sampling errors influence the quality of ore/waste selection. The following formula from Neufeld et al. (2006) is used to introduce random errors to the assays of all variables:

$$Z_{\text{with errors}} = (1 + y \times 0.05) \times Z_{\text{original}} \quad (7.8)$$

where y is a standard normal deviate; Z_{original} is original sample data; $Z_{\text{with errors}}$ is the data with random errors.

The errors are normally distributed and unbiased. The value of errors ranges from 0 % to more than 10 %. After the errors are introduced, OK estimates, dig limits lines and expected profit are re-calculated. A new ore/waste indicator map with digitized dig limits is in Figure 7.22. It is again obtained from an OK estimate. The OK estimate in this case is calculated using the BH samples with errors.

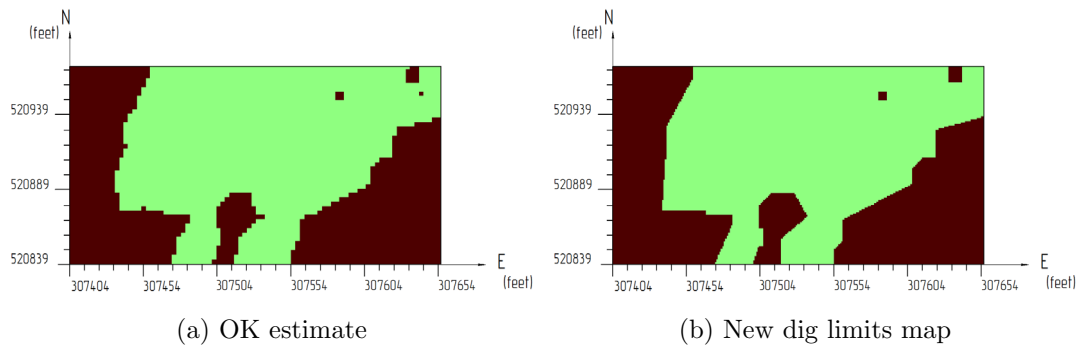


Figure 7.22: Ore/waste indicator map with digitized dig limits for the selection of ore (case with sample errors)

Figure 7.23 shows the mine bench discretized by the front end loader-truck scoops. The cases without dispatching errors and with 3' offset from a project position are provided. Each scoop is colored according to the expected profit. Then, the profit of each scoop is averaged and the final ore/waste indicator maps are obtained (Figure 7.24).

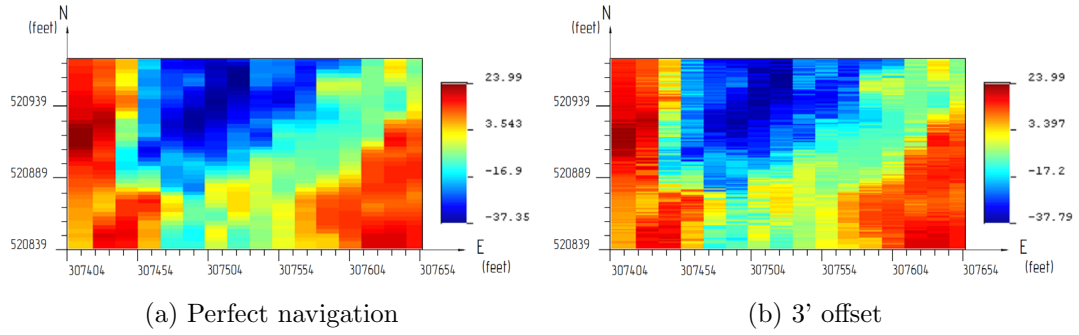


Figure 7.23: Change in expected profit for each scoop of excavating equipment due to 3' offset

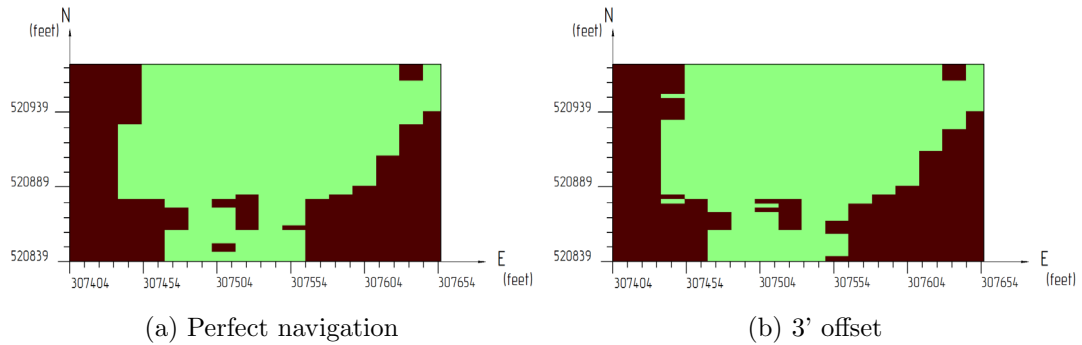


Figure 7.24: Change of ore/waste indicator maps for 'front end loader-truck' units due to 3' offset (TBT method)

The ore/waste indicator maps for dig limits case obtained in a similar way. Ore/waste indicators from the reference ore/waste maps (Figures 7.17 (b) and 7.22 (b)) serve as a basis for the selection of the bench. A truck unit is considered ore if it has more than 50 % probability of being ore. The bench is delimited by truck units similar to the TBT method (Figure 7.25). Irrespective to a grade control method, mined material is selected by truck units.

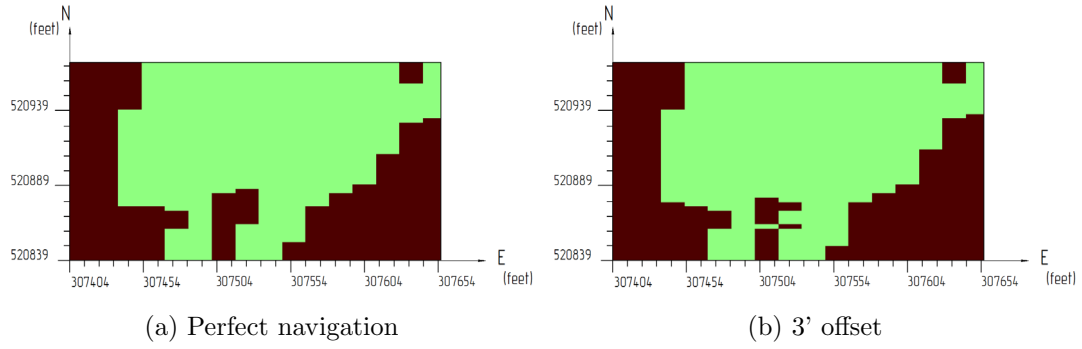


Figure 7.25: Change of ore/waste indicator maps for 'front end loader-truck' units due 3' offset (DL method)

Figures 7.26 and 7.27 represent the TBT and DL ore/waste indicator maps respectively obtained using 'hydraulic excavator-truck' units.

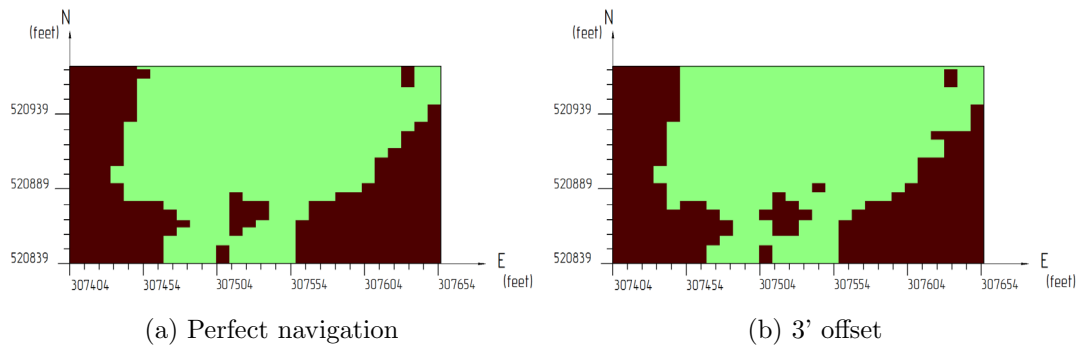


Figure 7.26: Change of ore/waste indicator maps for 'hydraulic excavator-truck units due 3' offset (TBT method)

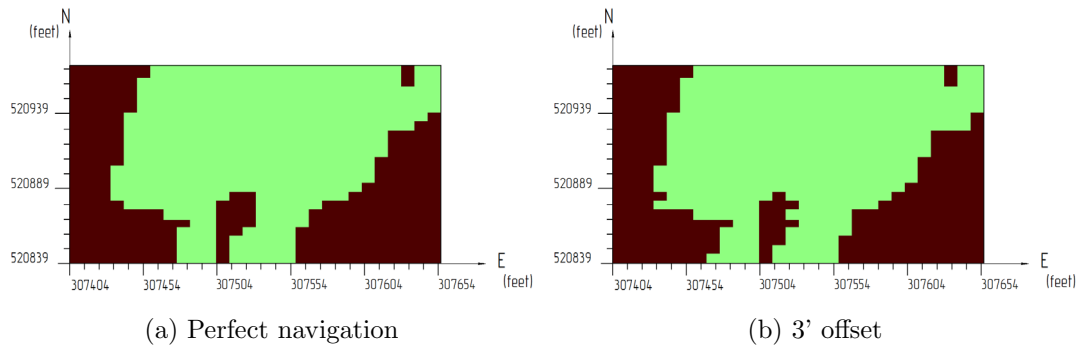


Figure 7.27: Change of ore/waste indicator maps for 'hydraulic excavator-truck' units due 3' offset (DL method)

Figures 7.28 and 7.29 show the TBT and DL ore/waste indicator maps respectively obtained using 'electric rope shovel-truck' units.

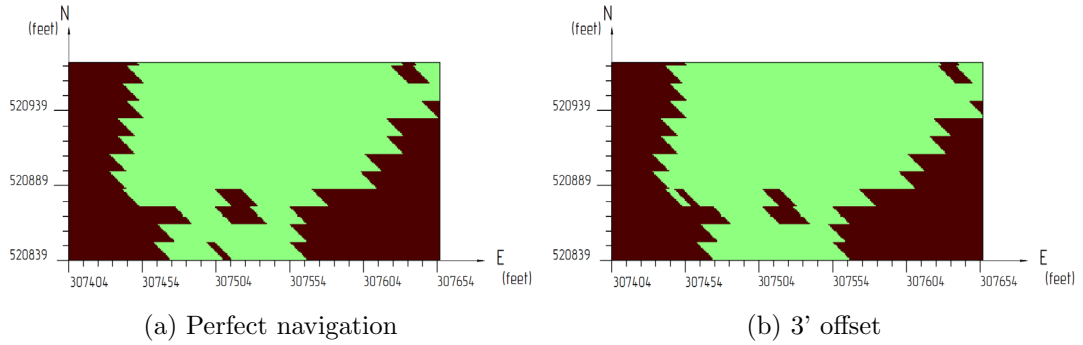


Figure 7.28: Change of ore/waste indicator maps for 'electric rope shovel-truck' units due to 3' offset (TBT method)

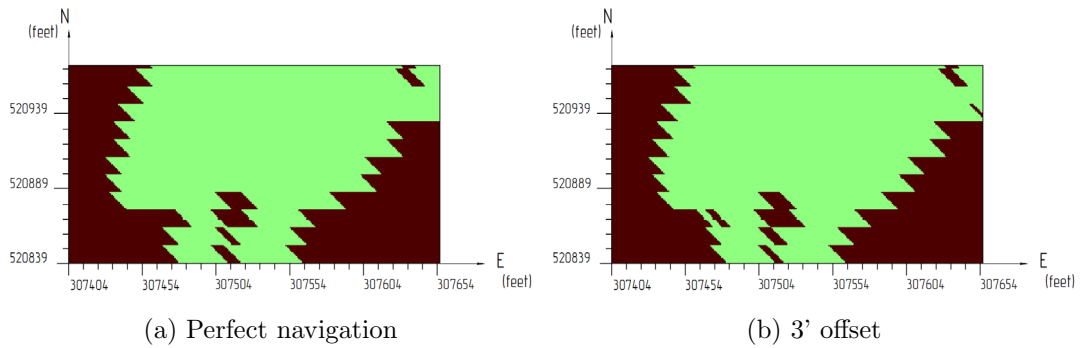


Figure 7.29: Change of ore/waste indicator maps for 'electric rope shovel-truck' units due to dispatching errors (DL method)

Tables 7.3 and 7.4 contain the comparison results of the TBT and DL methods without sample errors.

Table 7.3: Percentage of misclassified blocks produced by the TBT method with different degrees of navigation accuracy

	Equipment	Misclassification errors for different degrees of navigation accuracy, % (over 100 realizations)					Average, %
		0.00	1.00	2.00	3.00	4.00	
TBT method	Offset, feet	0.00	1.00	2.00	3.00	4.00	
	Front end loader	10.38	10.49	10.55	10.71	10.85	10.60
	Rope shovel	11.21	11.14	11.21	11.31	11.46	11.26
	Hydraulic excavator	10.36	10.32	10.20	10.29	10.44	10.32

Table 7.4: Percentage of misclassified blocks produced by the DL method with different degrees of navigation accuracy

	Equipment	Misclassification errors for different degrees of navigation accuracy, % (over 100 realizations)					Average, %
		0.00	1.00	2.00	3.00	4.00	
DL method	Offset, feet	0.00	1.00	2.00	3.00	4.00	
	Front end loader	11.32	11.30	11.41	11.62	12.24	11.58
	Rope shovel	12.02	12.19	12.36	12.35	12.56	12.30
	Hydraulic excavator	11.29	11.33	11.49	11.53	11.68	11.46

In some cases, due to random chance, grade control results improve after introducing dispatching errors. This is unrealistic and due to chance.

The above approach for calculating the percentage of misclassification is repeated for a data set with errors. All calculations for DL method are performed using the changed dig limits map from Figure 7.22 (b). For the TBT method, the total profit at each location is altered due to changes in the sample BH data. The resultant ore/waste indicator maps, delimited by the 'excavating equipment-truck' units, are compared to the initial ore/waste reference indicator map. The results are provided in Tables 7.5 and 7.6.

Table 7.5: Percentage of misclassified blocks produced by the TBT method with different degrees of navigation accuracy (accounting for sampling errors)

	Equipment	Misclassification errors for different degrees of navigation accuracy, % (over 100 realizations)					Average, %
		0.00	1.00	2.00	3.00	4.00	
TBT method	Offset, feet	0.00	1.00	2.00	3.00	4.00	
	Front end loader	12.01	11.91	11.91	12.01	12.10	11.99
	Rope shovel	12.20	12.26	12.39	12.49	12.47	12.36
	Hydraulic excavator	11.17	11.28	11.57	11.70	11.72	11.49

Table 7.6: Percentage of misclassified blocks produced by the DL method with different degrees of navigation accuracy (accounting for sampling errors)

	Equipment	Misclassification errors for different degree of navigation accuracy, % (over 100 realizations)					Average, %
		0.00	1.00	2.00	3.00	4.00	
DL method	Offset, feet	0.00	1.00	2.00	3.00	4.00	
	Front end loader	11.58	11.66	11.77	11.88	12.25	11.83
	Rope shovel	12.36	12.36	12.49	12.56	12.67	12.49
	Hydraulic excavator	11.63	11.66	11.51	11.66	11.87	11.66

Summary of the results and discussion

The truck-by-truck selection method is more flexible than dig limits approach. It implies making grade control decisions based on the expected profit of each scoop of excavating equipment. For this particular case study, the TBT method produced 8.9 % less misclassified blocks than the dig limits approach. This part of the case study does not aim to compare existing grade control procedure at Red Dog to the TBT approach. Therefore, a more reasonable resolution for short-term grade control models is used instead of the actual resolution used at Red Dog (25'×25'×25'). The effectiveness of grade control models at the actual resolution would be worse compared to the TBT grade control method.

The most effective excavating equipment for the short-term grade control is hydraulic excavator due to its maneuverability and the geometrical parameters of its bucket. Hydraulic excavator showed the best performance in all the cases. Rope shovel is considered to be the worst excavating equipment for grade control due to its digging constraints.

Sample errors impact the effectiveness of the TBT method more than DL method for this particular mine bench and modeling workflow. Sample errors caused 11.99 % decrease in the effectiveness of ore/waste classification for the TBT method and only 1.87 % for the DL method on average. It should also be mentioned that the current method to introduce sample errors might cause more than 10 % error for a sample. An appropriate assaying procedure does

not normally produce such large errors.

The size of the mine bench is relatively small compared to the size of the truck-based units. Therefore, the diversity of geological features does not have a significant impact on selectivity here. The dimensional parameters of scoops are too large compared to the ore/waste zones. For bigger benches with more complex geologic features and a larger number of ore/waste categories, the results of deterministic techniques would be worse compared to the TBT method (i.e. Chapter 6). The multivariate modeling workflow also may cause an impact on the effectiveness of TBT. The sensitivity of PPMT plus NS transformation in grade control has not been studied extensively.

7.8 Conclusions and Limitations

The effectiveness of each part of the case study is estimated separately on the example of one mine bench. It is done for a better control over results. It is difficult to objectively assess a combined effect of all grade control improvements, as the case study is partly artificially modeled. The results of such an assessment might not be representative. Overall, each part of the case study showed a significant improvement. The effectiveness of each part of the new grade control workflow is estimated by the total amount of misclassified blocks. The results can be summarized by the following statements:

i) The grid size of short-term grade control models have a significant impact on the correctness of the classification of mined material. The amount of misclassified mined material at the Red Dog mine may be decreased on 29.1 % by using a reasonable grid size for short-term grade control models.

ii) Using simulation instead of estimation at one of the reasonable grid sizes further improves the effectiveness of the ore/waste classification on 8.27 % (9.86 % and 10.75 % for simulation and estimation respectively)

iii) The impact of the blast movement displacement of rocks on the ore/waste

selection of mined material may be very significant depending on a particular blast. A simple and adjustable method for predicting post-blast positions of grades is offered.

iv) The TBT selection method represents the same principle as the simulation ore/waste classification approach but uses the selective units corresponding to one truck load. Using the TBT method instead of ordinary kriging in combination with dig limits results in 1.05 % less misclassified block on average among different types of excavating equipment.

v) The effectiveness of excavating equipment for grade control is governed by the geometrical parameters of shovel and the sequence of scoops.

vi) Dispatching errors impact both the TBT and DL methods: with increasing the distance of random offset from modeled position, the percentage of misclassified blocks increases.

vii) Sample errors may significantly affect the effectiveness of the TBT method over the DL method. This impact is believed to be dependent on the multivariate transformation scheme. For different transformation approaches, the impact of sample errors could be different. Nevertheless, even with a significant amount of sample errors, the performance of the TBT grade control method is still better than the performance of the dig limits grade control method on average.

It should be noted that a many assumptions are used for this case study. A reference model used for assessing the effectiveness of new developments is artificially constructed. It is a single realization of sequential Gaussian simulation. Nevertheless, all the univariate and multivariate relationships, as well as first and second order statistics, are reproduced in the reference models for each variable and the final ore/waste indicator map.

Utility functions for developing the reference ore/waste indicator map and for further calculations are assumed. Actual recovery equations for the variables of interest are not available for this case study. Therefore, final results do not

necessarily reflect the actual Red Dog philosophy for grade control.

Post-blast topography is artificially constructed. Actual post-blast topographic data are not available for this case study. An actual blast movement grade control would involve tuning *bmov* using additional input data.

Dig limits for the last part of the case study are hand drawn. There is no standard for developing the dig limit lines. The results are subject to the author's idea of appropriate dig limit polygons.

Chapter 8

Conclusions

A workflow for improved grade control is developed and presented. A new grade control paradigm addresses major sources of misclassification errors of mined material in open pit mines. A series of theoretical examples and a case study with real production data are constructed. Practical recommendations for improved grade control in open pit mines are provided. They may be used together or separately depending on the needs of a mine.

8.1 Summary of Contributions

Grade control decisions are based on limited data obtained from drillhole (DH) and blasthole (BH) samples. Grades at each unsampled location are predicted using estimation or simulation techniques. Practitioners usually construct grade control models using deterministic estimation methods and large grid sizes. Large grid sizes are used for obtaining grade control models at a resolution comparable to a selective mining unit (SMU) size. Low resolution of grade control models (large blocks) also allows easier drawing dig limit lines used in ore/waste selection. Theoretical experiments in this thesis show that using large grid sizes causes a loss of profit. Grade control models constructed using reasonable grid sizes show better results in grade control. The grid size

for grade control models should be considered with respect to the sample spacing. Theoretical experiments in Chapter 3 and the case study allow concluding that a reasonable grid size for grade control models should be in the range from 25 to 40 % of sample data spacing. It is not recommended to exceed 50 % of the sample data spacing. In most cases, the amount of missclassified material increases after this limit. An ordinary kriging grade control model for the Red Dog case study, constructed using a reasonable grid size, resulted in 4.4 % less misclassified blocks than the model constructed using the actual Red Dog grid size for grade control models.

Estimation is traditionally used for grade control at mines. Kriging methods are particularly popular. They produce robust predictions of grades at unsampled locations. Unfortunately, the estimates produced using kriging or other deterministic interpolation techniques are smooth and do not reproduce all the uncertainty in input grades. Estimation models for grade control are often constructed for each variable separately and then used for developing dig limit lines. This approach does not account for complex multivariate relationships between variables important for the recovery of metals. Simulation allows accounting for all the variables important for grade control at once. Multiple realizations of simulation are used to calculate the expected profit or loss of each grade control decision. The final decision brings the largest expected profit or the smallest expected loss. A theoretical experiment in Chapter 4 and the Red Dog case study in Chapter 7 illustrate different ways of using simulation for grade control. Simulation allows adjusting the grade control decisions depending on a particular technological process or technological constraints. In all provided examples, the simulation approach for grade control outperforms estimation compared to a reference distribution of grades: it produces less misclassified blocks. Once set up, the simulation approach for grade control can be used as easily as estimation. All important relationships between variables of interest and other aspects can be addressed by simulation. For the Red Dog

case study, simulation produced 0.9 % less misclassified blocks than estimation (even using a reasonable grid size). The more complex the relationships between variables and the more complicated the recovery formula, the more profitable simulation is for grade control.

Post-blast displacement of grades is, probably, the most important issue for improved grade control. All improvements in grade control can be compromised if a precise post-blast grade control model is not constructed. A method for predicting blast movement should be adjustable to different conditions and easy to use. A way to translate the pre-blast grades onto the post-blast surface without using dig limits is proposed in this thesis. *Bmov* program allows constructing pre-and post-blast 3-D models of mine bench using the pre- and post-blast topography. Pre- and post-blast user-defined polygons outline the boundaries of the pre- and post-blast 3-D models. The program applies an easy but robust principle of mapping the pre-blast grades onto the post-blast 3-D model. A block of a pre-blast 3-D model is associated to a correspondent block of a post-blast 3-D model using relative positions (indices) of the blocks inside the 3-D models. The indices are calculated with respect to the edges of the models in three orthogonal directions. It is possible to incorporate constraints and additional data to adjust the blast movement pattern according to site specific conditions.

Ore/waste delimitation of a mine bench using dig limits is replaced by the truck-by-truck (TBT) paradigm. Similar to simulation method for grade control, TBT implies making grade control decisions based on the expected profit from many realizations. The expected profit is then averaged inside grade control units representing one truck load. These truck-load units are developed beforehand with respect to particular excavating and hauling equipment. A way a particular piece of excavation equipment scoops a mine bench is taken into account. Having truck-load units placed in a correct order throughout the mine bench, it is possible to calculate the profit of each scoop and each truck

load. Therefore, the actual excavation process is modeled and the positions of each scoop are defined beforehand. A precise GPS dispatching system is required for this method. It should be mentioned that modern grade control methods with dig limits also require precise navigation. The TBT method is expected to be less effective in comparison to the DL method for very continuous grade distributions. The TBT method resulted in 1.05 % less misclassified blocks for the Red Dog case study. Both methods are used with optimized parameters for grade control models. Several types of excavating equipment are compared. The most effective type of the excavating equipment for grade control is determined to be a hydraulic excavator. Technological parameters of this type of excavating equipment permit flexible and selective excavation.

8.2 Limitations

Thousands of reference distributions are used for obtaining the recommendations in Chapter 3. Artificial reference and sample data is the only way to perform such a theoretical study. The effectiveness of estimation using real data may departure from the provided results due to the complexity of a real life geological settings. The distribution of data is known beforehand and statistically ideal. The amount of influencing factors could be increased. Some factors might be added or removed depending on a particular mine. Therefore, the reasonable range of grid sizes may be altered for each particular case; but the difference from the results provided in Chapter 3 is not expected to be significant.

The effectiveness of simulation over estimation is also checked using synthetic and partially conditioned distributions. Theoretically, simulation always outperforms estimation irrespective of the simulation workflow or a number of variables. However, real life results for grade control, especially, with only one variable may be different. Some cases may occur when estimation (i.e. ordinary

kriging) outperforms simulation. It specifically may happen when penalties for estimation and underestimation are equal. For asymmetric penalties, the effectiveness of simulation over estimation is more evident.

Simulation with more variables require a different approach. The impact of all variables on the recovery of a metal of interest or the quality of a final product should be properly accounted for. Correct utility and penalty functions for each variable should be developed for accurate profit and loss calculations for each grade control decision. Another issue is related to the process of multivariate modeling. Different multivariate transformation workflows can be used. The influence of different multivariate transformation techniques on short-term grade control could be studied more thoroughly.

The work of the blast movement program (*bmov*) is checked only for artificial topographic surfaces. It allows visualizing the principle of the post-blast mapping of grades. However, it is necessary to check the performance of the program with real data. The program uses gridded topography and user-defined polygons outlining the boundaries of pre- and post-blast benches. Therefore, the performance of *bmov* with the real data is controllable and expected to be stable. The program should be tuned to specific technological parameters of blasting and geological data. Some additional data such as blast measurement vectors are possible to incorporate into the program's code. Due to the complexity of the pre- and post-blast topographies, it is difficult to match the resolution of both models (number of nodes) in all directions. A better fit of the pre- and post-blast 3-D models is achieved for the topographic data gridded at a higher resolution. Working with high resolution models, in turn, will require more computation time.

The truck-by-truck (TBT) selection of grades uses the same principle as the simulation approach for grade control. It makes grade control decisions based on the expected profit of the units of mined material comparable to each truck load. The grade control decisions are made accounting for the actual

excavating process; each truck load is modeled beforehand. Therefore, it is very important to have a precise dispatching system to take advantage of more precise ore/waste classification.

Sample errors may adversely effect the effectiveness of the TBT method with simulation. It is not known how sensitive the TBT method is to particular multivariate transformation workflows. Currently, it is believed that sample errors are very important for optimal TBT performance.

8.3 Future Work

A more comprehensive research may be conducted to obtain the reasonable range for grid sizes relative to sample data. Theoretical results should be checked with real data from different types of deposits. Practical recommendations for different geological types of deposits could be developed.

Simulation is a more effective tool for grade control provided it is used properly. A number of different factors may influence its performance. More information should be gathered on the performance of simulation in different conditions. More practical recommendations for using simulation for short-term grade control should be developed. Prospectively, simulation should become a primary tool for grade control. Some new software may be developed to implement simulation for any number of variables.

The TBT method is an extension of the simulation approach. Different types of equipment are easy to implement with the TBT method. The influence of sample errors on the performance of the TBT method should be thoroughly investigated. The sensitivity of the TBT method to different multivariate transformation techniques should be studied and practical recommendations provided.

The computational time for the blast movement program can be improved using parallel processing and an optimized code. The principle of mapping

the pre-blast grades onto the post-blast 3-D models could be improved to fit with different blast movement scenarios. A function should be added into the program's code to incorporate additional blast movement measurement data.

References

- Barnett, R. M. (2015). Guide to multivariate modeling with the PPMT. *CCG guidebook series, vol. 20*, University of Alberta, Edmonton, AB, Canada.
- Barnett, R. M., Manchuk, J. G., & Deutsch, C. V. (2014). Projection pursuit multivariate transform. *Mathematical Geosciences*, 46(3), 337–359.
- Bender, W. L. (1999). *Back to basics: The fundamentals of blast design*.
- Bernoulli, D. (1954). Exposition of a new theory on the measurement of risk. *Econometrica: Journal of the Econometric Society*, 23–36.
- Caterpillar. (n.d.). *New hydraulic mining shovels: 6018/6018 FS*. Retrieved from http://www.cat.com/en_US/products/new/equipment/hydraulic-mining-shovels/hydraulic-mining-shovels/18421452.html
- Caterpillar. (n.d.-a). *New off-highway trucks: 777D*. Retrieved from http://www.cat.com/en_US/products/new/equipment/off-highway-trucks/off-highway-trucks/752351.html
- Caterpillar. (n.d.-b). *New wheel loaders: 992G*. Retrieved from http://www.cat.com/en_US/products/new/equipment/wheel-loaders/large-wheel-loaders/752946.html
- Cressie, N. (1990). The origins of kriging. *Mathematical geology*, 22(3), 239–252.
- Cunningham, C. V. B. (2005). The kuz-ram fragmentation model-20 years on. In *Proceedings of the Conference of European Federation of Explosives Engineers* (p. 201-210). Brighton.

- David, M. (1977). *Geostatistical ore reserve estimation*. Elsevier Scientific Publishing Company.
- Detour Gold. (2012). *Grade control and dilution management. Detour Lake Open Pit Gold Mine*. PDAC Technical sessions [PDF file]. Retrieved from http://s1.q4cdn.com/320803946/files/doc_presentations/DGC_12.03.06_PDAC%20Grade%20Control.pdf
- Deutsch, C. V., & Journel, A. G. (1998). *GSLIB: Geostatistical software library and user's guide* (2nd ed.). Oxford University Press.
- Deutsch, C. V., Magri, V. E., & Norrena, K. (2000). Optimal grade control using geostatistics and economics: methodology and examples. *Transactions-Society for mining metallurgy and exploration incorporated*, 308, 43–52.
- Dimitrakopoulos, R., & Godoy, M. (2014). Grade control based on economic ore/waste classification functions and stochastic simulations: examples, comparisons and applications. *Mining Technology*, 123(2), 90–106.
- Douglas, I., Rossi, M., & Parker, H. (1994). Introducing economics in grade control: the breakeven indicator method. *Preprints-Society of mining engineers of AIME*.
- Engmann, E., Ako, S., Bisiaux, B., Rogers, W., & Kanchibotla, S. (2013). Measurement and modelling of blast movement to reduce ore losses and dilution at ahafo gold mine in ghana. *Ghana Mining Journal*, 14, 27–36.
- Field, J. E., & Ladegaard-Pedersen, A. (1971). The importance of the reflected stress wave in rock blasting. *International Journal of Rock Mechanics and Mining Sciences & Geomechanics Abstracts*, 8(3), 213–226.
- Firth, I. R., & Taylor, D. L. (2003). Utilization of blast movement measurements in grade control. In *Proceedings of the 31th APCOM symposium on application of computers and operations research in the minerals industries*. Johannesburg, South Africa.
- Fitzgerald, M., York, S., Cooke, D., & Thornton, D. (2011). Blast monitoring

and blast translation–case study of a grade improvement project at the fimiston pit, kalgoorlie, western australia. In *Proceedings of the eighth international mining geology conference 2011* (pp. 285–298).

Franklin, J. A., & Katsabanis, T. (1996). *Measurement of blast fragmentation*. CRC Press.

Friedman, J. H. (1987). Exploratory projection pursuit. *Journal of the American statistical association*, 82(397), 249–266.

Giles, D. E. (n.d.). *Proof that the median minimizes the mean absolute deviation* [PDF file]. Retrieved from <http://web.uvic.ca/~dgiles/blog/median2.pdf>

Glacken, I. M. (1996). *Change of support by direct conditional block simulation* (Master’s thesis). Stanford University, Stanford, CA, USA.

Godoy, M., Dimitrakopoulos, R., & Costa, J. F. (2001). Economic functions and geostatistical simulation applied to grade control. In A.C. Edwards(Eds.), *Mineral Resource and Ore Reserve Estimation - The AusIMM Guide to Good Practice* (Vol. 52, p. 591-600). Melbourne, Australia: The Australasian Institute of Mining and Metallurgy.

Isaaks, E. H. (1991). *The application of Monte Carlo methods to the analysis of spatially correlated data* (Doctoral thesis). Stanford University, Stanford, CA, USA.

Isaaks, E. H., Barr, R., & Handayani, O. (n.d.). *Modeling blast movement for grade control* [PDF file]. Retrieved from <http://www.isaaks.com/files/Modeling%20%20Blast%20Heave%20for%20Open%20Pit%20Grade%20Control.pdf>

Isaaks, E. H., & Srivastava, R. M. (1989). *Applied geostatistics*. New York: Academic Press.

Isaaks, E. H., Treloar, I., & Elenbaas, T. (n.d.). *Optimum dig lines for open pit grade control* [PDF file]. Retrieved from [http://www.isaaks.com/files/Optimum%20Dig%20Lines%20for%](http://www.isaaks.com/files/Optimum%20Dig%20Lines%20for%20)

200open%20Pit%20Grade%20Control.pdf

- Journel, A. G. (1984). Mad and conditional quantile estimators. In *Geostatistics for natural resources characterization* (pp. 261–270). Springer.
- Journel, A. G. (1989). *Fundamentals of geostatistics in five lessons*. Wiley-Blackwell.
- Journel, A. G., & Huijbregts, C. J. (1978). *Mining geostatistics*. New York: Academic Press.
- Joy Global. (n.d.). *Electric rope shovels: P&H 1900AL*. Retrieved from <http://www.joyglobal.com/product-details/1900al>
- Kirkpatrick, S., Gelatt, C. D., & Vecchi, M. P. (1983). Optimization by simulated annealing. *Science*, 220(4598), 671–680.
- Komatsu. (n.d.). *Dump Trucks-Rigid - 830E-1AC*. Retrieved from <http://www.komatsu.com.au/Equipment/Pages/Dump%20Trucks%20-%20Rigid/830E-1AC.aspx>
- Konya, C. J., & Walter, E. J. (1991). *Rock blasting and overbreak control*. US Department of Transportation, Federal Highway Administration.
- Kutuzov, B. N., & Rubtsov, V. K. (1970). *Physics of explosive destruction of trocks* [in Russian]. Moscow, USSR: MGI.
- Kuznetsov, V. M. (1977). *Mathematical models of blasting* [in Russian]. Novosibirsk, USSR: Nauka.
- La Rosa, D., & Thornton, D. (2011). Blast movement modelling and measurement. In *Proceedings of the 35th APCOM symposium* (p. 244-247). Wollongong, NSW, Australia.
- Lavrentev, M. A., & Shabat, B. N. (1973). *Problems of hydrodynamics and their mathematical models* [in Russian]. Moscow, USSR: Nauka.
- Leite, F., Domingo, J., Carrasco, I., Gouveia, V., Navarro, I., & Lozano, F. (2014). *Dilution, ore grade and blast movement calculation model* [PDF file]. Retrieved from http://www.maxam.net/media/Default%20Files/civil_explosives/DilutionModelArticle.pdf

- Leuangthong, O. (2003). *Stepwise conditional transformation for multivariate geostatistical simulation* (Doctoral thesis). University of Alberta, Edmonton, AB, Canada.
- Leuangthong, O., Neufeld, C. T., & Deutsch, C. V. (2003). Optimal selection of selective mining unit (SMU) size. In *Proceedings of the 5th CCG Annual Conference*, (paper 116). Edmonton, AB, Canada: University of Alberta.
- Lusk, B., Silva, J., & Eltschlager, K. K. (2013). *Field testing and analysis of blasts utilizing short delays with electronic detonators* (Final Rep. No. S09AP15632). Lexington, KY: University of Kentucky.
- Maerz, N. H., Palangio, T. C., & Franklin, J. A. (1996). WipFrag image based granulometry system. In *Proceedings of the Fragblast 5 workshop on measurement of blast fragmentation, Montreal, Quebec, Canada* (pp. 91–99). AA Balkema.
- Matheron, G. (1963). Principles of geostatistics. *Economic geology*, *58*(8), 1246–1266.
- mining-technology.com. (n.d.). *Collahuasi copper mine, Chile*. Retrieved from <http://www.mining-technology.com/projects/collahuasi>
- Moore, D., Young, L., Modene, J., & Plahuta, J. (1986). Geologic setting and genesis of the red dog zinc-lead-silver deposit, western brooks range, alaska. *Economic Geology*, *81*(7), 1696–1727.
- Neufeld, C. T., Lyall, G., & Deutsch, C. V. (2006). Simulation of grade control, stockpiling and stacking for compliance testing of blending strategies. In *Proceedings of the 8th CCG Annual Conference*, (paper 306). Edmonton, AB, Canada: University of Alberta.
- Neufeld, C. T., Norrena, K. P., & Deutsch, C. V. (2007). Guide to geostatistical grade control and dig limit determination. *CCG guidebook series, vol. 1*, University of Alberta, Edmonton, AB, Canada.
- Norrena, K. P. (2007). *Decision making using geostatistical models of uncertainty* (Doctoral thesis). University of Alberta, Edmonton, AB, Canada.

- Norrena, K. P., & Deutsch, C. V. (2001). Automatic determination of dig limits subject to geostatistical, economic and equipment constraints. In *Proceedings of the 3rd CCG Annual Conference*, (paper 114). Edmonton, AB, Canada: University of Alberta.
- Ouchterlony, F. (2005). The Swebrec© function: linking fragmentation by blasting and crushing. *Mining Technology*, 114(1), 29–44.
- Persson, P.-A., Holmberg, R., & Lee, J. (1993). *Rock blasting and explosives engineering*. CRC press.
- Preece, D. S., Tawadrous, A., Silling, S. A., & Wheeler, B. (2015, August 26). *Modeling full-scale blast heave with three-dimensional distinct elements and parallel processing* [PDF file]. Retrieved from http://www.fragblast11.org/Media/Fragblast11/presentations/SESSION_10A.1030.pdf
- Preece, D. S., Tidman, J. P., & Chung, S. (1997, February 2-5). *Expanded rock blast modeling capabilities of DMC - BLAST, including buffer blasting*. Technical report published in the proceedings of the 13th Annual Symposium on Explosive and Blasting Research of the International Society of Blasting Engineers, Las Vegas, NV, USA. Retrieved from <http://www.osti.gov/scitech/servlets/purl/432902>
- Rossi, M. E., & Deutsch, C. V. (2014). *Mineral resource estimation*. Springer Science & Business Media.
- Shapurin, A. V., & Eschenko, A. A. (1970). *Investigation of relationships between the fragmentation of rocks, the positioning of charges, and the direction of blasting in the nkgok open pit* [in Russian] (Technical report). Kryvyi Rih, Ukraine: KGRI.
- Shepard, D. (1968). A two-dimensional interpolation function for irregularly-spaced data. In *Proceedings of the 1968 23rd ACM national conference* (pp. 517–524).
- Sheskin, D. J. (2003). *Handbook of parametric and nonparametric statistical*

procedures. CRC Press.

- Srivastava, R. M. (1987). Minimum variance or maximum profitability?. *CIM Bulletin*, 80(901), 63–68.
- Taylor, S. L. (1995). *Blast induced movement and its effect on grade dilution at the coeur rochester mine* (Master's thesis). University of Nevada, Reno, NV, USA.
- Teck Cominco Alaska Inc. (2009). *Red Dog Mine closure and reclamation plan. Supporting document B. Plan of operations [Final Plan]*. Retrieved from <http://dnr.alaska.gov/mlw/mining/largemine/reddog/publicnotice/pdf/sdb1.pdf>
- Teck Resources Limited. (n.d.). *2014 Annual Report*. Retrieved from <http://www.teck.com/Generic.aspx?PAGE=Teck%20Site/Investors%20Pages/Financial%20Reporting%20Pages/2014-Annual-Report>
- Thornton, D. (2009a). The application of electronic monitors to understand blast movement dynamics and improve blast designs. In *Proceedings of the 9th international symposium on rock fragmentation by blasting*, Fragblast (pp. 287–300).
- Thornton, D. (2009b). The implications of blast-induced movement to grade control. In *Proceedings of the 7th international mining geology conference* (pp. 147–154). Perth, WA, Australia.
- Thornton, D., Sprott, D., & Brunton, I. (2005). Measuring blast movement to reduce ore loss and dilution. In *Proceedings of the 31st annual conference on explosives and blasting technique*.
- Tordoir, A., Weatherley, D., Onederra, I., & Bye, A. (2009). A new 3D simulation framework to model blast induced rock mass displacement using physics engines. In *Proceedings of the 9th international symposium on rock fragmentation by blasting*, Fragblast (pp. 381–388).
- University of Colorado. (n.d.). *Proof that the mean minimizes the sum of squared errors* [PDF file]. Retrieved from <http://samiam.colorado>

[.edu/~mcclella/twt/sseproof.pdf](http://www.mcclella.twt.sseproof.pdf)

- Vasylchuk, Y. V., & Deutsch, C. V. (2015a). Assessing the effectiveness of using estimation methods versus simulation in ore/waste selection. In *Proceedings of the 17th CCG Annual Conference*, (paper 310). Edmonton, AB, Canada: University of Alberta.
- Vasylchuk, Y. V., & Deutsch, C. V. (2015b). A program for calculating an approximate blast movement for improved grade control. In *Proceedings of the 17th CCG Annual Conference*, (paper 311). Edmonton, AB, Canada: University of Alberta.
- Vasylchuk, Y. V., & Deutsch, C. V. (2015c). A short note on optimal kriging grid size relative to data spacing. In *Proceedings of the 17th CCG Annual Conference*, (paper 308). Edmonton, AB, Canada: University of Alberta.
- Vasylchuk, Y. V., & Deutsch, C. V. (2015d). A short note on truck-by-truck selection versus polygon grade control. In *Proceedings of the 17th CCG Annual Conference*, (paper 312). Edmonton, AB, Canada: University of Alberta.
- Verly, G. (2005). Grade control classification of ore and waste: A critical review of estimation and simulation based procedures. *Mathematical geology*, 37(5), 451–475.
- Wang, T., & Deutsch, C. V. (2009). Application of block LU simulation with an approximate model of coregionalization. In *Proceedings of the 11th CCG Annual Conference*, (paper 306). Edmonton, AB, Canada: University of Alberta.
- Wilde, B. J., & Deutsch, C. V. (2007a). Feasibility grade control (FGC):simulation of grade control on geostatistical realizations. In *Proceedings of the 9th CCG Annual Conference*, (paper 301). Edmonton, AB, Canada: University of Alberta.
- Wilde, B. J., & Deutsch, C. V. (2007b). A short note comparing Feasibility Grade Control with Dig Limit Grade Control. In *Proceedings of the 9th*

CCG Annual Conference, (paper 302). Edmonton, AB, Canada: University of Alberta.

Yang, R., Kavetsky, A., & McKenzie, C. (1989). A two-dimensional kinematic model for predicting muckpile shape in bench blasting. *International Journal of Mining and Geological Engineering*, 7(3), 209–226.

Yennamani, A. L. (2010). *Blast induced rock movement measurement for grade control at the phoenix mine* (Master's thesis). University of Nevada, Reno, NV, USA.

Yennamani, A. L., Aguirre, S., & Mousset-Jones, P. (2011). Blast-induced rock movement measurement for grade control. *Mining Engineering*, 63(2), 34–39.

Zhu, H. (1991). *Modeling mixtures of spatial distributions with integration of soft data* (Doctoral thesis). Stanford University, Stanford, CA, USA.

Appendix A

Input for Blast Movement Program

Table A.1: Parameter file for BMOV program

Parameters for Blast Movement Program

START OF PARAMETERS:

sgsim.out	- data file
pre.dat	- pre-blast surface file
post.dat	- post-blast surface file
pre-vert.dat	- pre-blast polygon vertices
post-vert.dat	- post-blast polygon vertices
2035	- project elevation of the bench bottom
1	- discretization constant
20	- matching number
bmov.out	- blast movement output

Table A.2: An example of vertices file

```
Data
2
x
y
10558.5 26157.5
10721.5 26157.5
10721.5 26057.5
10558.5 26057.5
10558.5 26157.5
```

Table A.3: An example of surface file

```
Surface file
4
X
Y
Elevation
10500.5 26000.5 2036.0
10501.5 26000.5 2036.0
10502.5 26000.5 2036.0
10503.5 26000.5 2036.0
10504.5 26000.5 2036.0
10505.5 26000.5 2036.0
10506.5 26000.5 2036.0
10507.5 26000.5 2036.0
10508.5 26000.5 2036.0
10509.5 26000.5 2036.0
10510.5 26000.5 2036.0
```